

UC San Diego

Research Theses and Dissertations

Title

New Tools and Insight for Recognition of Pseudo-Nitzschia Bloom and Toxic Incidence

Permalink

<https://escholarship.org/uc/item/3hk1d1sf>

Author

Quay, Jenny Elisabeth

Publication Date

2011-09-01

UNIVERSITY OF CALIFORNIA

SANTA CRUZ

**NEW TOOLS AND INSIGHT FOR RECOGNITION OF
PSEUDO-NITZSCHIA BLOOM AND TOXIN INCIDENCE**

A dissertation submitted in partial satisfaction
of the requirements for the degree of

DOCTOR OF PHILOSOPHY

in

OCEAN SCIENCES

by

Jenny Elisabeth Quay

September 2011

The Dissertation of Jenny E. Quay
is approved:

Professor Raphael M. Kudela, Chair

Professor Kenneth W. Bruland

Professor Peter T. Raimondi

Dr. G. Jason Smith

Tyrus Miller
Vice Provost and Dean of Graduate Studies

UMI Number: 3480360

All rights reserved

INFORMATION TO ALL USERS

The quality of this reproduction is dependent upon the quality of the copy submitted.

In the unlikely event that the author did not send a complete manuscript and there are missing pages, these will be noted. Also, if material had to be removed, a note will indicate the deletion.



UMI 3480360

Copyright 2011 by ProQuest LLC.

All rights reserved. This edition of the work is protected against unauthorized copying under Title 17, United States Code.



ProQuest LLC
789 East Eisenhower Parkway
P.O. Box 1346
Ann Arbor, MI 48106-1346

Copyright © by
Jenny Elisabeth Quay
2011

TABLE OF CONTENTS

DISSERTATION INTRODUCTION	1
CHAPTER ONE.....	7
<i>Development of a logistic regression model for the prediction of toxigenic Pseudo-nitzschia blooms in Monterey Bay, California</i>	
CHAPTER TWO.....	23
<i>Assessment of river discharge as a source of nitrate-nitrogen to Monterey Bay, California</i>	
CHAPTER THREE	74
<i>Application of Solid Phase Adsorption Toxin Tracking (SPATT) for field detection of the hydrophilic phycotoxins domoic acid and saxitoxin in coastal California</i>	
CHAPTER THREE (ADDENDUM)	91
<i>Update on the application of Solid Phase Adsorption Toxin Tracking (SPATT) for field detection of domoic acid</i>	
DISSERTATION CONCLUSION.....	95

ABSTRACT

NEW TOOLS AND INSIGHT FOR RECOGNITION OF *PSEUDO-NITZSCHIA* BLOOM AND TOXIN INCIDENCE

By

Jenny Elisabeth Quay

Pseudo-nitzschia is a cosmopolitan marine diatom which can cause the poisoning of humans, marine mammals, and birds through the production of the neurotoxin domoic acid and subsequent contamination of the marine food web. Severe poisoning events are induced when environmental conditions allow: (1) the rapid proliferation ('bloom') of resident toxic species of *Pseudo-nitzschia*, and/or (2) their enhanced toxin production, and (3) the conveyance of the toxin into prey items. The introduction of domoic acid into the food web was recognized as a public health concern along the coast of California following a *Pseudo-nitzschia* bloom and seabird mortality event in the Monterey Bay area in 1991, and blooms of *Pseudo-nitzschia* have since been observed in the region with regularity. Since the recognition of the public health concern posed by these recurrent harmful algal bloom (HAB) events, the California Department of Public Health (CDPH) has been charged with protecting the public from domoic acid intoxication through the Preharvest Shellfish Protection and Marine Biotxin Monitoring Program. This regulatory program (1) conducts, surveys, classifies and monitors commercial shellfish growing areas, and (2) monitors

numerous points along the California coastline for marine biotoxins in shellfish and toxigenic phytoplankton in the waters. While these regulatory efforts have successfully prevented significant injury to public health since they began, they remain relatively inefficient in terms of time, energy, and cost.

This thesis begins with an investigation of the environmental factors that contribute to *Pseudo-nitzschia* bloom formation in Monterey Bay (Chapter 1). The identification of nitrate and river discharge as seasonal bloom factors motivated an explicit evaluation and contextualization of river nitrate loading within the ‘upwelling-dominated’ region of Monterey Bay (Chapter 2). Finally, a new monitoring technology, Solid Phase Adsorption Toxin Tracking (SPATT), is presented, developed primarily for use by public health managers for more effective and efficient monitoring of domoic acid, the toxin produced by *Pseudo-nitzschia* and the ultimate cause for concern (Chapter 3, with addendum).

ACKNOWLEDGEMENTS

The text of this dissertation includes reprint[s] of the following previously published materials:

Lane, J. Q., Raimondi, P. T., Kudela, R. M. (2009) Development of a logistic regression model for the prediction of toxigenic Pseudo-nitzschia blooms in Monterey Bay, California. Marine Ecology Progress Series (383) 37-51.

Lane, J. Q., Roddam, C. M., Langlois, G. W., Kudela, R. M. (2011) Application of Solid Phase Adsorption Toxin Tracking (SPATT) for field detection of the hydrophilic phycotoxins domoic acid and saxitoxin in coastal California. Limnology and Oceanography: Methods (8) 645-660.

The text of this dissertation includes the following materials currently submitted for publication:

Lane, J. Q., Langlois, G.W., Kudela, R. M. (2010) Update on the application of Solid Phase Adsorption Toxin Tracking (SPATT) for field detection of domoic acid. Submitted for publication, Proceedings of the 14th International Conference on Harmful Algae.

Quay, J. E., Paradies, D. M., Worcester, K. R., Kudela, R. M. (2011) Assessment of river discharge as a source of nitrate-nitrogen to Monterey Bay, California. Submitted for publication, Estuaries and Coasts.

The co-author (Kudela) listed in these publications directed and supervised the research which forms the basis for the dissertation.

First and foremost, I would like to acknowledge and thank my Ph.D. advisor, Dr. Raphael Kudela. I am lucky and privileged to have studied under the guidance of such a dynamic and supportive researcher and mentor. There can be no repayment for what I owe for that, only recognition and respect for what has been given.

I would like to thank my committee members, Ken Bruland, Pete Raimondi, and Jason Smith. I could not have hoped for committee members more generous with

their time, energy, and attention. I will always remember our conversations and our work together. Especially, I will remember the curiosity and wonder I saw in each, and the grace with which they recognized, valued, and cultivated the same in me.

I would like to thank all of the countless volunteers, staff, labmates, and colleagues who willingly and generously contributed their time, attention, and energy in support of my research. I would like to thank the many donors, agencies, and foundations that provided the financial support that made my success a possibility.

I would like to thank my officemates, especially Michael Jacox and Ryan Paerl, for many years of advice, insight, honesty, and laughter. I would like to thank Kendra Hayashi and Meredith Howard for their unwavering support and friendship both within and beyond the laboratory walls.

I would like to thank my friends and my family who, while allowing me all of the time and space I needed to pursue my degree, never felt distant. The enjoyment of support so full of trust and integrity that it leaves no room for hesitation or expectation is my wish for all of us, especially those who question the world and seek to know it more completely.

Finally, to my own little family, Michael and Elvis, and for all of the trails we've left dusty and for those we have yet to blaze – all my love and gratitude.

DISSERTATION INTRODUCTION

Phytoplankton (from the Greek *phyton*, meaning “plant”, and *planktos*, meaning “wanderer”) are microscopic single-celled plants that form the base of the oceanic food web. Under certain environmental conditions (the provision of light, nutrients, etc.) phytoplankton can proliferate rapidly to form algal ‘blooms’. When such a proliferation is the cause of some deleterious effect it is referred to as a *harmful algal bloom* (a “HAB”), and consequences may range from those of aesthetics (e.g. foul smell, discoloration of the water) to those of public health (e.g. the introduction of toxins to the coastal food web). The consequence effected can depend on the type of phytoplankton that have bloomed, the environmental setting, the physiological state of the phytoplankton, etc.; each of these factors is a subject of study within the field of HAB ecology and dynamics.

This dissertation centers around the study of a cosmopolitan genus of harmful algae, *Pseudo-nitzschia*, that blooms frequently along the coast of California and in the study region of Monterey Bay. *Pseudo-nitzschia* is considered harmful through its production of a potent neurotoxin, domoic acid (DA). Domoic acid was first identified in Japan in the seaweed *Chondria armata Okamura* (Takemoto and Daigo 1958), and named according to its common name in Japanese, *domoi*. Confirmed as an ascaricidal (Asami et al. 1960), DA was frequently administered in Japan as a homeopathic remedy for parasitic infestations of roundworm in humans and animals. The neurotoxic effects of DA were discovered in 1989 when approximately 150

people became ill and 4 died following consumption of DA-laden shellfish harvested from Prince Edward Island on the Atlantic coast of Canada (Bates 1989; Wright et al. 1989; Perl et al. 1990). Estimated toxin loads (200 ppm) associated with the outbreak, coupled to a 10-fold safety factor, form the basis for the current regulatory action limit of 20 ppm in the United States (Wekell et al. 2004). Neurotoxic poisoning due to consumption of DA-laden prey or food items has been observed in marine mammals, birds, and humans (Addison and Stewart 1989; Bates 1989; Perl et al. 1990; Fritz et al. 1992; Beltrán et al. 1997; Lefebvre 2000; Scholin et al. 2000; Kreuder et al. 2005). The neurotoxicity of DA is attributed to its structural similarity to kainic acid, glutamic acid, and aspartic acid; the over-activation of glutamate receptors on nerve cell terminals causes an excessive influx of calcium ions into neurons through ion channels and, as a result, neuronal injury or cell death. The reader is referred to Lefebvre and Roberston (2010) for a complete review of DA (mechanism of neurotoxicity, structure, etc.) and human exposure risk.

The introduction of DA into the food web was recognized as a public health concern along the coast of California following a *Pseudo-nitzschia* bloom and seabird mortality event in the Monterey Bay area in 1991 (Fritz et al. 1992; Work et al. 1993), and blooms of *Pseudo-nitzschia* have since been observed within the region with regularity (Buck et al. 1992; Fritz et al. 1992; Work et al. 1993; Scholin et al. 2000; Trainer et al. 2001; Jester et al. 2008; Lane et al. 2009). Since the recognition of this public health concern, the California Department of Public Health (CDPH) has been charged with protecting the public from DA intoxication through the Preharvest

Shellfish Protection and Marine Biotxin Monitoring Program. This regulatory program (1) conducts, surveys, classifies and monitors commercial shellfish growing areas, and (2) monitors numerous points along the California coastline for marine biotoxins in shellfish and toxigenic phytoplankton in the waters. The latter depends on an extensive volunteer force for the collection, maintenance, sampling, and processing (shucking, homogenization, packaging, and shipment) of sentinel shellfish at field sites along the California coast. Analytical cost prohibits the analysis of all samples received by CDPH through these volunteer efforts, and the samples are prioritized by CDPH according to estimates of *Pseudo-nitzschia* abundance at the time of shellfish collection. In addition, CDPH enforces an annual quarantine of sport-harvested mussels from May 1 through October 31. While CDPH efforts have successfully prevented significant injury to public health since they began, they remain relatively inefficient in terms of time, energy, and cost.

Factors that improve growing conditions for land plants (fertilizer or nutrient input, adequate availability of light, etc.) similarly affect the coastal marine environment. Because *Pseudo-nitzschia* blooms pose a threat to human, marine mammal and bird health, the identification of specific environmental conditions associated with their formation are of interest; eutrophication (the enrichment of bodies of water by inorganic plant nutrients) via terrestrial freshwater runoff (Bird and Wright 1989; Trainer et al. 1998; Scholin et al. 2000), fluctuations in nutrient ratios (Marchetti et al. 2004) and upwelling processes (Buck et al. 1992; Trainer et al.

2000; Anderson et al. 2006) have been suggested as causative factors in Monterey Bay and elsewhere.

This thesis begins with an investigation of the environmental factors that contribute to *Pseudo-nitzschia* bloom formation in Monterey Bay (Chapter 1). The identification of nitrate and river discharge as seasonal bloom factors motivated an explicit evaluation and contextualization of river nitrate loading within the ‘upwelling-dominated’ region of Monterey Bay (Chapter 2). Finally, a new monitoring technology is presented, developed primarily for use by public health managers for more effective and efficient monitoring of DA, the toxin produced by *Pseudo-nitzschia* and the ultimate cause for concern (Chapter 3, with addendum).

References

- Addison, R. F., and J. E. Stewart. 1989. Domoic acid and the eastern Canadian molluscan shellfish industry. *Aquaculture* **77**: 263-269.
- Anderson, C. R., M. A. Brzezinski, L. Washburn, and R. M. Kudela. 2006. Circulation and environmental conditions during a toxigenic *Pseudo-nitzschia* bloom. *Marine Ecology Progress Series* **327**: 119-133.
- Asami, K., Y. Kawazoe, K. Kometani, and M. Hitosugi. 1960. Experimental evaluation of ascaricidal effects of domoic acid extracted from a sea weed Hanayanagi. *Japanese Journal of Parasitology* **9**: 290-293.
- Bates, S. S., C.J. Bird, A.S.W. de Freitas, R.A. Foxall, M. Gilgan, L.A. Hanic, G.R. Johnson, A.W. McCulloch, P. Odense, R. Pocklington, M.A. Quilliam, P.G. Sim, J.C. Smith, D.V. Subba Rao, E.C.D. Todd, J.A. Walter, and J.L.C. Wright. 1989. Pennate diatom *Nitzschia pungens* as the primary source of domoic acid, a toxin in shellfish from eastern Prince Edward Island, Canada. *Can. J. Fish. Aquat. Sci.* **46**: 1203-1215.
- Beltrán, A. S., M. Palafox-Uribe, J. Grajales-Montiel, A. Cruz-Villacorta, and J. L. Ochoa. 1997. Sea bird mortality at Cabo San Lucas, Mexico: Evidence that toxic diatom blooms are spreading. *Toxicon* **35**: 447-453.
- Bird, C. J., and J. L. C. Wright. 1989. The shellfish toxin domoic acid. *World Aquacult.* **20**: 40-41.
- Buck, K. R. and others 1992. Autecology of the diatom *Pseudonitzschia australis*, a domoic acid producer, from Monterey Bay, California. *Marine Ecology Progress Series* **84**: 293-302.
- Fritz, L., M. A. Quilliam, J. L. C. Wright, A. M. Beale, and T. M. Work. 1992. An outbreak of domoic acid poisoning attributed to the pennate diatom *Pseudonitzschia australis*. *Journal of Phycology* **28**: 439-442.
- Jester, R., K. Lefebvre, G. Langlois, V. Vigilant, K. Baugh, and M. W. Silver. 2008. A shift in the dominant toxin-producing algal species in central California alters phycotoxins in food webs. *Harmful Algae* **in press**.
- Kreuder, C. and others 2005. Evaluation of cardiac lesions and risk factors associated with myocarditis and dilated cardiomyopathy in southern sea otters (*Enhydra lutris nereis*). *American Journal of Veterinary Research* **66**: 289-299.
- Lane, J. Q., P. T. Raimondi, and R. M. Kudela. 2009. Development of a logistic regression model for the prediction of toxigenic *Pseudo-nitzschia* blooms in Monterey Bay, California. *Marine Ecology Progress Series* **383**: 37-51.
- Lefebvre, K., C. Powell, G. Doucette, J. Silver, P. Miller, P. Hughes, M. Silver, and R. Tjeerdema. 2000. Domoic acid-producing diatoms: probable cause of neuroexcitotoxicity in California sea lions. *Marine Environmental Research* **50**: 485.
- Lefebvre, K. A., and A. Roberston. 2010. Domoic acid and human exposure risks: A review. *Toxicon* **56**: 218-230.
- Marchetti, A., V. L. Trainer, and P. J. Harrison. 2004. Environmental conditions and phytoplankton dynamics associated with *Pseudo-nitzschia* abundance and domoic acid in the Juan de Fuca eddy. *Marine Ecology Progress Series* **281**: 1-12.
- Perl, T. M., L. Bédard, T. Kosatsky, J. C. Hockin, E. Todd, and R. S. Remis. 1990. An outbreak of toxic encephalopathy caused by eating mussels contaminated with domoic acid. *New England Journal of Medicine* **322**: 1775-1780.
- Scholin, C. A. and others 2000. Mortality of sea lions along the central California coast linked to a toxic diatom bloom. *Nature* **403**: 80-84.

- Takemoto, T., and K. Daigo. 1958. Constituents of *Chondria armata*. Chemical Pharmaceutical Bulletin **6**: 578-580.
- Trainer, V. and others 2000. Domoic acid production near California coastal upwelling zones, June 1998. Limnology & Oceanography **45**: 1818-1833.
- Trainer, V. L., N. G. Adams, B. D. Bill, B. F. Anulacion, and J. C. Wekell. 1998. Concentration and dispersal of a *Pseudo-nitzschia* bloom in Penn Cove, Washington, USA. Natural Toxins **6**: 113-126.
- Trainer, V. L., N. G. Adams, and J. C. Wekell. 2001. Domoic acid producing *Pseudo-nitzschia* species off the U.S. west coast associated with toxification events, p. 46-49. In G. M. Hallegraeff, S. I. Blackburn, C. J. Bolch and R. J. Lewis [eds.], Harmful Algal Blooms 2000. Intergovernmental Oceanographic Commission of UNESCO.
- Wekell, J. C., J. Hurst, and K. A. Lefebvre. 2004. The origin of the regulatory limits for PSP and ASP toxins in shellfish. Journal of Shellfish Research **23**: 927-930.
- Work, T. M. and others 1993. Domoic acid intoxication of brown pelicans and cormorants in Santa Cruz, California, p. 643-650. In T. J. Smayda and Y. Shimizu [eds.], Toxic phytoplankton blooms in the sea. Elsevier Science Publication B.V.
- Wright, J. L. C. and others 1989. Identification of domoic acid, a neuroexcitatory amino acid, in toxic mussels from eastern Prince Edward Island. Canadian Journal of Chemistry **67**: 481-490.

CHAPTER ONE



Development of a logistic regression model for the prediction of toxigenic *Pseudo-nitzschia* blooms in Monterey Bay, California

Jenny Q. Lane^{1,*}, Peter T. Raimondi², Raphael M. Kudela¹

¹Department of Ocean Sciences, University of California, 1156 High Street, Santa Cruz, California 95064, USA

²Department of Ecology and Evolutionary Biology, University of California, Center for Ocean Health, 109 Shaffer Road, Santa Cruz, California 95064, USA

ABSTRACT Blooms of the diatom genus *Pseudo-nitzschia* have been recognized as a public health issue in California since 1991 when domoic acid, the neurotoxin produced by toxigenic species of *Pseudo-nitzschia*, was first detected in local shellfish. Although these blooms are recurring and recognized hazards, the factors driving bloom proliferation remain poorly understood. The lack of long-term field studies and/or deficiencies in the scope of environmental data included within them hinders the development of robust forecasting tools. For this study, we successfully developed predictive logistic models of toxigenic *Pseudo-nitzschia* blooms in Monterey Bay, California, from a multi-project dataset representing 8.3 yr of sampling effort. Models were developed for year-round (annual model) or seasonal use (spring and fall–winter models). The consideration of seasonality was significant. Chlorophyll *a* (chl *a*) and silicic acid were predictors in all models, but period-specific inclusions of temperature, upwelling index, river discharge, and/or nitrate provided significant model refinement. Predictive power for unknown (future) bloom cases was demonstrated at $\geq 75\%$. In all models, our performing a chl *a* anomaly model and performing comparably to, or better than, previously described statistical models for *Pseudo-nitzschia* blooms or toxicity (the models presented here are the first to have been developed from long-term (>1.5 yr) monitoring efforts, and the first to have been developed for bloom prediction of toxigenic *Pseudo-nitzschia* species). The descriptive capacity of our models places historical and recent observations into greater ecological context, which could help to resolve historical alternation between the implication of freshwater discharge and upwelling processes in bloom dynamics.

KEY WORDS *Pseudo-nitzschia*, Predictive model, Logistic regression, Harmful algal bloom, Phytoplankton monitoring, Domoic acid

INTRODUCTION

Harmful algal blooms (HABs) can have severe deleterious consequences for local industry (e.g. shellfish, tourism), public health, and ecosystem health; in addition, the incidence of HABs appears to be increasing in both frequency and intensity (Hallegraeff 1993, Anderson et al. 2002, Gilbert et al. 2005). This trend, and its potential to inflict rising economic and societal costs, has encouraged the development of HAB forecasting tools in recent years (Schofield et al. 1999,

Johnson & Sakshaug 2000, Fisher et al. 2003). Many of these efforts have focused on the prediction and monitoring of dinoflagellate blooms and associated red tides, and successful prediction models for these types of HABs span a wide range of modeling approaches and complexity. One of the simplest approaches utilizes satellite-derived chlorophyll anomalies to identify potentially harmful blooms (e.g. Allen et al. 2008) or even species-specific blooms (Tomlinson et al. 2004). Issues associated with satellite-derived models (non-specificity, infrequent data) can be overcome by com-

*Email: jqlav@ucsc.edu

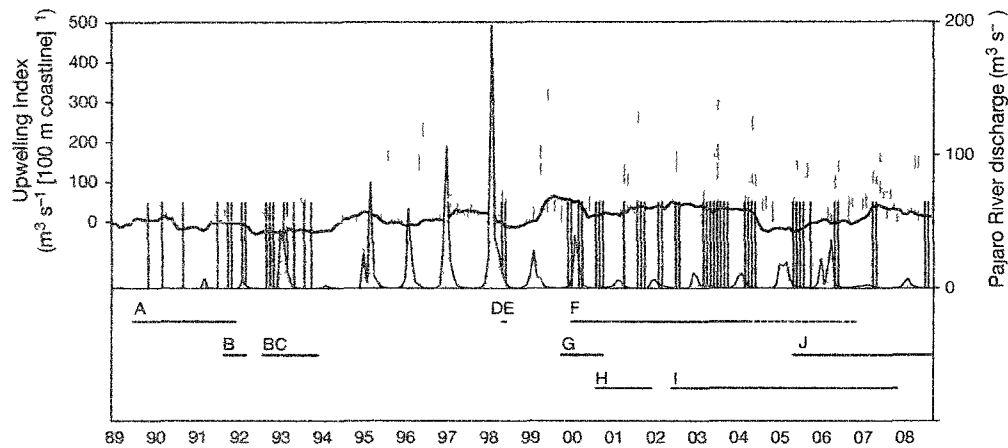


Fig. 1. Time series of bloom events as reported in published literature and in the modeling dataset used here. The time periods addressed by the various studies are indicated below the plot and are as follows: A: Buck et al. (1992); B: Walz et al. (1994); C: Walz (1995); D: Schomin et al. (2000); E: Trainer et al. (2000); F: Jester et al. (2009); G: Lefebvre et al. (2007b); H: Goldberg (2003); I: Center for Integrated Marine Technologies model dataset (present study); J: California Program for Regional Enhanced Monitoring for PhycoToxins model dataset (present study). Grey shading: time frame of data inclusion for the models developed in the present study. Vertical black bars: months for which blooms of toxicogenic *Pseudo-nitzschia* (cell concentration $>10,000$ cells l^{-1}) were reported. A 12 mo moving average of monthly upwelling anomaly (black line), the monthly upwelling index for $36^{\circ}N$, $122^{\circ}W$ (grey bars), and monthly mean Pajaro River discharge (area plot) are shown. Within the time frame of Jester et al. (2009) (F), note the negative values of the upwelling anomaly and the relatively high monthly mean river discharges over the span of summer 2004 through 2006 (dashed line). This period was identified by Jester et al. (2009) as a period of severely decreased *Pseudo-nitzschia* abundance.

blowing satellite data with other predictors, as is done in the Southwest Florida (USA) operational forecast for *Karenia brevis*. This model includes satellite data, wind predictions, and rule-based modeling to improve forecasting success (Stumpf et al. 2009). A similar approach integrating multiple environmental datasets was used for the European Harmful Algal Bloom Expert System (E-HABES): this predictive modeling approach uses fuzzy logic to identify blooms of *Nodularia spumigena*, *Dinophysis* spp., *Alexandrium minutum*, *K. mikimotoi*, and *Phaeocystis globosa* (Blauw et al. 2006). The authors state that fuzzy logic bridges the gap between purely empirical (statistical) predictions and fully deterministic models. Finally, seasonal initiation of HAB events and spatial/temporal distribution have been successfully predicted using fully coupled deterministic physical-biological models in the Gulf of Maine (USA) for *A. fundyense* (McGillivuddy et al. 2005). In contrast to these and other efforts, relatively little predictive skill has been developed for HABs of diatom species.

Toxicogenic species of the diatom *Pseudo-nitzschia* are producers of domoic acid, which can cause neurotoxic poisoning in humans (Addison & Stewart 1989; Bates et al. 1989) marine mammals (Lefebvre et al. 1999; 2002a; Scholin et al. 2000; Kreuder et al. 2005), and

birds (Fritz et al. 1992; Beltran et al. 1997). Since initial documentation in 1991, HABs of toxicogenic *Pseudo-nitzschia* have occurred in Monterey Bay, California, with regularity (Buck et al. 1992; Fritz et al. 1992; Work et al. 1993; Scholin et al. 2000; Trainer et al. 2001); the bulk of published *Pseudo-nitzschia* bloom data was generated through episodic, generally stand-alone research projects undertaken in reaction to these periodic events (Fig. 1). Because these studies were relatively short and episodic in nature, they typically relied on circumstantial observations or single variable correlations for identification of environmental conditions conducive to bloom formation. The constraints associated with this approach led to calls for long-term monitoring approaches (Trainer et al. 2000; Bates & Trainer 2006).

Despite the lack of long-term data, eutrophication via terrestrial freshwater runoff (Bird & Wright 1989; Trainer et al. 1996; Scholin et al. 2000), fluctuations in nutrient ratios (Marchetti et al. 2004), and upwelling processes (Buck et al. 1992; Trainer et al. 2000; Anderson et al. 2006) were implicated as prominent causative factors in historical literature, and our modeling design was developed with this historical ecological perspective in mind. While our data used for model development could not extend over the full time period

represented within the literature due to sampling and methodological inconsistencies, the range of ecological circumstances addressed are not unlike those encountered and implicated previously as triggers for HAB events (Fig. 1).

Our efforts follow 2 previous modeling studies that used shorter duration datasets. The first (Blum et al. 2006) was an attempt to model cellular domoic acid in a toxigenic strain of *Pseudo-nitzschia* (*Pseudo-nitzschia pungens* f. *multiseries*). In that study, 4 models were developed: 2 linear models demonstrated 'good predictive ability', but were developed from laboratory data that failed to address the scope of nutrient concentrations and ratios encountered in the field and were therefore not appropriate for use with field data. A third linear model and a logistic regression model were developed from combined laboratory data and field data collected from monospecific blooms of *P. pungens* f. *multiseries* off the coasts of Prince Edward Island (Canada), and Washington State (USA). Split-sample validations of these models (75% data used for model development; 25% reserved for model validation) demonstrated their 'adequate reliability', but the limited amount of field data (N = 46) and the predominance of restrictive laboratory data within the modeling dataset left the applicability of these models undetermined.

The second modeling study (Anderson et al. 2009) developed linear regression (hindcast) models of *Pseudo-nitzschia* blooms, particulate domoic acid, and cellular domoic acid, from: (1) a 'full' (remotely sensed and *in situ*) suite of predictor variables and (2) a 'remote-sensing only' suite of predictor variables. This study was limited in the amount of data available for model development (N = 72 to 89), but provided preliminary insight into *Pseudo-nitzschia* bloom mechanisms, including macronutrient control. Both model sets presented by Anderson et al. (2009) demonstrated high rates of false negative predictions, presumably due to the relatively limited dataset.

Here, we develop logistic regression models of toxigenic *Pseudo-nitzschia* blooms in Monterey Bay, California. This modeling exercise had 3 goals: (1) to develop *Pseudo-nitzschia* bloom models that are straightforward and useful in their application towards bloom monitoring, (2) through model development, to identify environmental variables that are significant factors in bloom incidence, and (3) to test the recurrence of these significant environmental variables in the previous *Pseudo-nitzschia* models described by Anderson et al. (2009) and Blum et al. (2006). The previous modeling efforts and this one are not wholly consistent in terms of scope, evaluated variables, or specific aim: Anderson et al. (2009) developed models of 'generic' *Pseudo-nitzschia* blooms, cellular domoic

acid, and particulate domoic acid from a 1.5 yr dataset collected from the Santa Barbara Channel, while Blum et al. (2006) developed models of particulate domoic acid from a mixture of experimental and field data. These previous studies and our efforts clearly differ in their region of interest and specific model subject. In the context of the present study, these disparities are an advantage, in that they allow for inter-model comparison capable of identifying factors that are likely to be universally significant to *Pseudo-nitzschia* bloom incidences and to the introduction of domoic acid into the marine environment through bloom proliferation. Thus, our model and the comparison of these 3 efforts should help to identify a common set of variables useful for predictive modeling of *Pseudo-nitzschia* in similar systems, such as major eastern boundary current regimes (Kudela et al. 2005).

We present 3 logistic regression models of toxigenic *Pseudo-nitzschia* blooms in Monterey Bay, California, as they occur throughout the year (annual model) and seasonally (spring and fall-winter models). A total of 31 environmental variables were evaluated, and 6 variables were identified as statistically significant for bloom prediction. This work is the first to present robust *Pseudo-nitzschia* bloom models developed from long-term monitoring data, and the first to evaluate eutrophication processes and seasonality in the prediction of *Pseudo-nitzschia* bloom incidences.

MATERIALS AND METHODS

Compilation of the model dataset. We compiled a dataset from publications that included *Pseudo-nitzschia* cell counts for Monterey Bay (Buck et al. 1992, Walz et al. 1994, Walz 1995, Villac 1996, Scholin et al. 2000, Goldberg 2003, Lefebvre et al. 2002b). Additional unpublished datasets were provided by Moss Landing Marine Laboratories (MLML), and internally generated through the Center for Integrated Marine Technologies (CIMT) and through the California Program for Regional Enhanced Monitoring for PhycoToxins (Cal-PreEMPT). Details on sampling and analytical methods for internally generated datasets are provided.

We obtained 2099 discrete cases from the above sources, 1156 of which were from surface waters (depth ≤ 5 m). All of the data were assessed to ensure methodological consistency, specifically: (1) unbiased sample collection and (2) true concurrency in environmental and *Pseudo-nitzschia* sampling. Of the 1071 cases remaining, 576 contained cell counts of toxigenic *Pseudo-nitzschia*. Not all data contained the same suite of environmental variables. For finalization of the modeling dataset, it was necessary to evaluate which data

were sufficiently complete, i.e. evaluate the minimal combination of variables sufficient for the development of a successful model. The receiver operating characteristic (ROC) was used to conduct this evaluation. ROC is a measure of model fit that scales like a traditional (US) academic point system (<0.6 = poor; 0.6 to 0.7 = fair; 0.7 to 0.8 = good; 0.8 to 0.9 = very good; >0.9 = excellent). Models developed from single, single and universally available (i.e. river discharge, upwelling index), and pairs of predictor variables failed to achieve 'very good' model fit accuracy. To achieve this level of accuracy, model development required concurrent macronutrient, chlorophyll *a* (chl *a*), and temperature variables in combination (Tables 1 & 2). Final inclusion of cases for the models presented therefore required sample collection from Monterey Bay surface waters, and toxigenic *Pseudo-nitzschia* cell counts (*P. multiseriata* and/or *P. australis*) with concurrent environmental measurements of seawater temperature, chl *a*, and macronutrients.

Internal data: sample collection. Samples were collected monthly from June 2002 to November 2007 from 11 stations throughout Monterey Bay as part of the CIMT project. PVC Niskin bottles (10 l volume fitted with silicone rubber band strings) mounted on an instrumented rosette were used to collect water from 5 m depth. Surface samples were collected from 2 stations by PVC bucket. Temperature data were obtained from a Seabird SBE-19 CTD deployed concurrently with water sampling.

Table 1. Evaluations of independent variable(s) as predictor variables were performed using all compiled literature and field data of toxic *Pseudo-nitzschia* in Monterey Bay at a depth ≤ 5 m (N = 576). The receiver operating characteristic (ROC) is a measure of model fit accuracy, where <0.6 = poor, 0.6 to 0.7 = fair, 0.7 to 0.8 = good, 0.8 to 0.9 = very good, and >0.9 is considered excellent. Inclusion of macronutrient, seawater temperature, and chlorophyll *a* as predictor variables was necessary to achieve 'very good' model fit accuracy. A key to variable names is provided in Table 2

Independent variable	N (cases)	Cases omitted	ROC
Salinity	427	149	0.462
Temp	493	83	0.573
ln(silicic acid)	516	60	0.614
ln(chl <i>a</i>)	497	79	0.618
ln(chl <i>a</i>), temp	473	103	0.638
ln(chl <i>a</i>), upwelling	492	84	0.638
ln(silicic acid), upwelling	516	60	0.713
ln(silicic acid), ln(chl <i>a</i>)	444	132	0.757
ln(nitrate), temp, ln(chl <i>a</i>)	419	157	0.766
ln(silicic acid), temp	438	138	0.785
ln(silicic acid), temp, ln(chl <i>a</i>)	422	154	0.848

Table 2. Complete list of the variables evaluated as independent (predictor) variables in the logistic regression models. X: all environmental variables and ratios, excluding temperature

Independent variable	Abbreviation	Units
Seawater temperature	Temp	°C
Total chlorophyll <i>a</i>	Chl <i>a</i>	$\mu\text{g l}^{-1}$
Nitrate	Nitrate	μM
Silicic acid	Silicic acid	μM
Ortho-phosphate	Phosphate	μM
Silicic acid (nitrate) ⁻¹	Silicic acid:nitrate	
Nitrate (silicic acid) ⁻¹	Nitrate:silicic acid	
Ortho-phosphate (nitrate) ⁻¹	Phosphate:nitrate	
Nitrate (ortho-phosphate) ⁻¹	Nitrate:phosphate	
Ortho-phosphate (silicic acid) ⁻¹	Phosphate:silicic acid	
Silicic acid (ortho-phosphate) ⁻¹	Silicic acid:phosphate	
Pajaro River discharge	Pajaro River	$\text{m}^3 \text{s}^{-1}$
San Lorenzo River discharge	San Lorenzo River	$\text{m}^3 \text{s}^{-1}$
Soquel River discharge	Soquel River	$\text{m}^3 \text{s}^{-1}$
Salinas River discharge	Salinas River	$\text{m}^3 \text{s}^{-1}$
Bakun upwelling index	Upwelling	$\text{m}^3 \text{s}^{-1}$
Ln(X + 1)	Ln(X)	

Shore-based surface samples were collected weekly from May 2005 to April 2008 from the Santa Cruz Municipal Wharf (36° 57.48' N, 122° 1.02' W) as part of the Cal-PreEMPT project using a PVC bucket or by integration of water samples collected from 3 discrete depths (0, 1.5, and 3 m) with a FieldMaster 1.75 l basic water bottle. Temperature was measured in the field by digital thermometer immediately following sample retrieval.

River discharge rates for the Salinas, San Lorenzo, Soquel, and Pajaro Rivers were obtained from the United States Geological Survey National Water Information System (<http://waterdata.usgs.gov/nwis/>). Bakun daily upwelling index values for the Monterey Bay region (36°N, 122°W) were obtained from the National Oceanographic and Atmospheric Administration Pacific Environmental Research Division (www.pfeg.noaa.gov/products/PFEL/).

Internal data: analytical methods. Samples for chl *a* were collected in duplicate and filtered onto uncombusted glass-fiber filters (Whatman GF/F) and processed using the non-acidification method (Welschmeyer 1994). Macronutrients (Nitrate plus nitrite [hereafter referred to as nitrate], silicic acid and ortho-phosphate) were stored frozen prior to analysis with a Lachat Quick Chem 8000 Flow Injection Analysis system using standard colorimetric techniques (Knepel & Bogren 2001, Smith & Bogren 2001a,b). *Pseudo-nitzschia* species identification and enumeration utilized species-specific large subunit rRNA-targeted

probes following standard protocols (Miller & Scholin 1998). Samples were enumerated with a Zeiss Standard 18 compound microscope equipped with a fluorescence illuminator 100 (Zeiss). Duplicate filters were prepared for each species and the entire surface area of each filter was considered in counting.

Model development. Logistic regression models were developed using MYSTAT Version 12.02.11. Logistic modeling is appropriate when the dependent variable is dichotomous (e.g. 0/1). Since our dataset contained continuous data of *Pseudo-nitzschia* abundance, logistic modeling required concatenation of *Pseudo-nitzschia* abundance data into a new dichotomous dependent variable (bloom/nonbloom) using a defined bloom threshold of 10,000 toxicogenic *Pseudo-nitzschia* cells l^{-1} (Lefebvre et al. 2002b, Fehling et al. 2006, Howard et al. 2007, Jester et al. 2009). Similar model results were obtained (not shown) when a criteria of 5000 cells l^{-1} was used.

Independent variables evaluated during model development are provided in Table 2. We used an automatic stepwise approach (forward, backward, and bidirectional) to identify the most significant subset. Variable selections were refined to (1) maximize the rate at which blooms were successfully predicted, (2) minimize the rate of false negative predictions, and (3) maximize model fit accuracy (ROC) while controlling for covariance among the independent variables. Variables exhibiting severe collinearity as determined by variance inflation factors and condition indices were considered mutually exclusive. Only significant variables ($p < 0.05$) were included in the final models. For the development of the 2 seasonal models, the data were partitioned according to the seasonal periods previously described for Monterey Bay (Pennington & Chavez 2000) while the entire dataset was used for development of the annual model. The final 3 models

are as follows: (1) year-round (annual model), (2) February 14 to June 30 (spring model), and (3) July 1 to February 13 (fall-winter model).

We compare our models to a simple bloom prediction method using chl *a* anomalies. Data from June 2004 to July 2008 were obtained from the LOBOVIZ website (www.mbari.org/lobo/loboviz.htm) for a nearshore mooring in Monterey Bay (M0), and a 30 d median chl *a* anomaly was calculated according to methods previously described for 60 d mean anomalies (Tomlinson et al. 2004, Wynne et al. 2006). The LOBOVIZ website was selected as a data source due to its ease of access and applicability. A median was employed in lieu of a mean since it has recently been recognized as the generally more appropriate value (R. Stumpf pers. comm.).

Translating probability into prediction, prediction-point assignment. When the model equation is solved, the user is presented with the probability of a bloom occurrence. The degree of probability that can be tolerated is referred to here as the prediction-point. Where the model solution, bloom probability, is greater than the prediction-point, the model predicts a bloom. Conversely, where the model solution is lower than the prediction-point, the probability of a bloom is considered sufficiently low to warrant a non-bloom prediction. The prediction-point must be pre-defined by either (1) the model developer for optimization of predictive power, or (2) the model user for selective risk management. We provide optimized prediction-points for each model and offer guidance for their adjustment. Optimized prediction-points were determined by generating model prediction failure rates over the full range of potential prediction-point assignments (0.000 to 1.000) at 0.005 increments (Fig. 2). The overall failure rate is minimized when the failure to predict blooms and failure to predict non-blooms are simulta-

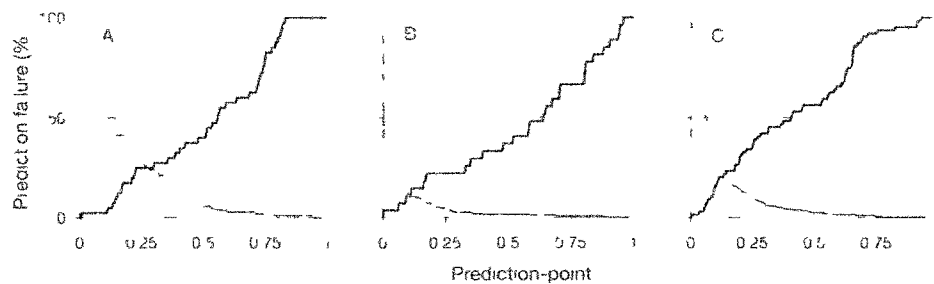


Fig. 2. Prediction failure rates for blooms (solid lines) and non-blooms (broken lines) for the spring (A), fall-winter (B), and annual (C) models along the range of possible prediction points. The prediction failure rate is defined as the rate at which the model fails to predict a case type (bloom or non-bloom). The overall prediction failure rate is minimized at the optimized prediction point where the 2 lines cross.

nously minimized. The optimized prediction point values therefore occur where the failure rate curves intersect (Fig. 2).

Model validation. A jackknife cross validation module was supplied by SYSTAT and used to validate model performance with respect to unknown (future) cases. This method is similar to the split sample bootstrap validation approach taken by Blum et al. (2006) except that it does not reduce the dataset that can be used for initial model development and it is an iterative process that allows for N instances of cross validation against unknown single cases. The cross validation was run with the model optimized prediction points and with user adjusted prediction points set according to the historical probability of blooms for Monterey Bay (2002 to 2005) calculated from an independent California Department of Public Health (CDPH) *Pseudo-nitzschia* bloom monitoring dataset. This historical probability is referred to as priors.

RESULTS

After removing those cases from the original ($N = 2099$) dataset that did not fulfill the specified quality criteria, 506 cases from 2002 to 2008 remained, 74 of which were classified as bloom cases. There was clear seasonality in these data: the rate of bloom incidence was 78% during the spring model period compared to a rate of 9% for the remainder of the year.

Logistic regression models are of the form

$$\text{LOGIT}(p) = \ln[p/(1-p)] = \beta_0 + \beta_1 z_1 + \beta_2 z_2 + \dots + \beta_k z_k \quad (1)$$

where p is the probability of the condition being modeled here, p represents the probability of a toxigenic *Pseudo-nitzschia* bloom, β_0 is a constant and $\beta_1, \beta_2, \dots, \beta_k$ are the regression coefficients of z_1, z_2, \dots, z_k respectively. The year-round (annual) and seasonal (spring and fall-winter) models are as follows:

Annual model

$$\text{LOGIT}(p) = 9.763 + 1.700[\ln(\text{silicic acid})] + 1.132[\ln(\text{chl } a)] - 0.800(\text{temp}) + 0.006(\text{upwelling}) \quad (2)$$

Spring model

$$\text{LOGIT}(p) = 5.835 + 1.398[\ln(\text{chl } a)] - 1.135[\ln(\text{silicic acid})] - 0.549(\text{temp}) \quad (3)$$

Fall-Winter model

$$\text{LOGIT}(p) = 10.832 - 5.026[\ln(\text{Pajaro River})] + 3.893[\ln(\text{silicic acid})] + 1.972[\ln(\text{chl } a)] + 0.652(\text{nitrate}) \quad (4)$$

The regression curve for the spring model is presented for visualization of how the model solution [LOGIT(p)] translates into a bloom probability (p) and through the

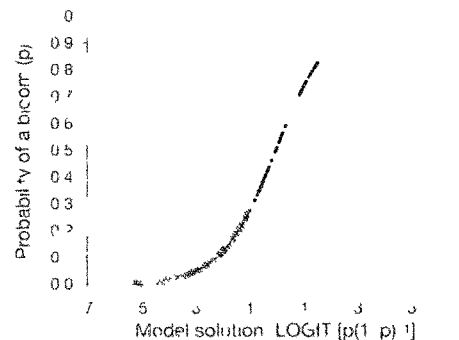


Fig. 3. The spring model logistic regression curve. Cases lying above the optimized prediction point (probability = 0.275) are predicted as blooms (●); cases lying below the optimized prediction point are predicted as non blooms (×).

implementation of a prediction point into a bloom or non bloom predictor (Fig. 3).

The models demonstrated very good to excellent model fit accuracy (Table 3). Other demonstrations of model proficiency include the determination of a model p value through calculation and evaluation of a likelihood ratio statistic and the determination of adjusted R^2 statistics, McFadden's ρ and Nagelkerke's R^2 for which values >0.2 are indicative of very good model fit (Hensher & Johnson 1981) (Table 3). Each of the models achieved a high level of statistical proficiency with 4 or fewer predictive variables.

Two predictive variables, $\ln(\text{chl } a)$ and $\ln(\text{silicic acid})$ were included in all models. The set of predictive variables used in the annual model and spring model were most similar, differing only in the inclusion of upwelling in the annual model. The fall-winter model is the most disparate of the 3 models with the variable set $\ln(\text{Pajaro River})$, nitrate, $\ln(\text{silicic acid})$ and $\ln(\text{chl } a)$. Of particular note is the omission of temp and upwelling from the fall-winter model and the inclusion of a river discharge variable, $\ln(\text{Pajaro River})$ and nitrate. All variables included in the models demonstrated extreme to maximum statistical significance.

The annual model did not emerge as an explicit sum of the 2 seasonal models. An annual model with $\ln(\text{Pajaro River})$ and nitrate included (not shown) achieves results very similar to those of the presented annual model but with slightly improved bloom and non bloom prediction. These variables however were non significant additions and caused inflation in the standard errors of the other (significant) variable coefficients; this is a general risk assumed when non significant predictors are included in any model (Menard 1995). The inclusion of additional variables in the

annual model also resulted in unacceptable levels of covariance (condition indices > 30). Dueling complexity and covariance restrictions likely promoted the usefulness of a 'composite' variable, such as upwelling, as a predictor within this, the most temporally comprehensive of the models.

Analysis of model performance at the default prediction-point (0.500) is useful, because it allows for an even comparison of predictive success under equalizing but unrealistic assumptions that: (1) blooms are evenly distributed throughout the year and (2) blooms are expected to occur with as much frequency as non-bloom conditions. As shown in Table 4, the development of seasonal models significantly enhanced pre-

dictive ability: the rate at which blooms were successfully predicted was 16% (spring model) and 19% (fall-winter model) greater than for the annual model. The rates of false positive prediction were slightly improved in the seasonal models. The rates of false negative prediction were more unequal among the models, and ranged most significantly between the two seasonal models.

Model performance at optimized prediction-points is summarized in Table 4; the fall-winter model demonstrated the highest rates of case prediction, followed by the annual and spring models, respectively. As with the default prediction-point, the rates of false negative prediction are most disparate among the seasonal models. The rates of false positive prediction are lowest for the seasonal models, but are increased overall with the implementation of the optimized prediction-points. The relatively high rates of false positive prediction result from a relatively low frequency of non-bloom predictions, which is an artifact of prediction-point optimization.

All of the models were assessed for predictive performance with unknown (future) cases by jackknife validation (Table 5). At the model-optimized prediction-points (Table 5), the rates at which blooms are successfully predicted are more comparable between the spring and annual models, and highest in the fall-winter model. Each model significantly out-performed a null model, improving bloom prediction by as much as 80%. This advantage does not extend to the prediction of non-bloom cases. The discrepancy in bloom versus non-bloom predictive improvement is a result of the model development, which focused on prediction of blooms. The Pearson's chi-squared test statistic for each model indicates extreme significance in the association of modeled predictions and the true outcome of future cases.

The models were also assessed by jackknife cross-validation under conditions simulating the application of 'user-adjusted' prediction-points. In Table 5, the application of 'low' prediction-points set by historical priors provides a demonstration of model performance in a period when future blooms occur with unexpectedly high frequency. The apparently conservative response is in part an artifact of logistic regression: logistic models generally guard against the misclassification of cases

Table 3. Model specifications and diagnostics for the logistic regression models presented in this study. The likelihood-ratio test is a test of the null hypothesis that the predictor variable coefficients are zero (i.e. have no predictive value), and can be evaluated for significance as a deviate chi-squared. McFadden's ρ^2 is a transformation of the likelihood-ratio statistic to mimic an R^2 statistic; values between 0.20 and 0.40 are considered very satisfactory (Hensher & Johnson 1981). The Nagelkerke's R^2 is based on both log likelihood and sample size. ROC, receiver operating characteristic

Predictor variables	Spring	Fall-Winter	Annual
	ln(silicic acid) ln(chl <i>a</i>) Temp	ln(silicic acid) ln(chl <i>a</i>) ln(Pajaro River) Nitrate	ln(silicic acid) ln(chl <i>a</i>) Temp Upwelling
N (total cases)	144	289	422
N (bloom cases)	40	27	64
ROC	0.848	0.943	0.860
Likelihood-ratio statistic	45.885	96.859	102.377
p-value	0.000	0.000	0.000
McFadden's ρ^2	0.270	0.540	0.285
Nagelkerke's R^2	0.394	0.616	0.376

Table 4. Prediction success and failure rates (%) at the default prediction-point of 0.500 and at model-specific optimized prediction-points. A modeled bloom probability higher than the prediction-point results in a bloom prediction. 'False negative' is the rate at which non-bloom predictions were incorrect. 'False positive' is the rate at which bloom conditions were predicted where none existed

	Spring	Fall-Winter	Annual
Default prediction-point			
Prediction-point	0.500	0.500	0.500
Blooms successfully predicted	60	63	44
Non-blooms successfully predicted	94	99	98
False negative	14	4	9
False positive	20	19	24
Model-optimized prediction-point			
Prediction-point	0.275	0.110	0.145
Blooms successfully predicted	75	89	77
Non-blooms successfully predicted	75	89	78
False negative	11	1	5
False positive	46	55	62

Table 5. Jackknife validation results for the logistic regression models at optimized prediction-points, where overall prediction error is minimized and at prediction-points equal to the priors of an independent California Department of Public Health (CDPH) bloom monitoring dataset. Improvement in bloom prediction is relative to the performance of a null model. Square brackets: negative scores

	Spring	Fall–Winter	Annual
Optimized prediction-points			
Prediction-point	0.275	0.110	0.145
Blooms successfully predicted (%)	75	89	77
Non-blooms successfully predicted (%)	76	89	77
False negative (%)	11	1	5
False positive (%)	45	55	62
Improvement in bloom prediction (%)	47	80	62
Improvement in non-bloom prediction (%)	4	[2]	[8]
Pearson's chi-squared (χ^2)	31.78	98.98	74.10
χ^2 p-value	0.000	0.000	0.000
CDPH priors prediction-points			
Prediction-point (priors)	0.101	0.066	0.081
Blooms successfully predicted (%)	98	93	91
Non-blooms successfully predicted (%)	42	82	60
False negative (%)	2	1	3
False positive (%)	61	65	71
Improvement in bloom prediction (%)	70	84	76
Improvement in non-bloom prediction (%)	[30]	[9]	[25]
Pearson's chi-squared (χ^2)	21.31	74.37	54.63
χ^2 p-value	0.000	0.000	0.000

belonging to the under-represented case group, a quality that makes them especially attractive for application in high-risk predictive contexts such as environmental regulation and clinical health (Fan & Wang 1998). The use of the CDPH priors is therefore an appropriate but conservative approach, increasing the probability of correctly identifying blooms ($\geq 91\%$ for all models), while reducing rates of false negative prediction ($\geq 3\%$ for all models), but at a cost to non-bloom prediction.

DISCUSSION

Model application: prediction-point adjustment

We sought to develop and deliver robust predictive models of toxigenic *Pseudo-nitzschia* blooms that were straightforward in their application. Further, we hoped to lay a framework for future modeling studies and independent model application, since this is the first time logistic regression has been applied to *Pseudo-nitzschia* bloom prediction. Providing these models with predetermined, optimized prediction-points satisfies the former; application of the models without end-user adjustment provides a statistically robust method for bloom prediction. Optioning how, and when, the optimized prediction-points can be adjusted satisfies

the latter; the ability to modify the prediction-points grants an opportunity to consider and integrate local bloom ecology, specifically frequency, within the model design.

Statistical models should be developed and implemented while remaining mindful of the system under investigation. In particular, the model should be developed and implemented with consideration of: (1) the general frequency at which blooms occur (the priors), (2) the prediction error rates that are inherent to the model, and (3) the cost of prediction error to the model user. The first of these is taken into account by the designation of an optimized prediction-point. Consideration of Points 2 and 3 is left to the discretion of the model user, since it is only necessary when the risk of a *specific type* of predictive error, rather than *overall* predictive error, needs to be reduced.

Use of a shifted prediction-point, rather than the default prediction-point, should be implemented whenever the probabilities of the 2 outcomes are significantly unequal (Neter et al. 1989). At present, blooms of *Pseudo-nitzschia* are relatively rare occurrences (Fig. 1). Because the probability of a bloom is generally not near 50%, a default prediction-point of 0.500 cannot provide optimized predictive capability. By the same reasoning, if a system generally demonstrates priors that are overwhelmingly different from our assumptions, the prediction-point can be reduced (inflated) to account for the more infrequent (frequent) occurrence, and therefore likelihood, of blooms. Similarly, if the cost of a certain type of incorrect prediction (false positive or false negative) is disproportionately high, the prediction-point can be adjusted to protect from that exaggerated cost. Fig. 2 may be used as a guide for balancing the probability of these errors and controlling their relative costs.

Shifting a prediction-point affects the predictive behavior of the model, always forcing compromise; Fig. 4 illustrates the trade-off between minimizing the number of blooms that the model fails to predict and minimizing the number of non-blooms that are identified as blooms. Reducing the prediction-point minimizes overall failure to predict a bloom by relaxing the criteria for bloom prediction. Conversely, increasing the prediction-point means that the criteria for bloom prediction are more strenuous, and blooms will be forecasted only when they are extraordinarily likely to occur.

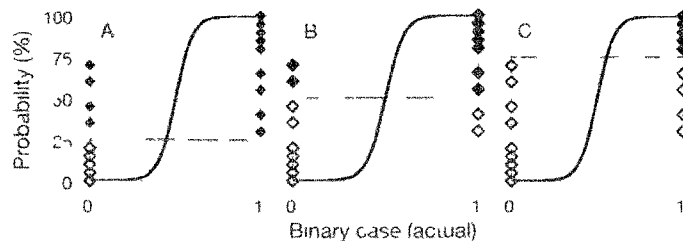


Fig. 4. A schematic diagram of a logistic regression with prediction points of 0.250 (A), 0.500 (B), or 0.750 (C). Cases lying on the 0 vertical axis are actual non bloom cases, cases lying on the 1 vertical axis are actual bloom cases. Filled symbols are predicted as blooms, open symbols are predicted as non blooms. Reducing the prediction point increases the number of cases that are predicted as blooms overall, maximizing the percent of actual blooms that are successfully predicted but reducing the percent of actual non blooms that are successfully predicted (A). Increasing the predictor point has the opposite effect (C).

Comparative model performance

In Table 6 we present the predictive performance of our annual and seasonal models compared to those of (1) a chl *a* anomaly (2) linear hindcasting models developed for *Pseudo nitzschia* blooms in the Santa Barbara Channel (Anderson et al. 2009) and (3) logistic regression models developed for pDA from a combination of field and experimental data (Blum et al. 2006).

Our logistic regression models were developed from the largest dataset to date and demonstrate a relatively high level of predictive capacity. Our models outperform the chl *a* anomaly model throughout the year and on a seasonal basis, although the predictive capacity of the chl *a* anomaly model was surprisingly comparable during the spring model period. Interestingly, the chl *a* anomaly model completely failed to predict blooms during the fall–winter model period. We suggest that dinoflagellate blooms, particularly common in Monterey Bay in the fall–winter model period, mask blooms of *Pseudo nitzschia* otherwise identified by the chl *a* anomaly. Conversely, the chl *a* anomaly works well in the spring model period when *Pseudo nitzschia* is more likely to be the dominant bloom organism. It should be noted that the chl *a* anomaly model is advantageous in that it is generally applicable to all potential HABs, particularly red tides (e.g. Kudela et al. 2008b; Ryan et al. 2008) and may therefore be a better model choice when not applied specifically for *Pseudo nitzschia* bloom prediction.

Table 6. Performance comparisons (%) among the annual and seasonal models developed in the present study and in previous *Pseudo nitzschia* modeling publications. Sensitivity is the rate at which the binary value 1 cases (blooms or high toxicity) were successfully predicted. Specificity is the rate at which the binary value 0 cases (non blooms or low toxicity) were successfully predicted. Improvement in bloom prediction is relative to the performance of a null model. Square brackets, negative scores.

Dependent variable	Toxicogenic <i>Pseudo nitzschia</i> bloom ^a	<i>Pseudo nitzschia</i> toxicity ^b	Coccolithic <i>Pseudo nitzschia</i> bloom	Toxicogenic <i>Pseudo nitzschia</i> bloom ^c
Annual				
Sensitivity	77	77	75	39
Specificity	78	75	93	72
False negative	5		25	5
False positive	62		7	88
Improvement in bloom prediction	61			31
N	422	139	75	182
Spring				
Sensitivity	75			50
Specificity	75			62
False negative	11			10
False positive	46			71
Improvement in bloom prediction	47			35
N	144			65
Fall–Winter				
Sensitivity	89			0
Specificity	89			77
False negative	1			3
False positive	55			100
Improvement in bloom prediction	80			(2.6)
N	289			117

^aPresent study

^bBlum et al. (2006)

Anderson et al. (2009)

^cStudy of chl *a* anomaly (present study)

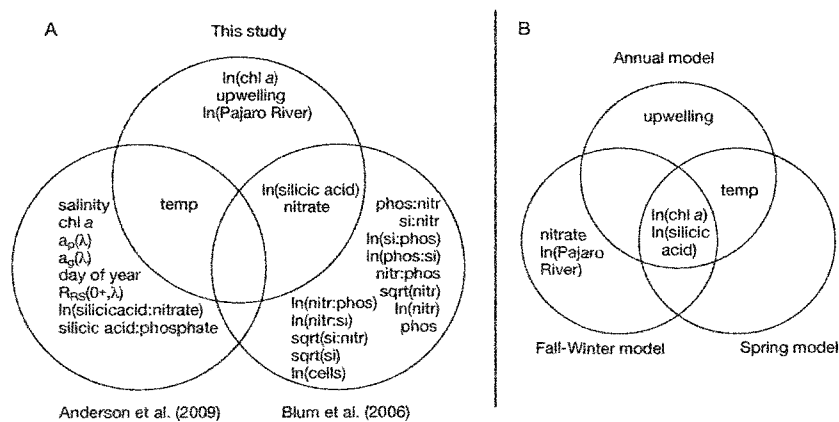


Fig. 5. Venn diagrams illustrating the shared and unique variables included in models of *Pseudo-nitzschia* ecophysiology shown within the present study, Anderson et al. (2009), and Blum et al. (2006) (A) and included in the annual, spring, and fall–winter models (B). Nutrient abbreviations for Blum et al. (2006) are as follows—phos: phosphate; si: silicic acid; nitr: nitrate. Variable abbreviations used in Anderson et al. (2009) are as follows— $a_p(\lambda)$: particulate absorption [412–665 nm]; $a_g(\lambda)$: CDOM absorption [412–665 nm]; $R_{rs}(0+\lambda)$: remote-sensing reflectance [412–665 nm]. 'Sqrt': square-root operation

Inter-study patterning: recurrent predictor variables

Fig. 5A illustrates the predictor variables that are shared and not shared between the models developed by Blum et al. (2006), Anderson et al. (in press), and in the present study. While the regions of interest and, in some cases, the dependent variable differ between these studies, the similarities and differences shared between the models can provide insight into universal patterns of *Pseudo-nitzschia* ecophysiology and, in turn, indicate which variables may be fundamental to future monitoring and modeling.

Seawater temperature was identified as a significant predictor whenever it was included in a study for evaluation. In all cases, a negative relationship was demonstrated between temperature and the dependent variable. Cold surface temperatures are often associated with upwelling, one of the processes previously identified as a causative factor of *Pseudo-nitzschia* blooms. The direct assessment of the upwelling index was unique to the present study; where it emerged as a predictor variable, it had a weak positive association with *Pseudo-nitzschia* bloom incidence.

Silicic acid (ln-transformed) and nitrate both emerged as predictors in models developed for *Pseudo-nitzschia* toxicity (Blum et al. 2006) and in the models developed here. In both studies, the patterns agree: association with the dependent variable is negative for silicic acid and positive for nitrate. While neither variable emerged as an individual predictor in the models developed by Anderson et al. (2009), a negative relationship was demonstrated between the silicic acid to

nitrate ratio and blooms of *Pseudo-nitzschia*, indicating a possibly confounded negative and positive relationship between blooms and silicic acid and nitrate, respectively.

Additional recurrent patterns are suggested by variables that are related, but not explicitly shared, between the studies. Anderson et al. (2009) chose not to evaluate river discharge as a model variable, but presented a *Pseudo-nitzschia* bloom model and a cellular toxicity model that included particle absorption and absorption of chromophoric dissolved organic matter (CDOM), variables which are associated with significant recent river discharge events (Warrick et al. 2004, 2007). In both models, high particulate absorption was negatively associated with the dependent variable, suggesting a direct negative relationship between high river discharge and *Pseudo-nitzschia* blooms. Our fall–winter model, which addresses the time period in which 'first flush' and high discharge events generally occur, also demonstrates a direct negative relationship between river discharge and bloom incidence. The consideration of seasonality when modeling river discharge and blooms and the patterning of blooms and high discharge events through time reveal complexity in this relationship, as discussed in the next subsection.

Infra-study (seasonal) patterning: ecological context and implications

The predictor variables shared and not shared between the annual, spring, and fall–winter models

are presented in Fig 5B effectively zooming in on the modeled relationships with a lens of added dimension and ecological context. The 2 most similar models are the annual and spring models; this is not entirely surprising given that the majority of *Pseudo nitzschia* blooms occur in the springtime (Fig 1). Upwelling is the only predictor unique to the annual model; its omission from the spring model may arise from a general predominance of upwelling throughout the spring model period. The independent variables in the spring model exhibited particular propensity for covariation. It is would further suggest that *Pseudo nitzschia* bloom dynamics in Monterey Bay are largely dominated by a specific environmental forcing: the upwelling over the spring model period.

The fall-winter model includes oceanic periods that are not fully defined, generally dominated by upwelling processes. All of the models including the fall-winter model demonstrate that conditions of low silicic acid and concurrently high chl *a* are associated with blooms of toxic *Pseudo nitzschia* in Monterey Bay. The fall-winter model however includes 2 unique predictor variables: nitrate (positive coefficient) and Pajaro River discharge (negative coefficient). The inclusion of nitrate in the fall-winter model suggests that the macronutrient control observed by Anderson et al (2009) specifically the negative relationship between *Pseudo nitzschia* blooms and the ratio of silicic acid to nitrate may have been underscored by confounding seasonal relationships. Our results are therefore similar to those presented by Anderson et al (2009) but are either more specific due to the explicit assessment of seasonality or representative of a similar relationship more heavily impacted by eutrophication. Annual dissolved inorganic nitrate loading via terrestrial storm runoff is relatively low in the region addressed by Anderson et al (2009) however nitrate input via storm runoff can be significant during winter runoff events (McPherson et al 2007).

The association of fall-winter blooms with conditions of high nitrate suggests that a nitrate eutrophication process is uniquely significant during this period. Notably, the Pajaro River in Monterey Bay introduces disproportionately high nitrate loads (CLEAN 2006, 2007) on a strictly seasonal basis. In our dataset blooms within the fall-winter model period occurred during periods of minimal freshwater discharge while blooms within the spring model period occurred during periods of decreasing river discharge following a flush event (Fig 1). We also observed this pattern within the broader time series in which blooms are generally not associated with peak discharge events and occur either with the declining shoulder of a high river discharge event or with a period marked by minimal discharge (Fig 1; note that a 4 yr period of

relatively high discharge between 1994 and 1998 accompanies an absence of data (not necessarily an absence of blooms). As described by the models, river discharge through concentrated low flow periods and load events may provide a eutrophic source of nitrate conducive to seasonal bloom formation while allowing immediate bloom formation during periods of peak discharge.

Although not observed in the modeling dataset compiled here, one independent study recently reported a shift in toxin-producing species associated with an overall restructuring of the phytoplankton community for Monterey Bay (Jester et al 2009). Jester et al (2009) used a similar dataset to ours (Monterey Bay 2000 to 2006); the discrepancy in *Pseudo nitzschia* abundance observations between the datasets may be due to differences in spatial coverage. The shift in toxin-producing species was defined by a sharp decline in the incidence of toxic *Pseudo nitzschia* in the summer of 2004 which persisted until the end of the study in 2006. This period was marked by anomalously low upwelling conditions and anomalously

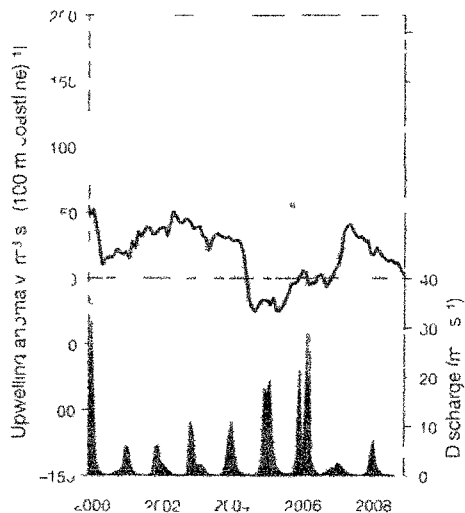


Fig 6 Monthly upwelling anomaly for 36 N 122 W (grey bars) with a 12 month moving average trendline (black line) and the monthly mean discharge to the Pajaro River (grey line) for the period from 2000 to 2008. An independent study addressing toxicogen *Pseudo nitzschia* abundance in Monterey Bay for the period from 2000 to 2006 identified the summer 2004 period as a harmful species shifting point (from *Pseudo nitzschia* to *Alexandrium* and *Dinophysis*) and showed the summers from 2004 through 2006 to be periods of severely decreased *Pseudo nitzschia* abundance (greyed area) (Jester et al 2009). This shifted period demonstrates relatively low upwelling and high river discharge activity.

high periods of river discharge (Fig. 6) conditions which our models identify as non conducive to toxicogenic *Pseudo nitzschia* blooms. Both of these conditions were alleviated in 2007, marked by a significant toxicogenic *Pseudo nitzschia* bloom event in Monterey Bay (Jester et al. 2009). A bloom of toxicogenic *Pseudo nitzschia* was also observed in 2008 (data not shown). According to the models and these observations, climatological conditions associated with low upwelling and high river discharge conditions may be conducive to suppressed toxicogenic *Pseudo nitzschia* bloom activity. The forecast of these conditions may now translate into the anticipation of large scale shifts, such as the shift in toxin producing species described by Jester et al. (2009).

Bloom modeling versus toxin modeling

The monitoring of domoic acid for public health purposes is carried out continually by the CDPH and focuses quite appropriately on the protection of human health from domoic acid intoxication. This monitoring effort is more accurately described as the monitoring of domoic acid bioaccumulation in sentinel shellfish supplies (*Mytilus californianus*). Modeling or monitoring efforts that are focused on toxin load alone, while useful and appropriate for regulatory purposes, obviously do not allow for the estimation or monitoring of *Pseudo nitzschia* blooms, which can be highly variable in their toxicity (Trainer et al. 2002; Marchetti et al. 2004; Anderson et al. 2006). This variability translates into a weak relationship between toxin bioaccumulation and toxicogenic *Pseudo nitzschia* abundance, evidenced here by CDPH/Cal PreEMPT project data compiled from study sites in northern central and southern California over a 3 yr time period (Fig. 7). Note that there were cases where extreme bloom concentrations of toxicogenic *Pseudo nitzschia* were associated with sub regulatory toxin levels (<20 $\mu\text{g g}^{-1}$), but no observed cases where sub bloom concentrations of toxicogenic *Pseudo nitzschia* were associated with toxin levels approaching the regulatory limit in shellfish. Logistic regression models developed for toxicogenic *Pseudo nitzschia* blooms can therefore be used for detection of both acute and sub acute toxic bloom events, while models developed for domoic acid alone will fail to address the injection of toxin into the system via sub acute bloom events. This is a significant failure inherent to all toxin models, since chronic or early life stage exposure to sub lethal levels of domoic acid are increasingly being recognized as an emerging threat to both human health and wildlife (Kreuder et al. 2005; Goldstein et al. 2008; Gratton et al. 2008; Ramsdell & Zabka 2008; M. Miller pers. comm.). By providing

estimations of all toxicogenic *Pseudo nitzschia* bloom events, whether low or high in toxicity, *Pseudo nitzschia* bloom models have the unique ability to address this emerging threat. Ideally, future models should be developed for both cell abundance (present study) and for toxin production (Blum et al. 2006; Anderson et al. 2009). While the domoic acid data associated with the cases used herein were insufficient for inclusion of a toxin component, a 2 step model would maximize both regulatory monitoring and our understanding of the ecophysiological conditions associated with toxin production.

CONCLUSIONS

The models presented here demonstrate toxicogenic *Pseudo nitzschia* bloom classification rates of $\geq 75\%$. These predictive success rates are comparable to or improved over those reported for previous models of toxicity and generic *Pseudo nitzschia* blooms. The assessment of our model alongside a cell abundance anomaly model, a useful tool designed for the detection of HABs, more generally demonstrates the capacity for improved predictive ability through more rigorous model development. Although we have reported the largest modeling dataset to date, consisting of 506 cases from 2002 to 2008, the removal of approximately 75% of the full dataset highlights the need for more consistent data collection. The parameters common to the 3

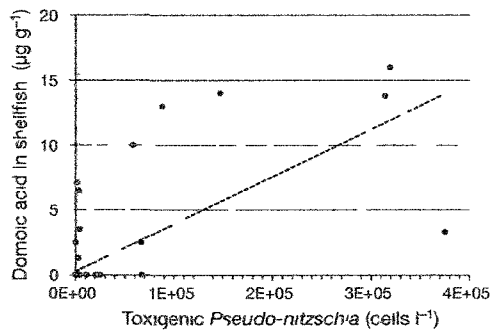


Fig. 7. Micrograms of domoic acid per gram shellfish plotted against counts of toxicogenic *Pseudo nitzschia*. Data are from study sites in northern central and southern California monitored from 2005 to 2007 by Cal PreEMPT in conjunction with the California Department of Public Health. Domoic acid never approached the regulatory limit of 20 $\mu\text{g domoic acid g}^{-1}$ shellfish when toxicogenic *Pseudo nitzschia* concentrations were at sub-bloom levels, i.e. <10,000 cells l^{-1} (shaded area), and only began to approach the regulatory limit at cell concentrations that were significantly higher than <10,000 cells l^{-1} . The dashed line shows the results of a linear regression for domoic acid toxicity versus cell abundance.

regional models developed for the west coast of the United States (Fig. 5A) provide direction for the design of ongoing and future HAB monitoring. We note that several parameters identified as being important (e.g. urea [Lioward et al. 2007, Kudela et al. 2008a], lithium [Subba Rao et al. 1998], ammonium [Trainer et al. 2007], iron and copper [Rue & Bruland 2001, Maldonado et al. 2002, Wells et al. 2005]) were not included for evaluation and could potentially further improve model prediction. All models included macronutrient variables as predictors of toxicogenic *Pseudo nitzschia* blooms, indicating the influence of upwelling and possibly cultural eutrophication on toxicogenic *Pseudo nitzschia* bloom proliferation. The seasonal significance of river discharge during periods associated with weak upwelling suggests that both natural (upwelling) and cultural (freshwater discharge) eutrophication processes and the timing and seasonality of these processes are significant factors influencing toxicogenic *Pseudo nitzschia* bloom dynamics. Although our models are specific to Monterey Bay, we have identified several factors common to all 3 modeling efforts for *Pseudo nitzschia*. Given appropriate validation data, we suggest that some variant of this reduced subset of environmental variables could be applied to other regions, particularly similar coastal upwelling systems where *Pseudo nitzschia* is prevalent (e.g. the west coast of the United States and Baja Mexico, the southern Benguela, and the Iberian peninsula; Bates et al. 1998, Kudela et al. 2005, Fawcett et al. 2007).

Acknowledgements. We thank P. L. Miller (University of California Santa Cruz, UCSC) and the CalPREEMPT team for contributing to the modeling dataset. We gratefully acknowledge the significant contribution made by M. W. Silver (UCSC) to the CIMT dataset and thank CIMT participants for their efforts. We thank G. J. Smith and K. Hayashi for their contribution to the MLML dataset. Special thanks to G. W. Langlois (CDPH) for providing shellfish toxicity data and an independent *Pseudo nitzschia* monitoring dataset. Three anonymous reviewers contributed significantly to the improvement of this manuscript. Partial funding was provided by NOAA MERHAB Award NA04NOS4780229 (CalPREEMPT), NOAA Award NA16OC2936 (CIMT) and as a fellowship (JQL) from an anonymous donor through the Center for the Dynamics and Evolution of the Land-Sea Interface (CDELSI). This contribution is part of the Global Ecology and Oceanography of Harmful Algal Blooms (GEOHAB) Core Research Project on Harmful Algal Blooms in Upwelling Systems and is MERHAB (Monitoring and Evert Response for Harmful Algal Blooms) Publication Number 70.

LITERATURE CITED

Addison RF, Stewart JE (1989) Domoic acid and the eastern Canadian mussel shellfish industry. *Aquaculture* 77: 263-269
 Allen I, Smyth T, Siddorn J, Holt M (2008) How well can we forecast high biomass algal bloom events in a eutrophic

coastal sea? *Harmful Algae* 8:70-76
 Anderson DM, Gilbert PM, Burkholder JM (2002) Harmful algal blooms and eutrophication: nutrient sources, composition and consequences. *Estuaries* 25:704-726
 Anderson CR, Brzezinski MA, Washburn L, Kudela R (2006) Circulation and environmental conditions during a toxicogenic *Pseudo nitzschia* bloom in The Santa Barbara Channel, California. *Mar Ecol Prog Ser* 327:119-133
 Anderson CR, Siegel DA, Kudela RM, Brzezinski MA (2009) Empirical models of toxicogenic *Pseudo nitzschia* blooms: potential use as a remote detection tool in the Santa Barbara Channel. *Harmful Algae* 8:478-492
 Bates SS, Trainer VL (2006) The ecology of harmful diatoms. In: Graneli E, Turner J (eds) *Ecology of harmful algae*. Vol. 189. Springer Verlag Heidelberg, p.81-93
 Bates SS, Burd CJ, de Freitas ASW, Foxall RA and others (1989) Pennate diatom *Nitzschia pungens* as the primary source of domoic acid: a toxin in shellfish from eastern Prince Edward Island, Canada. *Can J Fish Aquat Sci* 46:1203-1215
 Bates SS, Garrison DL, Horner RA (1998) Bloom dynamics and physiology of domoic acid producing *Pseudo nitzschia* species. In: Anderson D, Cembella A, Hallegraeff G (eds) *Physiological ecology of harmful algal blooms*. Springer Verlag Heidelberg, p.267-292
 Beltran AS, Palafox Uribe M, Grayiles Montiel J, Cruz Villacorta A, Ochoa JL (1997) Sea bird mortality at Cabo San Lucas, Mexico: evidence that toxic diatom blooms are spreading. *Toxicon* 35:447-453
 Bird CJ, Wright JLC (1989) The shellfish toxin domoic acid. *World Aquac* 20:40-41
 Blouw AN, Anderson P, Estrada M, Johansen M and others (2006) The use of fuzzy logic for data analysis and modeling of European harmful algal blooms: results of the HABFS project. *Afr J Mar Sci* 28:365-369
 Plum I, Subba Rao DV, Pan Y, Swainathan S, Adams NG (2006) Development of statistical models for prediction of the neurotoxin domoic acid levels in the pennate diatom *Pseudo nitzschia pungens f. multiseries* utilizing data from cultures and natural blooms. In: Subba Rao DV (ed) *Algal cultures: analogues of blooms and applications*. Science Publishers, Enfield, NH, p.891-916
 Burk KR, Uttal Cooke L, Pilsbain CH, Roelke DL and others (1992) Autecology of the diatom *Pseudonitzschia australis*, a domoic acid producer from Monterey Bay, California. *Mar Ecol Prog Ser* 84:293-302
 CCLFAN (Central Coast Long Term Environmental Assessment Network) (2006) 2004-2005 annual report. Available at: www.cclean.org/ftp/CLEAN%20Final%2004-05.pdf
 CLEA (Central Coast Long Term Environmental Assessment Network) (2007) Program overview 2001-2006. Available at: www.cclean.org/ftp/CLEAN%2001-06%20Overview%20copy.pdf
 Fan X, Wang L (1996) Comparing linear discriminant function with logistic regression for the two group classification problem. Annual Meeting of the American Educational Research Association, San Diego, CA (April 13-17, 1996)
 Garcia A, Pardo CC, Borrad S, Corbeira A, Kudela RM (2007) Contrasting wind patterns and toxicogenic phytoplankton in the southern Benguela upwelling system. *Mar Ecol Prog Ser* 348:19-31
 Fehling J, Davidson K, Bolch C, Tett P (2006) Seasonality of *Pseudo nitzschia* spp. (Bacillanophyceae) in western Scottish waters. *Mar Ecol Prog Ser* 323:91-105
 Fisher WS, Malone FC, Gathina JD (2003) A pilot project to detect and forecast harmful algal blooms in the northern Gulf of Mexico. *Environ Monit Assess* 81:373-381

- Fritz L, Quilliam MA, Wright JC, Beal VM, Work TM (1992) An outbreak of domoic acid poisoning attributed to the pennate diatom *Pseudo-nitzschia australis*. *J Phycol* 28: 439–442
- Gilbert PM, Anderson DM, Centre IP, Craneh F, Scilner KG (2007) The global complex phenomena of harmful algal blooms. *Oceanogr Phy (Washington DC)* 18: 136–147
- Coldberg JD (2003) Domoic acid in the benthic food web of Monterey Bay, California. Master's thesis, California State University Monterey Bay, Monterey, CA
- Corduneanu T, Mazet JAK, Zabka TS, Lanquar G, and others (2008) Novel symptomatology and changing epidemiology of domoic acid toxicosis in California sea lions (*Zalophus californianus*) and increasing risk to marine mammal health. *Proc R Soc Lond B Biol Sci* 275: 257–276
- Crafton LM, Roberts S, Tian R, V. Poushey C, and others (2008) Domoic acid neurotoxicity in Native Americans in the Pacific Northwest: human health project methods and update. In: *Proc 4th Symp on Harmful Algal Blooms in the US*. US National Office for Harmful Algal Blooms
- Halvraeff GM (1993) A review of harmful algal blooms and their apparent global increase. *Phycologia* 32: 79–99
- Hensher DA, Johnson LW (1981) Applied discrete choice modeling. *Crmon Helm*, London
- Howard MA, Cochlan WP, Ladizinsky N, Kudrinskiy RM (2007) Nitrogenous preference of toxicogenic *Pseudo-nitzschia australis* (Bacillariophyceae) from field and laboratory experiments. *Harmful Algae* 3: 206–217
- Jester K, Lefebvre K, Langous C, Vigilant V, Baugh K, Silver MW (2009) A shift in the dominant toxin-producing algal species in central California during phytoplankton food webs. *Harmful Algae* 8: 291–298
- Johansen C, Stoknes E (2000) Monitoring of harmful algal blooms along the Norwegian coast using remote optical methods. *S Afr J Mar Sci* 22: 309–321
- Kirupel K, Bogren K (2001) Determination of orthopterosolones by flow injection analysis in seawater. *QuickChem Method* 31: 113–011 H. In: *Saline methods of analysis*. Lachat Instrument, Milwaukee, WI
- Kreuder C, Miller MA, Lowins J, Conrad PA, Carpenter TE, Jessup DA, Mazet JA (2005) Evaluation of cardiac lesions and risk factors associated with myocarditis and dilated cardiomyopathy in southern sea otters (*Enhydra lutris nereis*). *Am J Vet Res* 66: 289–299
- Kuljevac R, Pitcher G, Probyn T, Ferreira F, Mouta T, Trainer V (2005) Harmful algal blooms in coastal upwelling systems. *Oceanography (Washington DC)* 16: 184–197
- Kudela RM, Lane IQ, Cochlan WP (2008a) The potential role of anthropogenically derived nitrogen in the growth of harmful algal blooms in California, USA. *Harmful Algae* 8: 10–110
- Kudela RM, Ryan JP, Blakely MD, Lane IQ, Peterson TD (2008b) Linking the physiology and ecology of *Cochlo-dinium* to the underlying and harmful algal bloom events: a comparative approach. *Harmful Algae* 7: 278–292
- Lefebvre KA, Powell CL, Busma RM, Doerthe CJ, and others (1999) Detection of domoic acid in northern anchovies and California sea lions associated with an unusual mortality event. *Nat Toxins* 7: 83–92
- Lefebvre KA, Bargu S, Kikuchi T, Sive MV (2002a) From sandbars to blue whales: the pervasiveness of domoic acid. *Toxicol* 40: 971–977
- Lefebvre KA, Silvert MW, Coale SL, Tjeerdtina RS (2002b) Domoic acid in planktivorous fish in relation to toxic *Pseudo-nitzschia* cell densities. *Mar Biol* 40: 625–631
- Maldonado MT, Hughes MP, Rae EL, Wells ML (2002) The effect of Fe and Cu on growth and domoic acid production by *Pseudo-nitzschia multiseriens* and *Pseudo-nitzschia australis*. *Limnol Oceanogr* 47: 515–526
- Marchetti A, Trainer VL, Harrison PJ (2004) Environmental conditions and phytoplankton dynamics associated with *Pseudo-nitzschia* abundance and domoic acid in the Juan de Fuca eady. *Mar Ecol Prog Ser* 281: 1–12
- McCillicuddy JJ, Anderson D, Lynch D, Townsend D (2005) Mechanisms regulating large scale seasonal fluctuations in *Alevandrium lundveense* populations in the Gulf of Maine: results from a physical biological model. *Deep Sea Res* 52: 2698–2714
- McPhee Shaw EL, Seigel DA, Washburn L, Przeznanski MA, Jones JL, Lydecker A, Melack J (2007) Mechanisms for nutrient delivery to the inner shelf observations from the Santa Barbara Channel. *Limnol Oceanogr* 52: 1748–1766
- Menard S (1995) Applied logistic regression analysis. *Sage*, Thousand Oaks, CA
- Miller PE, Scholin CA (1999) Identification and enumeration of cultured and wild *Pseudo-nitzschia* (Bacillariophyceae) using species-specific LSU rRNA targeted fluorescent probes and filter-based whole cell hybridization. *J Phycol* 34: 371–382
- Neter J, Wasserman W, Kutner M (1989) Applied linear regression models. *Irwin*, Homewood, IL
- Pennington JT, Chavez FP (2000) Seasonal fluctuations of temperature, salinity, nitrate, chlorophyll and primary production at station H3/M1 over 1989–1996 in Monterey Bay, California. *Deep Sea Res* 47: 941–973
- Ramsdell JS, Zabka TS (2008) *In utero* domoic acid toxicity to fetal basis of adult disease in the California sea lion (*Zalophus californianus*). *Mar Drugs* 6: 262–290
- Rue E, Buland K (2001) Domoic acid binds to a specific protein: a possible role for the toxin produced by the marine diatom *Pseudo-nitzschia*. *Mar Chem* 76: 127–134
- Ryan JP, Govert JR, King SA, Bissett WP, and others (2008) A coastal ocean extreme bloom incubator. *Geophys Res Lett* 35: L126J2. doi:10.1029/2008GL034081
- Schiffeld O, Grzymalski T, Bissett WP, Kirkpatrick GJ, Miller DF, Molone MA, Roesler CS (1999) Optical monitoring and forecasting systems for harmful algal blooms: possibility of pipe dream? *J Phycol* 35: 1477–1496
- Schoen CA, Head F, Doucette CJ, Benson S, and others (2000) Mortality of sea lions along the central California coast linked to a toxic diatom bloom. *Nature* 403: 80–84
- Smith P, Bogren K (2001a) Determination of nitrate and/or nitrite in brackish seawater by flow injection analysis colorimeter. *QuickChem Method* 31: 107–041 E. In: *Saline methods of analysis*. Lachat Instruments, Milwaukee, WI
- Smith P, Bogren K (2001b) Determination of silicate in brackish or seawater by flow injection analysis colorimeter. *QuickChem Method* 31: 114–271 C. In: *Saline methods of analysis*. Lachat Instruments, Milwaukee, WI
- Stumpf R, Tomlinson M, Calkins J, Kirkpatrick B, and others (2009) Status assessment for an operational algal bloom forecast system. *J Mar Syst* 76: 151–161
- Subba Rao TS, Pan Y, Mukherjee K, and others (2002a) Prediction of domoic acid by *Pseudo-nitzschia multiseriens* Hasle affected by lithium. *PSZN I Mar Ecol* 19: 31–36
- Tomlinson MC, Stumpf RP, Ramnarayanan V, Truby EW, and others (2004) Evaluation of the use of SeaWiFS image for detecting *Karenia brevis* harmful algal blooms in the eastern Gulf of Mexico. *Remote Sens Environ* 91: 293–303
- Trainer VL, Adams NC, Bill BD, Anulacion BF, Wekell JC (1998) Concentration and dispersal of a *Pseudo-nitzschia*

- bloom in Penn Cove, Washington, USA. *Nat Toxins* 6: 113–126
- Trainer VL, Adams NG, Bill BD, Stehr CM and others (2000) Domoic acid production near California coastal upwelling zones. June 1998. *Limnol Oceanogr* 45: 1818–1833
- Trainer VL, Adams NG, Wekell JC (2001) Domoic acid producing *Pseudo-nitzschia* species off the U.S. west coast associated with toxication events. In Hallegraeff GM, Blackburn SI, Bolch CJ, Lewis RJ (eds) *Harmful algal blooms 2000*. Intergovernmental Oceanographic Commission of UNESCO, Paris, p 46–49
- Trainer VL, Hickey RM, Horner RA (2002) Biological and physical dynamics of domoic acid production off the Washington coast. *Limnol Oceanogr* 47: 1438–1446
- Trainer VL, Cochlan WP, Erickson A, Bill BD, Cox FH, Borcherdt JA, Lefebvre KA (2007) Recent domoic acid closures of shellfish harvest areas in Washington State inland waterways. *Harmful Algae* 6: 449–459
- Villac MC (1996) Synecology of the genus *Pseudo-nitzschia*. H. Petragallo from Monterey Bay, California, USA. PhD dissertation, Texas A&M University, College Station
- Walz PM (1995) *Pseudo-nitzschia* species and domoic acid in Monterey Bay, CA. PhD dissertation, University of California, Santa Cruz
- Walz PM, Garrison DL, Graham WM, Cathey MA, Tjeerdema RS, Silver MW (1994) Domoic acid-producing diatom blooms in the Monterey Bay, California, 1991–1993. *Nat Toxins* 2: 271–279
- Warrick JA, Mertes LAK, Siegel DA, Mackenzie C (2004) Estimating suspended sediment concentrations in turbid coastal waters of the Santa Barbara Channel with SeaWiFS. *Int J Remote Sens* 25: 1995–2002
- Warrick JA, DiGiacomo PM, Weisberg SB, Nezhin NP and others (2007) River plume patterns and dynamics within the Southern California Bight. *Cont Shelf Res* 27: 2427–2448
- Wells ML, Trick CG, Cochlan WP, Hughes MP, Trainer VL (2005) Domoic acid: the synergy of iron, copper, and the toxicity of diatoms. *Limnol Oceanogr* 50: 1908–1917
- Welschmeyer NA (1994) Fluorometric analysis of chlorophyll *a* in the presence of chlorophyll *b* and pheopigments. *Limnol Oceanogr* 39: 1985–1992
- Work TM, Beale AM, Fitz L, Quilham MA, Silver M, Buck K, Wright JLC (1993) Domoic acid intoxication of brown pelicans and cormorants in Santa Cruz, California. In Smayda TJ, Shimizu Y (eds) *Toxic phytoplankton blooms in the sea*. Elsevier Science Publication B.V., Amsterdam, p 643–650
- Wynne T, Stumpf R, Richardson A (2006) Discerning resuspended chlorophyll concentrations from ocean color satellite imagery. *Cont Shelf Res* 26: 2583–2597

Editorial responsibility: Matthias Seaman, Oldendorf/Luhe, Germany

Submitted September 25, 2008, Accepted March 5, 2009
 Proofs received from author(s) April 21, 2009

CHAPTER TWO

Assessment of river discharge as a source of nitrate-nitrogen to Monterey Bay,

California

Jenny E. Quay*¹, David M. Paradies², Karen R. Worcester³, Raphael M. Kudela¹

* Corresponding author

¹ Department of Ocean Sciences, University of California Santa Cruz
1156 High Street, Santa Cruz, California 95064
Email: JennyEQuay@gmail.com
Phone: (510) 684-8193, Fax: (831) 459-4882

² Bay Foundation of Morro Bay, 601 Embarcadero, Suite 11, Morro Bay, California
93442

³ Central Coast Water Quality Control Board, 895 Aerovista Place, Suite 101, San
Luis Obispo, California 93401

Abstract

Coastal regions within eastern boundary currents are generally considered to be ‘upwelling-dominated,’ promoting the assumption that, relative to upwelling, river contributions of nitrogen-nitrate (N_{NO_3}) to these systems are insignificant. We use 10 years of daily estimates to evaluate the relative contribution of river and upwelling N_{NO_3} loads introduced to Monterey Bay, an open embayment along the ‘upwelling-dominated’ California coastline. At low temporal resolutions upwelling does dominate the region in terms of N_{NO_3} loads, but is inconsistent at higher-resolution timescales of ecological relevance (days-to-weeks): river loading, compared to upwelling loading, can predominate with significant frequency (28% of days per year). We observe an onshore-offshore gradient in river influence even at low (annual) temporal resolution. Based on the Nitrogen Indicator for Coastal Eutrophication Potential (N-ICEP), river load trends indicate that eutrophication potential may become more severe and should be monitored at multiple temporal resolutions within a local and global context.

Keywords: eutrophication, rivers, coastal upwelling, nitrate, ICEP, California.

Introduction

Historically, freshwater nitrogen delivery to Monterey Bay CA, has been presumed to be negligible due to the much greater magnitude and spatial scale of nitrate introduction by wind-driven upwelling (Kudela and Chavez 2004), and many investigations of its hydrography either omit the consideration of fluvial impacts or determine them to be minor (Bolin and Abbott 1963; Breaker and Broenkow 1994; Olivieri and Chavez 2000; Pennington and Chavez 2000; Ramp et al. 2005; Rosenfeld et al. 1994; Shulman et al. 2010). Regional blooms of the toxigenic diatom *Pseudo-nitzschia*, however, have alternately been linked to river discharge and upwelling processes, suggesting that river discharge may influence the ecology of this region. A recently published model for toxigenic *Pseudo-nitzschia* blooms in Monterey Bay, California (Lane et al. 2009) reconciles these viewpoints through the consideration of seasonality: seasonal modeling identified Pajaro River discharge and nitrate concentration as significant predictors when upwelling is seasonally low (Bolin and Abbott 1963; Pennington and Chavez 2000). As described by the models, river discharge may provide a source of nitrogen conducive to seasonal bloom formation, while allaying immediate bloom formation during periods of peak discharge. This empirically-derived description indicates a relationship between river discharge events and bloom incidence that is biphasic: blooms are suppressed during high-discharge ('flush') events, but subsequently promoted by the high nitrate/declining discharge conditions which follow. The Pajaro River introduces disproportionately large nitrate loads on a highly seasonal basis, and is frequently

paired with nitrate in descriptions of changing regional water quality: nitrate concentration in the Pajaro River has risen from <0.1 mM in the 1950's to levels that regularly exceed the drinking-water standard of 0.714 mM in more recent years (Ruehl et al. 2007). As a result of this conditioning, the Pajaro and Salinas rivers and their vicinities are now designated as impaired for nitrate by the Clean Water Act [303 (d)]. The identification of river discharge as a seasonally significant factor in *Pseudo-nitzschia* bloom formation, and the recognition of substantially elevated nitrate concentrations in rivers such as the Pajaro and the Salinas, suggest that the historical perspectives on the relative significance (or insignificance) of freshwater nitrogen loading to the Monterey Bay system may be based on assumptions that no longer apply. The present study is in part a reevaluation of the temporal and spatial scales over which those assumptions may or may not be valid.

The previous empirical (statistical) model linking nitrate, wind-driven upwelling, and river discharge clearly did not account for all possible sources of nitrogen to Monterey Bay. We acknowledge the limitations introduced through our approach [e.g. we do not address N_{NO_3} input from sources such as advection, atmospheric deposition, internal tide flux, or nitrification (Mackey et al. 2010; Rosenfeld et al. 1994; Shea and Broenkow 1982; Wankel et al. 2007; Ward 2005)] but we emphasized the utility of a simple first-order comparison. This contribution provides a first-order assessment of whether the common approach that omits rivers as a component in complex model building or nutrient budgeting is inviolate, and is intended to provide a framework for evaluation. A comprehensive nutrient budget for Monterey Bay is

beyond the scope of this study. Similarly, while we index the eutrophication risk of Monterey Bay rivers according to their potential to promote new production of non-siliceous algae through nutrient delivery (a particularly relevant exercise in Monterey Bay, where dinoflagellate blooms occur with regularity), the investigation of how this potential may or may not be fulfilled is beyond the scope of this paper and is addressed elsewhere (Armstrong et al. 2007; Kudela and Chavez 2004; Kudela et al. 2004; Kudela et al. 2008a; Kudela and Peterson 2009; Kudela et al. 2008b; Ryan et al. 2008).

A comparison of annual nitrate loading by freshwater discharge versus upwelling has previously been described for the Santa Barbara Channel (Warrick et al. 2005). In that study, the authors recognized that “although [river nutrient] contributions are significantly less than upwelling inputs to the channel, they are highly pulsed and supply nutrients in significantly different proportions and at different times of the year compared to upwelling”. At the northern extreme of the California Current System (CCS), similar comparative studies of the Columbia River also describe river nitrate contributions that are relatively small, but indicate that “despite the relatively small contributions on a seasonal basis, the Columbia River can be important as a local source during periods of downwelling or weak upwelling winds” (Hickey and Banas 2008). While the significance of river nitrate supply and cultural eutrophication in non-upwelling coastal systems is well-documented (Billen and Garnier 2007; Bricker et al. 2007; Cloern 2001; Conley et al. 2009; Heisler et al. 2008; Howarth 2008; Howarth et al. 2000; Justic et al. 1995a; Justic et al. 1995b; Li et al. 2007;

Ludwig et al. 2009; Spruill and Bratton 2008; Turner and Rabalais 1991; Turner and Rabalais 1994), the Santa Barbara Channel and the Columbia River region provide unique examples of river/upwelling nitrate input comparisons from an upwelling-dominated system. These previous studies were constrained to river/upwelling load assessments at coarse (annual or seasonal) temporal resolution; nonetheless, these comparisons either suggest or demonstrate the significance of temporality as opposed to load magnitude alone. Here we present the first comparative study of river nitrate supply relative to that of upwelling at a temporal resolution greater than seasonal, and the first comparative study from the central region of the CCS.

We compare annual, monthly and daily nitrate-nitrogen (N_{NO_3}) loads introduced to Monterey Bay by rivers and by wind-driven upwelling over a 10 y period (Jan 2000 – Aug 2009). We describe N_{NO_3} input to Monterey Bay by wind-driven upwelling using two methods to calculate the upwelling index (UI): (1) the Pacific Fisheries Environmental Laboratory (PFEL) UI for 36N 122W, based on the offshore component of Ekman transport (Bakun 1973), and (2) UI from wind velocities observed at the Monterey Bay Aquarium Research Institute (MBARI) M1 mooring, also using the offshore component of Ekman transport. We describe N_{NO_3} input to Monterey Bay by rivers according to load models developed for seven Central California Ambient Monitoring Program (CCAMP) Coastal Confluences monitoring sites within Monterey Bay (Figure 1), and compare our annual N_{NO_3} load estimates to those developed through a simpler modeling approach used by the Central Coast Long-term Environmental Assessment Network (CCLEAN). Upwelling N_{NO_3} loading

and river N_{NO_3} loading are compared through time to identify trends in loads across the 10 y period for which data are available. To understand and recognize the influence of river N_{NO_3} loading and upwelling N_{NO_3} loading across the marine receiving waters of Monterey Bay, we describe the general patterns of river and upwelling N_{NO_3} loading through a hydrological year (i.e. as annual climatologies), and compare them to analogous patterns of surface nitrate concentration at the Santa Cruz Municipal Wharf (SCMW), and at moorings M0 (8 km offshore), M1 (18 km offshore), and M2 (56 km offshore).

We further analyze two independent data sets to characterize nutrient source waters and nutrient receiving waters according to their nutrient stoichiometry. Nitrogen species omitted in our analysis include urea-nitrogen (N_{UREA}) and ammonium-nitrogen (N_{NH_4}). While the contribution of nitrogen as N_{UREA} and N_{NH_4} loading is generally less than the contribution of nitrogen as N_{NO_3} , the introduction of N_{UREA} and N_{NH_4} may have a disproportionate influence on harmful algal bloom (HAB) dynamics: recent studies indicate that *Pseudo-nitzschia* growth dynamics and toxicity vary according to N-substrate supplied for growth (Armstrong et al. 2007; Radan 2008). In recognition of their potentially differential impact, the stoichiometries for N_{UREA} and N_{NH_4} relative to N_{NO_3} are provided.

Lastly, Monterey Bay rivers are further characterized using the Nitrogen Indicator of Coastal Eutrophication Potential (N-ICEP) index, which summarizes in a single figure the relevant information provided both by the absolute and relative values of

the nitrogen and silica fluxes delivered by large river systems to identify systems susceptible to or impacted by eutrophication (Billen and Garnier 2007).

Materials and Methods

Estimation of daily N_{NO_3} loads: upwelling—Upwelling nitrate load was calculated by taking the product of an upwelling index (UI; vertical mass transport of upwelling source water per day) and the nitrate concentration of upwelling source water (estimated from daily average water temperature, described below). Both components of this approach [(1) the load calculation as a product of mass transport and nitrate concentration, and (2) the estimation of nitrate concentration from temperature] allow for derivation of upwelling nitrate supply or surface nitrate concentration, often for the approximation of new production (Chavez and Toggweiler 1995; Dugdale et al. 1989; Garside and Garside 1995; Kamykowski 1987; Kamykowski and Zentara 1986; Kudela and Chavez 2000; Kudela and Dugdale 1996; Messie et al. 2009; Olivieri 1996; Olivieri and Chavez 2000; Pennington et al. 2010; Toggweiler and Carson 1995). We use two independent time series of UI estimates to generate two (local and regional) estimates of N_{NO_3} upwelling loading to Monterey Bay. The first series of UI estimates were obtained from the National Oceanographic and Atmospheric Administration Pacific Fisheries Environmental Laboratory (PFEL; www.pfel.noaa.gov). The PFEL derives UI for 26 positions along the Eastern Pacific coast; the PFEL UI for 36N 122W (Figure 1) is readily available and represents variations in coastal upwelling for the Monterey Bay region. The

second series of UI estimates was calculated from wind vector data (using a MATLAB [Mathworks Inc.] script originally developed by L. Breaker) using daily averaged wind velocities at mooring M1 (<http://dods.mbari.org/lasOASIS>). As with the PFEL UI estimates, UI at M1 is an estimate of vertical mass transport derived from Ekman's theory of mass transport due to wind stress (Smith 1995). The derivations of PFEL UI and M1 UI differ, however, according to: (1) the location at which the UI is derived (PFEL UI is for an offshore region centered south of Monterey Bay while M1 is centrally located within Monterey Bay; Figure 1), and (2) the source of the wind stress data/estimates used for the calculation of Ekman transport (the PFEL UI is calculated from geostrophic wind stresses derived from surface atmospheric pressure fields provided by the U.S. Navy Fleet Numerical Meteorological and Oceanographic Center, while the M1 UI is calculated from observed winds at mooring M1).

The UI describes the quantity (mass) of source water being upwelled from depth; the delivery of nitrate load through this transport process is calculated by taking the product of UI (vertical mass transport) and the nitrate concentration of upwelling source water. This requires, then: (1) a definition of upwelling source (i.e. depth) in Monterey Bay, and (2) estimation of the nitrate concentration of the upwelling source water. In Monterey Bay and for the California Current System, the depth of upwelling source water has been described and validated elsewhere as 60 m (Kudela and Chavez 2000; Messie et al. 2009; Olivieri 1996). We use this approximation to satisfy the two requirements specified above, as follows: (1) the

characteristics of upwelling source water are those of water at 60 m depth, and (2) the nitrate concentration of upwelling source water ($[\text{NO}_3]$) can be estimated according to the 60 m temperature record from MBARI mooring M1 (<http://dods.mbari.org/lasOASIS>) and the following temperature-nitrate relationship, established previously from 6 y of M1 mooring data (Olivieri and Chavez 2000):

$$[\text{NO}_3] = 0.6075(T)^2 - 19.078(T) + 149.436$$

The product of a concentration (daily average nitrate in upwelling source water, estimated from source-water temperature measurements and an established temperature-nitrate relationship) and a flux (daily average vertical mass transport: UIs by PFEL and from observed wind stress at M1) is a load – here, daily average nitrate load according to regional and local upwelling indices.

Estimation of daily N_{NO_3} loads: rivers—All major stream and river discharges to the ocean from southern San Mateo County to Santa Barbara County have been monitored monthly since 2001 through CCAMP coastal confluences monitoring, characterizing the primary sources of freshwater discharge to the ocean in this area. Daily N_{NO_3} loads (and Si loads, where available for the purpose of N-ICEP calculations) were calculated by application of a CCAMP stream flow model to macronutrient concentrations at daily resolution for the following streams and rivers: San Lorenzo River, Soquel Creek, Aptos Creek, Pajaro River, Salinas River, Carmel

River, and Big Sur River (Figure 1). Salinas River N_{NO_3} load estimates include those introduced to Monterey Bay through the Moss Landing Harbor entrance.

The CCAMP stream flow model was developed to enhance stream flow information presented within the National Hydrography Dataset Plus (NHD+) geospatial framework (U.S. Environmental Protection Agency and the U.S. Geological Survey 2005) The CCAMP model uses Unit Runoff Model (UROM) estimates provided in the NHD+ geospatial framework to develop more spatially and temporally explicit estimates of flow (i.e. it describes flow at CCAMP Coastal Confluence monitoring sites at daily resolution). Unmodified, the NHD+ UROM model can provide annual average daily flows for each medium resolution hydrographic stream reach. The underlying NHD+ approach uses five United States Geological Survey (USGS) stream gages from the Hydro-Climatic Data Network (HCDN) within a 322 km (200 mile) radius as calibration gages to produce an estimation of average daily flows for each stream reach, accounting for upstream watershed area and other climatic and hydrologic features. The CCAMP stream flow model reconciles the following issues inherent in the NHD+ UROM model: (1) a spatial scale of 322 km is insufficient to resolve California hydrologic climate regimes, (2) anthropogenic influences on stream and river flows are beyond the scope of the NHD+ effort, (3) USGS gage network measurements provide high temporal data density and low spatial data density, while (4) stream transect method measurements provide low temporal data density, high accuracy and improved spatial density.

CCAMP enhancements to the NHD+ UROM model include selection of one to three USGS gages that more directly represent localized flow conditions at the site of interest. In some cases the gage may reside on the same stream system. Ratios are developed between gaged daily flow measurements and the UROM mean daily flow at each gage location, and if more than one gage is used these ratios are averaged. Mean daily flow ratios are then multiplied by the NHD+-derived annual mean daily flow at the discharge location of interest to estimate flow at that location and point in time. Gage choice is optimized by evaluating performance against CCAMP measured stream flows collected monthly along a ten-point cross section using a Marsh-McBirney conductive probe flow meter and setting rod. Modeled and observed flow estimates match closely (data not shown) and linear correlation of modeled and observed flow demonstrate an excellent model representation of observed flow variability ($R^2 > 0.94$ for the seven Coastal Confluence sites addressed in this study).

Monthly macronutrient data were collected by CCAMP in accordance with California State Board's Surface Water Ambient Monitoring Program Quality Assurance Program Plan (www.waterboards.ca.gov/water_issues/programs/swamp/). Depth-integrated samples are collected into 1 L plastic bottles from the center of the stream flow or thalweg and immediately placed in cold ice chests (4 °C) for transport to the analyzing laboratory (BC Laboratories, Inc.). Macronutrient concentration estimates were derived to daily resolution by linear interpolation of monthly measurements.

Error associated with linear interpolation of monthly macronutrient measurements was examined in more detail as part of the CCAMP monitoring program using high frequency nitrate concentration data from an in-situ ultraviolet spectrophotometer sensor, deployed by Monterey Bay Aquarium Research Institute through its Land Ocean Biogeochemical Observatory (LOBO) network. The L03 sensor is located at the lower end of the Old Salinas River in Moss Landing Harbor. This instrument collects nitrate readings continuously at an hourly interval and has been in operation since 1994. Its location in a tidal area presents additional sources of variability that would not be encountered were the sensor located in a non-tidal riverine environment. We adapted this data for use by selecting daily measurements collected at salinity low points. We extracted monthly interval measurements from this dataset and used the subset to create a daily linear interpolation of nitrate concentrations. Linear regression between the measured and interpolated daily concentrations produced a significant relationship ($p < 0.001$, $R^2 = 0.53$). When averaged daily interpolated concentrations were compared to averaged measured concentrations for the period of record, the interpolated values underestimated average concentrations by 3%. An additional round of validation was performed for the CCAMP N_{NO_3} daily load estimates using an independent data set (P3 Project, described below). This exercise allowed for validation of the CCAMP-modeled N_{NO_3} daily loads with N_{NO_3} loads calculated from direct measurement of macronutrients (UCSC) and discharge rates (USGS) and demonstrated high precision of CCAMP N_{NO_3} load estimation (RMSD = 10.7%, N = 100).

Non-CCAMP confluence monitoring and coastal sampling—River and creek samples were collected by volunteers and staff at the California Department of Fish and Game (CDFG) as part of the Pathogens Pollution Project (P3 Project). Sampling was conducted monthly (May 2007 – Sept 2008) at six CCAMP Coastal Confluences monitoring locations described previously (all except Aptos Creek), and from 2 additional sites (Waddell Creek and Scott Creek; Figure 1). Macronutrient grab samples were collected into acid-washed polyethylene terephthalate (PETE) bottles and transported to the analyzing laboratory (UCSC) in a cooler with blue ice. The grab samples were filtered upon arrival either by syringe-filtration (Whatman® 0.2 µm GD/X) or canister-filtration (Poretics® 0.6 µm polycarbonate membrane; <100mm Hg). Filtrates for ammonium and urea analyses were collected into 50 mL polypropylene (PP) centrifuge tubes (Corning®); previous tests have confirmed that these tubes are contaminant free for both urea and ammonium. Filtrates for macronutrient analysis [nitrate plus nitrite, silicic acid, and ortho-phosphate (hereafter referred to as phosphate)] were collected in 20 mL low-density polyethylene (LDPE) vials and stored frozen at -20 °C until analysis. Macronutrients were analyzed with a Lachat Quick Chem 8000 Flow Injection Analysis system using standard colorimetric techniques (Knepel and Bogren 2001; Smith and Bogren 2001a; Smith and Bogren 2001b). Ammonium samples were manually analyzed using a fluorescence method (Holmes et al. 1999). Urea samples were manually analyzed using the diacetylmonoxime thiosemicarbazide technique (Price and Harrison 1987) modified

to account for a longer time period and lower digestion temperature (Goeyens et al. 1998).

Shore-based macronutrient sampling was conducted weekly at SCMW (Figure 1) as part of the California Program for Regional Enhanced Monitoring for PhycoToxins (Cal-PReEMPT) project. Samples were collected from the surface with a PVC bucket (Jan – Aug 2006) or were mixtures of water samples collected from three discrete depths (0, 1.5 and 3 m) with a FieldMaster 1.75 L basic water bottle (Aug 2006 – Nov 2009). Offshore macronutrient sampling was conducted approximately monthly June 2002 – November 2007 at eleven stations throughout Monterey Bay as part of the Center for Integrated Marine Technology (CIMT) program. Ten-liter PVC Niskin bottles (refitted with silicone rubber band strings) mounted on an instrumented rosette were used to collect water from 0, 5, 10 and 25 m depth. At two of the stations surface (0 m) samples were collected using a PVC bucket. All Cal-PReEMPT and CIMT grab samples were processed and analyzed for macronutrients at UCSC as described for P3 Project macronutrient samples. For the development of nitrate-salinity mixing curves, CIMT cruises were categorized *a priori* according to concurrent Pajaro River discharge (USGS 11159000) as either (a) ‘high river flow’ (≥ 80 CFS), or (b) ‘ambient’.

Data used for the development of monthly climatologies of nearshore/offshore nitrate at three MBARI moorings (M0, M1, M2; Figure 1) were obtained from the LOBOViz 3.0 LOBO Network Data Visualization website, which is managed and maintained as a public data source by MBARI (www.mbari.org/lobo/loboviz).

Surface nitrate data were obtained at hourly resolution for the timeframes over which they were available [M0 (Aug 2004 – Jul 2009), M1 (Oct 2009 – Jun 2010), M2 (Jul 2002 – Jun 2010)].

River basin characterization per the Indicator for Coastal Eutrophication

Potential (ICEP) index—In addition to nutrient stoichiometries, we characterize the Pajaro and Salinas rivers according to their ICEP indices for nitrogen export. The ICEP index for nitrogen export (hereafter referred to as N-ICEP) is defined as

$$\text{N-ICEP} = [\text{NFlx} / (14 \times 16) - \text{SiFlx} / (28 \times 20)] \times 106 \times 12 \quad (1)$$

where NFlx and SiFlx are the mean specific fluxes of total nitrogen and dissolved silica (Si), respectively, delivered at the outlet of the river basin, expressed in kg N km⁻² d⁻¹ and kg Si km⁻² d⁻¹. The N-ICEP index is expressed in kg C km⁻² d⁻¹; the scaling of the index according to watershed area allows unbiased comparisons between large river systems (Billen and Garnier 2007). Si daily loads were available in the CCAMP data as a partial record (November 2007 – July 2009). The daily average N_{NO3} and Si loads were used for the calculation of monthly average N-ICEP. Annual N-ICEP for the Pajaro and Salinas Rivers are provided for hydrological years (July – June) 2004 and 2005 based on annual loads previously reported by CCLEAN (CCLEAN 2006; CCLEAN 2007) and from CCAMP load data for hydrological year 2008 (July 2008 – June 2009).

Results

N_{NO3} from rivers and upwelling: load comparison — N_{NO_3} loading into Monterey Bay by rivers and by wind-driven upwelling is shown in Figure 2 at annual (Figure 2A), monthly (Figure 2B), and daily (Figure 2C) resolution; N_{NO_3} loading statistics are presented in Table 1. River N_{NO_3} input from rivers is 2 orders-of-magnitude lower than N_{NO_3} input by wind-driven upwelling at lower (annual and monthly) temporal resolutions, timescales over which previous comparative analyses have been conducted (e.g. Warrick et al. 2005). The 2 orders-of-magnitude difference between river and upwelling N_{NO_3} input is not consistently observed at higher (daily and weekly) resolution (Figure 3), where N_{NO_3} input from rivers is maintained while N_{NO_3} input by wind-driven upwelling is relatively lower or zero during some winter months. These 2-4 week periods of comparatively higher river N_{NO_3} input coincide with periods of southerly winds and/or wind relaxation, when river flows and river N_{NO_3} input remain positive (river loading is switched ‘on’) while daily mean upwelling is essentially zero (loading by upwelling is switched ‘off’). The day-to-day recurrence of this circumstance throughout our 10 y time series is 28%; this statistic generally reflects the proportion of days for which daily mean upwelling was zero (or negative, in instances of downwelling). River input is generally not significant compared to upwelling N-loading when the analysis is constrained to days where upwelling wind stress is positive, and when only load magnitude (but not temporality) is considered (Table 1).

In addition to their constancy as a source of N_{NO_3} , rivers differ from upwelling in their annual loading character; the greater proportion of river N_{NO_3} load is introduced over relatively short periods during the rainy season, and the transformation of river N_{NO_3} loading into cumulative sum profiles across hydrological years demonstrates the ‘stepped’ character of river loading (Figure 4). Upwelling contributes most significantly towards its cumulative load total in the early and late periods of the hydrological year, when the percent contribution from rivers is relatively small. Conversely, plateaus in the upwelling annual cumulative load profiles coincide with periods of the year when rivers are contributing the bulk of their annual N_{NO_3} load, generally across the mid-point of the hydrological year (i.e. winter). The characteristics described for the cumulative sum N_{NO_3} loading profiles are consistent across years: the profiles in Figure 4B (cumulative sum, in percentage units) are similar for all years, even those which precede and follow years of relatively high absolute loading, e.g. 2004 and 2005 (Figure 4A).

Linear salinity-nitrate mixing curves developed for CIMT cruises categorized *a priori* according to concurrent river discharge as either (a) ‘high flow’ or (b) ‘ambient’ showed a reversal in the salinity-nitrate relationship according to river state, although linear correlations were not statistically significant. Under conditions of high river flow, the relationship between nitrate and salinity was inverse ($\alpha = -0.3047$), while during ‘ambient’ conditions the relationship was positive ($\alpha = 1.130$). Based on the ‘high-flow’ mixing curve developed from the regional cruise data, we would expect the freshwater endmember to Monterey Bay (i.e. the freshwater source

of nitrate) to have a nitrate concentration of 13.58 μM . This estimate agrees well with average nitrate concentrations of ‘typical’ Monterey Bay rivers (e.g. San Lorenzo: 16.45 μM , Scotts Creek: 7.16 μM) but is 1-2 orders of magnitude lower than the nitrate concentrations described by P3 Project data for the significant freshwater sources to Monterey Bay (i.e. the Pajaro and Salinas rivers), suggesting: (1) a conservative regression, and/or (2) under-representation of extreme-event conditions in the P3 dataset. Evaluation of the endmember concentration estimate should be performed with sensitivity to high-flow conditions, which were potentially missed by monthly P3 Project sampling but accounted for in the CCAMP flow models. The peak N_{NO_3} load from the Pajaro River, calculated according to the USGS annual peak streamflow (5,110 cfs; 05 April 2006) and our ‘high-flow’ freshwater endmember nitrate concentration estimate (13.58 μM) is lower but within an order-of-magnitude of the CCAMP load estimate (2,378 versus 13,749 kg N_{NO_3}). Both P3 and CCAMP data support the high-flow mixing curve regression, but suggest that the endmember concentration may be slightly underestimated (e.g. by rainwater dilution, spatial distribution of cruise sampling, etc.).

A significant correlation exists at the two moorings located furthest offshore (M1 and M2; Figure 5C-D) for monthly climatological surface nitrate concentrations and N_{NO_3} loading by upwelling; the correlations weaken and become statistically insignificant at the more inshore stations M0 and SCMW (Figure 5A-B). The correlation between river N_{NO_3} loading and surface nitrate is strongest at the most

inshore location, SCMW, and maintains statistical significance at the next most inshore station (M0), but is not significant at the offshore moorings (Figure 5E-H).

N_{NO3} from rivers and upwelling: trend comparison—Mann-Kendall trend analysis of N_{NO3} loading by rivers and by wind-driven upwelling revealed a difference in trends for the 10 y loading record used in this study. River N_{NO3} loading exhibited a positive (slope of 0.012) trend; upwelling loading trend was non-negative, but its slope was zero (Table 2). Trend results for upwelling N_{NO3} load estimates were the same whether the load estimates were based on UI at Monterey Bay mooring M1 (UI according to locally observed winds) or PFEL estimates for 36N 122W (UI according to wind stress derived from mean surface atmospheric pressure fields). The absence of a trend in upwelling N_{NO3} loading over the time-period addressed in our study (2001-2009) is consistent with observations of intra-annual oceanographic and climatic variability in Monterey Bay (e.g. phase changes, regime shifts) which would preclude monotonic trends, including (1) increased nitrate at 60 m from 1998-2005, with (2) increased water column stratification after 2003 and a concomitant reduction in near-surface nitrate (Chavez et al. 2006).

While our trend analysis for upwelling is an accounting of changes in its strength and potential (i.e. wind-stress, thermocline depth, etc.), our use of a static temperature-nitrate relationship, albeit with precedent, would prevent the identification of a trend caused by changes in source water mass (and its properties) for upwelling. Since our focus is riverine N_{NO3} loading (positive trend), failure would result in missing a (positive) trend in the upwelling N_{NO3} loading. According to two

parameters which are representative of the temperature-nitrate relationship, the Nitrate Depletion Temperature (NDT; (Kamykowski and Zentara 2003; Kamykowski et al. 2002) and the coefficient of the linear nitrate-temperature regression (α), calculated for each year from 2000 – 2010 from daily averages of temperature and nitrate at MBARI mooring M1 (Figure 1), there is a significant trend in the nitrate-temperature relationship across this period ($p < 0.05$), but one which would translate to decreasing N_{NO_3} loading (and a progressive over-estimation of upwelling N_{NO_3} loads) across the decade. According to our trend analysis and this preliminary evaluation of inter-annual variability in the temperature-nitrate relationship at M1, we find no evidence of a positive trend in upwelling N_{NO_3} loading. A negative trend, potentially masked by our use of a single nitrate-temperature across years, may in fact exist. Thus we conservatively identify a positive trend in river N_{NO_3} loading and no trend in upwelling loading. Given the relatively short (10 y) data set we do not discount the possibility that other trends would be evident in longer time series.

Differential loading: nutrient source stoichiometry—The Redfield-Brzezinski nutrient ratio, where C:N:Si:P = 106:16:15:1 (Brzezinski 1985; Redfield 1934), is commonly used for marine waters; in comparison, six of the eight fluvial sources would be enriched according to Si >> P > N (Table 3). The remaining 2 rivers, the Pajaro and Salinas, would be enriched according to N > Si > P with the Salinas demonstrating extreme nitrogen enrichment (N >> Si > P). All rivers are enriched with Si relative to P; this is especially pronounced in the 2 southernmost rivers (Carmel and Big Sur). The Salinas and the Pajaro Rivers have their outfalls in the

mid-Bay region, making them distinct from the other rivers in terms of both nutrient stoichiometry (as relatively nitrogen-enriched) and outfall locale (Figure 1). The prevalence of additional nitrogen species (N_{UREA} and N_{NH4} , collectively referred to as N_X) was also evaluated; for all rivers, N_{NO3} is the most prevalent of the 3 nitrogen species that were quantified (N_{NO3} , N_{UREA} , N_{NH4}).

The nutrient stoichiometry of Monterey Bay waters from shipboard sampling (0, 5, 10 and 25 m) shows relatively low surface N_{NO3} with values approaching the Redfield-Brzezinski ratio with increased depth (Table 3). Ratios of $N_{NO3}:N_X$ in surface waters measured throughout Monterey Bay are low compared to $N_{NO3}:N_X$ ratios of the major rivers (Pajaro and Salinas), and equivalent to $N_{NO3}:N_X$ ratios for the northernmost rivers (e.g. Waddell Creek). Nutrient stoichiometry in integrated water (0, 1.5, 3 m) from SCMW resembled that of Monterey Bay surface waters, but with relatively lower N_{NO3} for all ratios. Unlike rivers and offshore Monterey Bay, N_{NO3} was not the predominant nitrogen species at SCMW: N_{UREA} was generally 3-fold higher than N_{NO3} , while $N_{NO3}:N_{NH4}$ approached 1:1 (Table 3).

Eutrophication risk assessment—Monthly N-ICEP values for the Pajaro and Salinas rivers are shown in Figure 6. While there is clear variability in monthly N-ICEP, the Pajaro River was characterized by positive N-ICEP values from early- to mid-year (Jan – Aug 2008, Mar – Jul 2009) while N-ICEP for the Salinas River was significantly positive only for 2 months in early 2009 (February and March). Annual N-ICEP indices for the hydrological years 2004 and 2005 were positive for the Salinas River ($0.15 \text{ kg C km}^{-2} \text{ d}^{-1}$ in both years). These annual N-ICEP figures,

determined from annual loads reported by CCLEAN, are in agreement with the annual N-ICEP determined from CCAMP data for the hydrological year 2008 ($0.12 \text{ kg C km}^{-2} \text{ d}^{-1}$). Annual N-ICEP indices for the Pajaro River were consistently negative in the hydrological years 2004 and 2005, as determined from CCLEAN load data (-2.08 and -1.07 , respectively), and in the hydrological year 2008, as determined from CCAMP load data ($-0.05 \text{ kg C km}^{-2} \text{ d}^{-1}$).

Discussion

Riverine N_{NO_3} loading along an 'upwelling-dominated' coastline—While a comprehensive nutrient budget for Monterey Bay is beyond the scope of this study, we provide here a first-order comparison to assess whether the common approach that omits rivers as a component in complex model building or nutrient budgeting is inviolate. This study elucidates a competitive capacity; the significance of this within the context of a comprehensive regional nutrient budget is that said capacity has been proven against the nutrient source classically identified as dominant (i.e. wind-driven coastal upwelling).

N_{NO_3} load comparisons are available for the Columbia and Santa Clara rivers, near the northern and southern termini of the California Current System, respectively (Hickey and Banas 2008; Hickey et al. 2010; Warrick et al. 2005). These studies provide reference points from opposite ends of the California Current System in which Monterey Bay is centrally located, and from regions which differ significantly in hydrological setting and climate. The Columbia River is a significant source of

freshwater discharge, contributing 77% of the drainage along the west coast of the United States of America north of San Francisco (Barnes et al. 1972). Nitrate input by the Columbia River is an order-of-magnitude lower than nitrate input by coastal upwelling in the outfall region, but has been shown to maintain the ecosystem during periods when upwelling is depressed (Hickey and Banas 2008; Hickey et al. 2010; Kudela et al. 2010). To the south, the Santa Clara River drains a much smaller and drier watershed, but one which is heavily influenced by patterns of land-use (agricultural and urban). For this relatively dry system in the southern CCS, river nitrate input is 2-3 orders of magnitude lower than nitrate input by upwelling, but nutrient contributions from the river are regarded as significant due to differences in nutrient quality (i.e. Si:N:P for upwelled waters was 16:5:1; the same ratio for rivers was 13:10:1), and input timing.

Our evaluation of N_{NO_3} loading to Monterey Bay by rivers and by wind-driven upwelling confirms the significance of river N_{NO_3} load timing and indicates that temporality, and not simply magnitude, must be taken into consideration – even in a region identified as one that is dominated by coastal upwelling. Our comparison of river and upwelling N_{NO_3} loads on annual and monthly timescales affirms the classification of Monterey Bay as an upwelling-dominated region (the minimum differences between nitrate input from rivers and from upwelling were 2 orders of magnitude for annual and monthly timescales), but also affirms this classification as a generality. Most water quality monitoring programs cannot describe river nitrate loading on a daily basis, and the present study is the first to compare river and

upwelling nitrate inputs at sub-seasonal resolution. As such, this study is the first to describe nitrate inputs within a region of the CCS at the temporal resolution at which regional discharge and upwelling events are often defined (e.g. wind-relaxation events, ‘first flush’ discharge events) and relevance to phytoplankton response has been described by others (Malej et al. 1995; Small and Menzies 1981; Walsh et al. 1977). We note that only when our order-of-magnitude load comparison was conducted at this ecologically relevant temporal resolution (Beman et al. 2005) did the rate at which rivers exceed wind-driven upwelling as a nitrate source become apparent (28%; Figure 3). Similarly, the refined development of salinity-nitrate mixing curves from regional cruise data according to river flow status (‘high flow’ versus ‘ambient’) demonstrates: (1) regional riverine influence sufficient to cause a reversal in the salinity-nitrate mixing curve, i.e. a negative correlation between nitrate and salinity in Bay waters when river flow is high, and (2) further evidence for regional riverine N_{NO_3} source importance under high flow conditions, indicated by the similarity between average nitrate concentrations in ‘typical’ Monterey Bay rivers with the freshwater N_{NO_3} endmember concentration predicted by the ‘high flow’ salinity-nitrate mixing curve.

Onshore-to-offshore gradient in N_{NO_3} source climatology correlations—Our comparison of upwelling and river N_{NO_3} loading was designed to address N_{NO_3} loading for Monterey Bay. In our comparison, the refinement of temporal scale (annual to monthly to weekly/daily) identified periods when N_{NO_3} loads from rivers surpassed those introduced by upwelling across an entire region, while the

climatological comparisons from nearshore to offshore (Figure 5) provide some indication of the cross-shelf gradient. The development of surface nitrate climatologies at discrete locations spanning the onshore-to-offshore distance encompassed by Monterey Bay (SCMW, M0, M1, M2; Figure 1) indicates the predominance of river N_{NO_3} loading even on a broad temporal scale at discrete nearshore (but still ‘oceanographic’) observational locations. While there is strong correlation between the climatology of surface nitrate and the climatology of N_{NO_3} loading by upwelling at the offshore stations M1 and M2, the correlation becomes insignificant further inshore. Conversely, the correlation between the climatologies for surface nitrate and N_{NO_3} loading by rivers is strongest at the most inshore station (SCMW), and weakens with increasing distance offshore. These onshore/offshore correlation gradients for river N_{NO_3} loading and for N_{NO_3} loading by upwelling suggest that the relative significance of N_{NO_3} river loading cannot be ignored, even without regard to temporality, at inshore locations such as SCMW and M0. The relative importance of this loading suggests an enhanced capacity to influence algal growth and harmful algal bloom dynamics within the onshore coastal zone, nearest to coastal communities and economies (Anderson et al. 2008; Anderson et al. 2002; Glibert et al. 2005a; Glibert et al. 2005b; Howarth 2008; Kudela et al. 2006; Kudela et al. 2008a).

The southward advection of upwelling waters from an upwelling center immediately to the north of Monterey Bay has been observed during upwelling events (Ramp et al. 2009; Ramp et al. 2005; Rosenfeld et al. 1994), but this delivery requires

sustained winds of 10 m s^{-1} on the order of a week (Ramp et al. 2005). A recent publication synthesizing the results of two Autonomous Ocean Sampling Network (AOSN) field experiments described in one case (August 2006) a failure to simulate salinity and temperature fields (demonstrated successfully for August 2003) using a nested, data assimilating model supported by focused, high-resolution sampling of the upwelling center (Shulman et al. 2010). The model simulations in August 2006 overestimated surface and sub-surface salinity fields and were not improved through assimilation of glider data from the upwelling center to the north of the Bay. New consideration of minor, but evidently important, N_{NO_3} sources to Monterey Bay (Mackey et al. 2010; Wankel et al. 2007), have also demonstrated circumstances when these processes exert significant influence within an ‘upwelling dominated’ regime. Our correlation of surface N_{NO_3} climatologies to river and upwelling N_{NO_3} loading climatologies (Figure 5) indicates the predominance of river N_{NO_3} loading on a *broad temporal scale* at nearshore locations. Under circumstances of high river flow, we identify evidence of this predominance on a *broad spatial scale*: the development of salinity-nitrate mixing curves from regional cruise data according to river flow condition (‘high-flow’ versus ‘ambient’) demonstrates a sign reversal in the salinity-nitrate relationship (i.e. an inverse relationship between nitrate and salinity) during periods of high river flow.

Implications for water quality monitoring programs—While there are several ongoing water quality monitoring programs in the Monterey Bay region, the CCAMP dataset was used for this study because (1) it afforded estimates of river nitrate loads

at daily resolution, and (2) it had been generated from continual monitoring over the longest timespan (2000 – 2009). In these two respects, the CCAMP dataset is unique in its capacity to identify long-term trends in water quality, to estimate total river loads of pollutants to the ocean, and to provide benchmark data for flow model validation. Related but simpler modeling efforts utilizing CCAMP data have been employed in previous studies, including epidemiological evaluations of spatial risk to marine mammals (or their food items) of various land-based pathological diseases, based on animal location relative to freshwater outflows and other pollution sources (Miller et al. 2002; Miller et al. 2006; Miller et al. 2005; Stoddard et al. 2008). While a long-term, high resolution dataset was necessary for the primary purpose of this study (upwelling/river N_{NO_3} load comparison), it is useful to consider whether the higher precision modeling required to generate daily river load estimates is necessary for annual estimates of riverine N_{NO_3} loads. For the hydrological years 2004 and 2005, annual load estimates from six monitoring locations are available for comparison from CCAMP and CCLEAN [Aptos Creek (2005 only), San Lorenzo River, Soquel Creek, Pajaro River, Carmel River, Big Sur River (2004 only); Figure 1]. Across these sites, annual N_{NO_3} load estimates agreed in both years to within an order-of-magnitude. The largest discrepancies between the annual load estimates occurred for the rivers with relatively small drainage areas (Carmel River and Big Sur River in 2004; Aptos Creek and Soquel Creek in 2005); for all other rivers, the factor difference between CCLEAN and CCAMP annual load estimates ranged from < 1 to 3. In both 2004 and 2005, the CCLEAN estimates of total N_{NO_3} river load to

Monterey Bay were lower than the estimates from CCAMP, and this difference is not wholly unexpected: annual loads generated by CCLEAN were presumed to be underestimates since CCLEAN calculated daily loads from each monthly grab sample (from measured N_{NO_3} and NHD+ modeled discharge), averaged the daily loads across the hydrological year, and multiplied the average by the number of days in the hydrological year (365). While the approach taken by CCLEAN is simple and less time-intensive, the resulting annual load calculations were reported as “estimates, based on individual grab samples, (which) may underestimate actual loads because high loads associated with episodic storm events are not consistently sampled” (CCLEAN 2007). Since CCAMP annual load estimates are annual sums of daily loads, they have the potential to more precisely resolve N_{NO_3} loads introduced during episodic high-flow (‘flush’) events. Our comparison of CCAMP annual load estimates with those generated by CCLEAN suggests that the simpler approach (CCLEAN) is adequate for large-scale (Bay-wide, annual) estimates. Where higher precision is required, large-scale estimates generated by programs such as CCLEAN could be augmented with data provided by programs designed to characterize river contributions during episodic events (e.g. ‘First Flush’ monitoring, with the addition of flow measurement or estimation). The significance of local water quality data may be more effectively extended to the coastal environment if, either individually or in concert, water quality programs include the parameters required for calculation of N-ICEP (and the analogous index for phosphate, P-ICEP) on daily, weekly, monthly, and annual timescales.

Differential loading among Monterey Bay rivers—In most years, the annual N_{NO_3} loads introduced by the Pajaro and the Salinas rivers comprise >95% of total annual river N_{NO_3} load to Monterey Bay (Figure 7). While the relative contributions from the Pajaro and Salinas are consistently large, the relative contributions from each of the two rivers are variable. Within the 2001 – 2009 timeframe, 2005 and 2006 stand out as years of relatively high freshwater discharge: mean annual discharge from the Salinas River was an order-of-magnitude higher in 2005 – 2006 than across the other years (16.7 versus $1.7 \text{ m}^3 \text{ s}^{-1}$). In these high discharge years, the Salinas River dominated (Figure 7). Conversely, in years of low to moderate discharge, the Pajaro River tends to dominate. The unusually high contribution of N_{NO_3} from the Big Sur River in 2009 is unexplained, but presumed to be an artifact of severe wildfires that affected the region in the summer of 2008, and the drainage of burned landscape over the 2009 rainy season.

While we can illustrate disproportionate N_{NO_3} loading by the Pajaro and Salinas Rivers by comparing annual N_{NO_3} load contributions (Figure 7) and nutrient ratios (Table 3), the N-ICEP index provides added insight into the character of the Salinas and Pajaro River basins. The N-ICEP refers to the potential for new primary production (non-siliceous algae only) based upon the nutrient fluxes delivered by a river system. The N-ICEP represents the relevant information contained in both absolute and relative values of nitrogen and silica fluxes delivered by large river systems (Billen and Garnier 2007). The damming of rivers and reservoir construction (increased retention of biogenic silica), urbanization (increased discharge of low Si:N

wastewater) and agriculture (increased nitrogen, thereby decreasing Si:N) all promote positive N-ICEP values, while rivers draining pristine watersheds are rich in silica and low in nitrogen (Billen and Garnier 2007; Table 3, this study), resulting in negative N-ICEP values. Our analysis of N-ICEP is constrained to the Salinas and Pajaro rivers since (1) the ICEP is designed for relatively large-scale river systems, and (2) N_{NO_3} loading by the Pajaro and Salinas regularly contributes >95% of total river N_{NO_3} loading on a consistent basis (Figure 7). Although the N-ICEP indices of the 5 additional rivers included in the CCAMP dataset are unavoidably inflated in terms of absolute value (an artifact of inserting a small drainage area into the N-ICEP calculation), they trend strongly negative in the winter months and trend to less negative values through the remainder of the year. As expected, the most consistent and extreme negative N-ICEP indices are observed in rivers that drain relatively pristine watersheds (e.g. Big Sur River; data not shown).

The monthly N-ICEP figures reveal extended periods during which the Pajaro River is characterized by positive N-ICEP (e.g. Jan – Aug 2008, Figure 6) while on an annual basis (e.g. for the 2008 hydrological year) the Pajaro River was characterized by negative N-ICEP. As with our comparisons between N_{NO_3} loading from upwelling and from river discharge, considerable information is gained by comparing annual and monthly patterns. Billen and Garnier (2007) recommended calculation of the N-ICEP on varying timescales (daily, monthly, yearly) according to the surface area of the impacted coastal marine zone and the residence time of freshwater masses within it. Our monthly comparison of the Pajaro River and Salinas

River N-ICEP indexes is informative but necessarily limited, and the monitoring of Si and N should be adjusted (or implemented) within water quality assessment programs to afford the regular determination of N-ICEP at sub-annual resolution. A thorough evaluation of N-ICEP for Monterey Bay rivers requires more extensive collection of high-resolution Si and N_{NO_3} loading data than were available for this study, and future assessments should be undertaken across various temporal resolutions selected according to the question and conditions under consideration.

Broad implications—Our preliminary assessment of N-ICEP for Monterey Bay rivers identifies it as a useful index for the characterization of large rivers within the Monterey Bay region, one which allows comparison of Monterey Bay rivers to rivers from different climatic regions of the world now and into the future. A recent collection of N-ICEP values based upon measured (versus modeled) load data demonstrates a general association of positive N-ICEP for river basins draining to the Mediterranean Sea, Black Sea, Baltic Sea and the North Atlantic and negative N-ICEP for rivers draining to the North and South Pacific, South Atlantic, the Arctic, and the Indian Ocean (Garnier et al. 2010). Our identification of the Salinas River as consistently positive N-ICEP highlights the Salinas River as an exception to these general patterns. Worldwide, N-ICEP generally increases with population density, and shifts to a positive value in river basins with >30% agricultural land (Garnier et al. 2010). The Pajaro River N-ICEP appears to be shifting towards a positive value (-2.08, -1.07, and -0.05 kg C km⁻² d⁻¹ in 2004, 2005 and 2008, respectively), in agreement with previous observations of increasing agricultural activity and water

quality impairment within the watershed (Los Huertos et al. 2001; Ruehl et al. 2007). As the longest continual monitoring program addressing nutrient loading to central California coastal waters, the 10 y of CCAMP N_{NO_3} load data used for this study provided a unique opportunity to assess the presence of intra-decadal load trending. The positive trend identified in Monterey Bay river N_{NO_3} loads (CCAMP; 2000 – 2009), and the increasing N-ICEP values in the Pajaro River both suggest that N-ICEP values will continue trending positive in the absence of intervention. Industrialized countries in Europe and the United States have seen N-ICEP values stabilize or decrease as a result of nitrogen removal in wastewater treatment and increases in the efficiency of agricultural nitrogen use; positive trends for Monterey Bay river N-ICEP values suggest a trajectory more similar to areas such as the Japanese and Chinese Seas, Indian and South African coasts, where rapidly increasing agricultural production and fast urbanization have led to increased N-ICEP across a 30 year period (1970 – 2000; Garnier et al. 2010).

There is increasing scientific consensus that eutrophication plays a role in the development, persistence, and expansion of HABs in the United States and worldwide (Anderson et al. 2008; Heisler et al. 2008; Kudela et al. 2008a). More generally, regions that are not strongly influenced by riverine nutrient sources may exhibit strong responses by the phytoplankton community to relatively small changes in loading and stoichiometry; for example, the Washington and Oregon coast appear to be poised to shift from N-limitation to P or Si-limitation with very moderate increases in N-loading to the Columbia River (Kudela and Peterson 2009). This

susceptibility can be introduced or augmented by climatological events such as El Niño, when river outflows provide significant macronutrient loads to nutrient-deplete surface coastal waters (Castro et al. 2002; Wilkerson et al. 2002); these conditions can induce a significant phytoplankton response (Friederich et al. 2002; Kudela and Chavez 2004) and have been implicated in HAB conditions leading to mass wildlife mortality (Scholin et al. 2000). While toxigenic blooms of *Pseudo-nitzschia* in Monterey Bay are predominantly associated with upwelling conditions on an annual basis, the influence of river discharge becomes apparent on a seasonal basis (Lane et al. 2009). Our demonstration here of the predominance of river N_{NO_3} loading on short timescales (~28% of the time), the onshore-offshore gradient of its influence, and its upward temporal trend, indicate that rivers are exerting significant (and increasing) influence within a coastal upwelling system. Based on previous descriptions of the linkage between HABs and eutrophication (Anderson et al. 2008; Heisler et al. 2008; Kudela et al. 2008a; Lane et al. 2009), this influence, and its strengthening, should be expected to enhance the development, persistence and expansion of phytoplankton blooms, including HABs, in coastal waters of the present day and of the future.

Acknowledgements

We thank Dane Hardin (Applied Marine Sciences) and Marc Los Huertos (CSU Monterey Bay) for their guidance and suggestions. We appreciate the assistance of Gary Conley and Bridget Hoover (Monterey Bay National Marine Sanctuary), Melissa Blakely (UCSC), Larry Breaker (Moss Landing Marine Laboratories), and the staff and volunteers of the Pathogens Pollution (P3) Project and the Central Coast Ambient Monitoring Program (CCAMP). This manuscript was substantially improved by comments from Michael Jacox, Ryan Paerl, and two anonymous reviewers. Partial funding was provided as a Benjamin and Ruth Hammett Award for Research on Climate Change; a Science, Technology, Engineering, Policy and Society (STEPS) Institute Graduate Student Research Award; and a Center for the Dynamics and Evolution of the Land-Sea Interface (C.DELSI) Graduate Student Research Award. Additional funding was provided as a fellowship (JQL) from an anonymous donor through C.DELSI and from National Science Foundation project OCE-9912361 (RMK) and NOAA Awards NA04NOS4780239 and NA08NOS4730382. This contribution is part of the Global Ecology and Oceanography of Harmful Algal Blooms (GEOHAB) Core Research Project on Harmful Algal Blooms in Upwelling Systems, and is Monitoring and Event Response to Harmful Algal Blooms (MERHAB) Publication #XXX.

References

- Anderson, D. M. and others 2008. Harmful algal blooms and eutrophication: Examining linkages from selected coastal regions of the United States. *Harmful Algae* **8**: 39-53.
- Anderson, D. M., P. M. Glibert, and J. M. Burkholder. 2002. Harmful algal blooms and eutrophication: nutrient sources, composition, and consequences. *Estuaries* **25**: 704-726.
- Armstrong, M. D., W. P. Cochlan, N. Ladizinsky, and R. M. Kudela. 2007. Nitrogenous preference of toxigenic *Pseudo-nitzschia australis* (Bacillariophyceae) from field and laboratory experiments *Harmful Algae* **6**: 206-217.
- Bakun, A. 1973. Coastal upwelling indices, west coast of North America, 1946-71. NOAA Technical Report. United States Department of Commerce.
- Barnes, C. A., A. C. Duxbury, and B. A. Morse. 1972. Circulation and selected properties of the Columbia River effluent at sea, p. 41-80. *In* A. T. Pruter and D. L. Alverson [eds.], *The Columbia River Estuary and Adjacent Ocean Waters*. University of Washington Press.
- Beman, J. M., K. R. Arrigo, and P. A. Matson. 2005. Agricultural runoff fuels large phytoplankton blooms in vulnerable areas of the ocean. *Nature* **434**: 211-214.
- Billen, G., and J. Garnier. 2007. River basin nutrient delivery to the coastal sea: Assessing its potential to sustain new production of non-siliceous algae. *Mar Chem* **106**: 148-160.
- Bolin, R. L., and D. P. Abbott. 1963. Studies on the marine climate and phytoplankton of the central coastal area of California, 1954-1960, p. 23-45. *California Cooperative Oceanic Fisheries Investigations Report*. Hopkins Marine Station of Stanford University.
- Breaker, L. C., and W. W. Broenkow. 1994. The circulation of Monterey Bay and related processes. *Oceanography and Marine Biology* **32**: 1-64.
- Bricker, S. B. and others 2007. Effects of nutrient enrichment in the nation's estuaries: a decade of change. *Harmful Algae* **8**.
- Brzezinski, M. A. 1985. The Si:C:N ratio of marine diatoms: interspecific variability and the effect of some environmental variables. *J Phycol* **21**: 347-357.
- Castro, C. G. and others 2002. Nutrient variability during El Nino 1997-98 in the California current system off central California. *Prog Oceanogr* **54**: 171-184.
- CCLEAN. 2006. Central Coast Long-term Environmental Assessment Network (CCLEAN): annual report 2004-2005.
- . 2007. Central Coast Long-term Environmental Assessment Network (CCLEAN): regional monitoring program overview 2001-2006.
- Chavez, F. and others 2006. Seeing the future in a stratified sea. Monterey Bay Aquarium Research Institute 2006 annual report.
- Chavez, F. P., and J. R. Toggweiler. 1995. Physical estimates of global new production: the upwelling contribution. *In* C. P. Summerhayes, K. C. Emeis, M. V. Angel, R. L. Smith and B. Zeitzschel [eds.], *Upwelling in the Ocean: Modern Processes and Ancient Records*. J. Wiley and Sons.
- Cloern, J. E. 2001. Our evolving conceptual model of the coastal eutrophication problem. *Mar Ecol-Prog Ser* **210**: 223-253.
- Conley, D. J. and others 2009. Controlling eutrophication: nitrogen and phosphorus. *Science* **323**: 1014-1015.

- Dugdale, R. C., A. Morel, A. Bricaud, and F. P. Wilkerson. 1989. Modeling new production in upwelling centers: A case study of modeling new production from remotely sensed temperature and color. *Journal of Geophysical Research* **94**: 18119-18132.
- Friederich, G. E., P. M. Walz, M. G. Burczynski, and F. P. Chavez. 2002. Inorganic carbon in the central California upwelling system during the 1997-1999 El Nino-La Nina event. *Prog Oceanogr* **54**: 185-203.
- Garnier, J., A. Beusen, V. Thieu, G. Billen, and L. Bouwman. 2010. N:P:Si nutrient export ratios and ecological consequences in coastal seas evaluated by the ICEP approach. *Global Biogeochem Cy* **24**: -.
- Garside, C., and J. C. Garside. 1995. Euphotic-zone nutrient algorithms for the Nabe and EqPac study sites. *Deep-Sea Research Part II: Topical Studies in Oceanography* **42**: 335-347.
- Glibert, P. M., D. M. Anderson, P. Gentien, E. Granéli, and K. G. Sellner. 2005a. The global, complex phenomena of harmful algal blooms. *Oceanography* **18**: 136-147.
- Glibert, P. M. and others 2005b. The role of eutrophication in the global proliferation of harmful algal blooms: new perspectives and new approaches. *Oceanography* **18**: 198-209.
- Goeyens, L., N. Kindermans, M. A. Yusuf, and M. Elskens. 1998. A room temperature procedure for the manual determination of urea in seawater. *Estuarine, Coastal and Shelf Science* **47**: 415-418.
- Heisler, J. and others 2008. Eutrophication and harmful algal blooms: A scientific consensus. *Harmful Algae* **8**: 3-13.
- Hickey, B. M., and N. S. Banas. 2008. Why is the Northern End of the California Current System So Productive? *Oceanography* **21**: 90-107.
- Hickey, B. M. and others 2010. River Influences on Shelf Ecosystems: Introduction and synthesis. *J Geophys Res-Oceans* **115**: -.
- Holmes, R. M., A. Aminot, R. Kerouel, B. A. Hooker, and B. J. Peterson. 1999. A simple and precise method for measuring ammonium in marine and freshwater ecosystems. *Canadian Journal of Fisheries and Aquatic Sciences* **56**: 1801-1808.
- Howarth, R. W. 2008. Coastal nitrogen pollution: A review of sources and trends globally and regionally. *Harmful Algae* **8**: 14-20.
- Howarth, R. W. and others 2000. Nutrient pollution of coastal rivers, bays, and seas. *Issues in Ecology* **7**: 1-15.
- Justic, D., N. N. Rabalais, and R. E. Turner. 1995a. Stoichiometric Nutrient Balance and Origin of Coastal Eutrophication. *Mar Pollut Bull* **30**: 41-46.
- Justic, D., N. N. Rabalais, R. E. Turner, and Q. Dortch. 1995b. Changes in Nutrient Structure of River-Dominated Coastal Waters - Stoichiometric Nutrient Balance and Its Consequences. *Estuar Coast Shelf S* **40**: 339-356.
- Kamykowski, D. 1987. A Preliminary Biophysical Model of the Relationship between Temperature and Plant Nutrients in the Upper Ocean. *Deep-Sea Res* **34**: 1067-1079.
- Kamykowski, D., and S. J. Zentara. 1986. Predicting plant nutrient concentrations from temperature and sigma-T in the upper kilometer of the world ocean. *Deep-Sea Res* **33**: 89-105.
- . 2003. Can phytoplankton community structure be inferred from satellite-derived sea surface temperature anomalies calculated relative to nitrate depletion temperatures? *Remote Sens Environ* **86**: 444-457.

- Kamykowski, D., S. J. Zentara, J. M. Morrison, and A. C. Switzer. 2002. Dynamic global patterns of nitrate, phosphate, silicate, and iron availability and phytoplankton community composition from remote sensing data. *Global Biogeochem Cy* **16**: -.
- Knepel, K., and K. Bogren. 2001. Determination of orthophosphorous by flow injection analysis in seawaters: QuickChem Method 31-113-01-1-H. Saline Methods of Analysis. Lachat Instruments.
- Kudela, R., and F. Chavez. 2004. The impact of coastal runoff on ocean color during an El Niño year in Central California. *Deep-Sea Res Pt II* **51**: 1173-1185.
- Kudela, R., W. Cochlan, and A. Roberts. 2004. Spatial and temporal patterns of *Pseudo-nitzschia* species in central California related to regional oceanography *In* J. H. L. K.A. Steidinger, C.R. Tomas, and G.A. Vargo [ed.], *Harmful Algae 2002*. Florida Fish and Wildlife Conservation Commission, Florida Institute of Oceanography and Intergovernmental Oceanographic Commission of UNESCO, Paris.
- Kudela, R. M., and F. P. Chavez. 2000. Modeling the impact of the 1992 El Niño on new production in Monterey Bay, California. *Deep-Sea Research II* **47**: 1055-1076.
- Kudela, R. M., W. P. Cochlan, T. D. Peterson, and C. G. Trick. 2006. Impacts on phytoplankton biomass and productivity in the Pacific Northwest during the warm ocean conditions of 2005. *Geophys Res Lett* **33**.
- Kudela, R. M., and R. C. Dugdale. 1996. Estimation of new production from remotely-sensed data in a coastal upwelling regime. *Adv Space Res* **18**: 791-797.
- Kudela, R. M. and others 2010. Multiple trophic levels fueled by recirculation in the Columbia River plume. *Geophys Res Lett* **37**: -.
- Kudela, R. M., J. Q. Lane, and W. P. Cochlan. 2008a. The potential role of anthropogenically derived nitrogen in the growth of harmful algae in California, USA *Harmful Algae* **8**: 103-110.
- Kudela, R. M., and T. D. Peterson. 2009. Influence of a buoyant river plume on phytoplankton nutrient dynamics: What controls standing stocks and productivity? *J Geophys Res-Oceans* **114**: -.
- Kudela, R. M., J. P. Ryan, M. D. Blakely, J. Q. Lane, and T. D. Peterson. 2008b. Linking the physiology and ecology of *Cochlodinium* to better understand harmful algal bloom events: A comparative approach. *Harmful Algae* **7**: 278-292.
- Lane, J. Q., P. T. Raimondi, and R. M. Kudela. 2009. Development of a logistic regression model for the prediction of toxigenic *Pseudo-nitzschia* blooms in Monterey Bay, California. *Marine Ecology Progress Series* **383**: 37-51.
- Li, M. T., K. Q. Xu, M. Watanabe, and Z. Y. Chen. 2007. Long-term variations in dissolved silicate, nitrogen, and phosphorus flux from the Yangtze River into the East China Sea and impacts on estuarine ecosystem. *Estuar Coast Shelf S* **71**: 3-12.
- Los Huertos, M., L. E. Gentry, and C. Shennan. 2001. Land use and stream nitrogen concentrations in agricultural watersheds along the central coast of California. *ScientificWorldJournal* **1 Suppl 2**: 615-622.
- Ludwig, W., E. Dumont, M. Meybeck, and S. Heussner. 2009. River discharges of water and nutrients to the Mediterranean and Black Sea: Major drivers for ecosystem changes during past and future decades? *Prog Oceanogr* **80**: 199-217.
- Mackey, K. R. M. and others 2010. Influence of atmospheric nutrients on primary productivity in a coastal upwelling region. *Global Biogeochem Cy* **24**: -.
- Malej, A., P. Mozetic, V. Malacic, S. Terzic, and M. Ahel. 1995. Phytoplankton responses to freshwater inputs in a small semi-enclosed gulf (Gulf of Trieste, Adriatic Sea). *Marine Ecology Progress Series* **120**: 111-121.

- Messie, M., J. Ledesma, D. D. Kolber, R. P. Michisaki, D. G. Foley, and F. P. Chavez. 2009. Potential new production estimates in four eastern boundary upwelling ecosystems. *Prog Oceanogr* **83**: 151-158.
- Miller, M. A. and others 2002. Coastal freshwater runoff is a risk factor for *Toxoplasma gondii* infection of southern sea otters (*Enhydra lutris nereis*). *Int J Parasitol* **32**: 997-1006.
- Miller, W. A. and others 2006. *Salmonella* spp., *Vibrio* spp., *Clostridium perfringens*, and *Plesiomonas shigelloides* in marine and freshwater invertebrates from coastal California ecosystems. *Microb Ecol* **52**: 198-206.
- . 2005. New genotypes and factors associated with *Cryptosporidium* detection in mussels (*Mytilus* spp.) along the California coast. *Int J Parasitol* **35**: 1103-1113.
- Olivieri, R. A. 1996. Plankton dynamics and the fate of primary production in the coastal upwelling ecosystem of Monterey Bay, California. University of California Santa Cruz.
- Olivieri, R. A., and F. P. Chavez. 2000. A model of plankton dynamics for the coastal upwelling system of Monterey Bay. *Deep-Sea Research II* **47**: 1077-1106.
- Pennington, J. T., and F. P. Chavez. 2000. Seasonal fluctuations of temperature, salinity, nitrate, chlorophyll and primary production at station H3/M1 over 1989-1996 in Monterey Bay, California. *Deep-Sea Research II* **47**: 947-973.
- Pennington, J. T., G. E. Friederich, C. G. Castro, C. A. Collins, W. E. Wiley, and F. P. Chavez. 2010. The northern and central California coastal upwelling system. *In* K. Liu, L. Atkinson, R. Quiñones and L. Talaue-McManus [eds.], *Carbon and nutrient fluxes in continental margins*. Springer.
- Price, N. M., and P. J. Harrison. 1987. Comparison of Methods for the Analysis of Dissolved Urea in Seawater. *Mar Biol* **94**: 307-317.
- Radan, R. 2008. Nutrient uptake and toxicity of *Pseudo-nitzschia cuspidata*: a laboratory and field based experiment. San Francisco State University.
- Ramp, S. R. and others 2009. Preparing to predict: The Second Autonomous Ocean Sampling Network (AOSN-II) experiment in the Monterey Bay. *Deep-Sea Res Pt II* **56**: 68-86.
- Ramp, S. R., J. D. Paduan, I. Shulman, J. Kindle, F. L. Bahr, and F. Chavez. 2005. Observations of upwelling and relaxation events in the northern Monterey Bay during August 2000. *J Geophys Res-Oceans* **110**: -.
- Redfield, A. C. 1934. On the proportions of organic derivations in sea water and their relation to the composition of plankton, p. 177-192. *In* R. J. Daniel [ed.], *James Johnstone Memorial Volume*. University Press of Liverpool.
- Rosenfeld, L. K., F. B. Schwing, N. Garfield, and D. E. Tracy. 1994. Bifurcated flow from an upwelling center: a cold water source for Monterey Bay. *Cont Shelf Res* **14**: 931-964.
- Ruehl, C. R. and others 2007. Nitrate dynamics within the Pajaro River, a nutrient-rich, losing stream. *J N Am Benthol Soc* **26**: 191-206.
- Ryan, J. P. and others 2008. A coastal ocean extreme bloom incubator. *Geophys Res Lett* **35**.
- Scholin, C. A. and others 2000. Mortality of sea lions along the central California coast linked to a toxic diatom bloom. *Nature* **403**: 80-84.
- Shea, R. E., and W. W. Broenkow. 1982. The role of internal tides in the nutrient enrichment of Monterey Bay, California. *Estuarine, Coastal and Shelf Science* **15**: 57-66.
- Shulman, I., S. Anderson, C. Rowley, S. Derada, J. Doyle, and S. Ramp. 2010. Comparisons of upwelling and relaxation events in the Monterey Bay area. *J Geophys Res-Oceans* **115**: -.

- Small, L. F., and D. W. Menzies. 1981. Patterns of primary productivity and biomass in a coastal upwelling region. *Deep-Sea Research (a): Oceanographic Research Papers* **28**: 123-149.
- Smith, P., and K. Bogren. 2001a. Determination of nitrate and/or nitrite in brackish or seawater by flow injection analysis colorimeter: QuickChem method 31-107-04-1-E. *Saline Methods of Analysis*. Lachat Instruments.
- . 2001b. Determination of silicate in brackish or seawater by flow injection analysis colorimeter: QuickChem Method 31-114-27-1-C. *Saline Methods of Analysis*. Lachat Instruments.
- Smith, R. L. 1995. The physical processes of coastal ocean upwelling systems. *In* C. P. Summerhayes, K. C. Emeis, M. V. Angel, R. L. Smith and B. Zeitzschel [eds.], *Upwelling in the Ocean: Modern Processes and Ancient Records*. J. Wiley and Sons.
- Spruill, T. B., and J. F. Bratton. 2008. Estimation of groundwater and nutrient fluxes to the Neuse River estuary, North Carolina. *Estuar Coast* **31**: 501-520.
- Stoddard, R. A. and others 2008. Risk factors for infection with pathogenic and antimicrobial-resistant fecal bacteria in northern elephant seals in California. *Public Health Rep* **123**: 360-370.
- Toggweiler, J. R., and S. Carson. 1995. What are upwelling systems contributing to the ocean's carbon and nutrient budgets? *In* C. P. Summerhayes, K. C. Emeis, M. V. Angel, R. L. Smith and B. Zeitzschel [eds.], *Upwelling in the Ocean: Modern Processes and Ancient Records*. J. Wiley and Sons.
- Turner, R. E., and N. N. Rabalais. 1991. Changes in Mississippi River Water-Quality This Century. *Bioscience* **41**: 140-147.
- . 1994. Coastal Eutrophication near the Mississippi River Delta. *Nature* **368**: 619-621.
- U.S. Environmental Protection Agency and the U.S. Geological Survey. 2005. National Hydrography Dataset Plus - NHDPlus.
- Walsh, J. J., T. E. Whittedge, J. C. Kelley, S. A. Huntsman, and R. D. Pillsbury. 1977. Further transition-states of Baja California upwelling ecosystem. *Limnol Oceanogr* **22**: 264-280.
- Wankel, S. D., C. Kendall, J. T. Pennington, F. P. Chavez, and A. Paytan. 2007. Nitrification in the euphotic zone as evidenced by nitrate dual isotopic composition: Observations from Monterey Bay, California. *Global Biogeochem Cy* **21**: -.
- Ward, B. B. 2005. Temporal variability in nitrification rates and related biogeochemical factors in Monterey Bay, California, USA. *Marine Ecology Progress Series* **292**: 97-109.
- Warrick, J. A., L. Washburn, M. A. Brzezinski, and D. A. Siegel. 2005. Nutrient contributions to the Santa Barbara Channel, California, from the ephemeral Santa Clara River. *Estuarine, Coastal and Shelf Science* **62**: 559-574.
- Wilkerson, F. P., R. C. Dugdale, A. Marchi, and C. A. Collins. 2002. Hydrography, nutrients and chlorophyll during El Nino and La Nina 1997-99 winters in the Gulf of the Farallones, California. *Prog Oceanogr* **54**: 293-310.

Table 1. Comparative statistics for nitrogen as nitrate (N_{NO_3}) loading by rivers monitored as part of the Central Coast Ambient Monitoring Program (CCAMP; Coastal Confluences) and by wind-driven upwelling according to observed daily mean winds at Monterey Bay mooring M1 (36.75N 122.03W) and according to daily mean upwelling index (UI) estimates issued by the Pacific Fisheries Environmental Laboratory (PFEL) for 36N 122W.

	Rivers (CCAMP)	Upwelling (M1 / PFEL)
Average N_{NO_3} load ($\times 10^9$ kg y^{-1})	0.001	0.3 / 0.7
Days of positive N_{NO_3} load	100%	73% / 87%
Days (river load > UI load)	28%	-- / --
Days (river load > UI load); UI > 0	1%	-- / --
Mean relative contribution (% y^{-1})	0.4 (range: 0.1–1.3)	>99 / --

Table 2. Sen's slope estimates from Mann-Kendall trend analysis of 10 y (01 Jan 2000 through 06 Aug 2009) of daily nitrogen loadings (nitrogen as nitrate; kg) to Monterey Bay by rivers monitored as part of the Central Coast Ambient Monitoring Program (CCAMP; Coastal Confluences), and by wind-driven upwelling according to observed daily mean winds at Monterey Bay mooring M1 (36.75N 122.03W) and according to daily mean upwelling index (UI) estimates issued by the Pacific Fisheries Environmental Laboratory (PFEL) for 36N 122W.

	Rivers (CCAMP)	Upwelling (M1 and PFEL)
Upward	0.012 ($p = 0.000$)	0.000 ($p = 0.000$)
Downward	$p > 0.05$	$p > 0.05$
<i>n</i>	3506	3503

Table 3. Nutrient ratios, expressed in phosphate (P), silica (Si), and nitrogen [urea-nitrogen (N_{UREA}) nitrate-nitrogen (N_{NO_3}); ammonium-nitrogen (N_{NH_4})]. Ratios were determined from river and creek grab samples collected monthly (May 2007 – Sept 2008) from rivers and creeks throughout Monterey Bay as part of the Pathogens Pollution Project. Stoichiometries for onshore/offshore receiving waters are provided from cruise samples collected monthly at stations throughout Monterey Bay (Center for Integrated Marine Technology; 2002 – 2007); stoichiometries for inshore receiving waters are from integrated-depth (0, 1.5, 3 m) samples collected weekly at the Santa Cruz Municipal Wharf (SCMW; 2005 – 2009). For comparison, nutrient ratios for the Mississippi River, Santa Clara River, and upwelled water in the Santa Barbara (SB) Channel are included (Justic et al. 1995a; Warrick et al. 2005).

	Si:P	Si: N_{NO_3}	N_{NO_3} :P	N_{NO_3} : N_{UREA}	N_{NO_3} : N_{NH_4}
Waddell Creek	291	50	3	4	5
Scott Creek	213	56	5	4	2
San Lorenzo River	108	24	5	8	5
Soquel Creek	175	133	2	6	7
Pajaro River	290	0.4	356	100	34
Salinas River	228	0.1	3277	424	884
Carmel River	443	55	7	18	29
Big Sur River	673	128	3	9	28
— —					
Mississippi River	14	0.9	15	n/a	n/a
Santa Clara River	16	3	5	n/a	n/a
— —					
Monterey Bay (0 m)	23	2	9	5	5
Monterey Bay (5 m)	20	2	9	4	7
Monterey Bay (10 m)	14	1	10	38	11
Monterey Bay (25 m)	13	1	12	54	28
SB Channel upwelling	13	1	10	n/a	n/a
— —					
SCMW	30	6	5	0.3	0.8

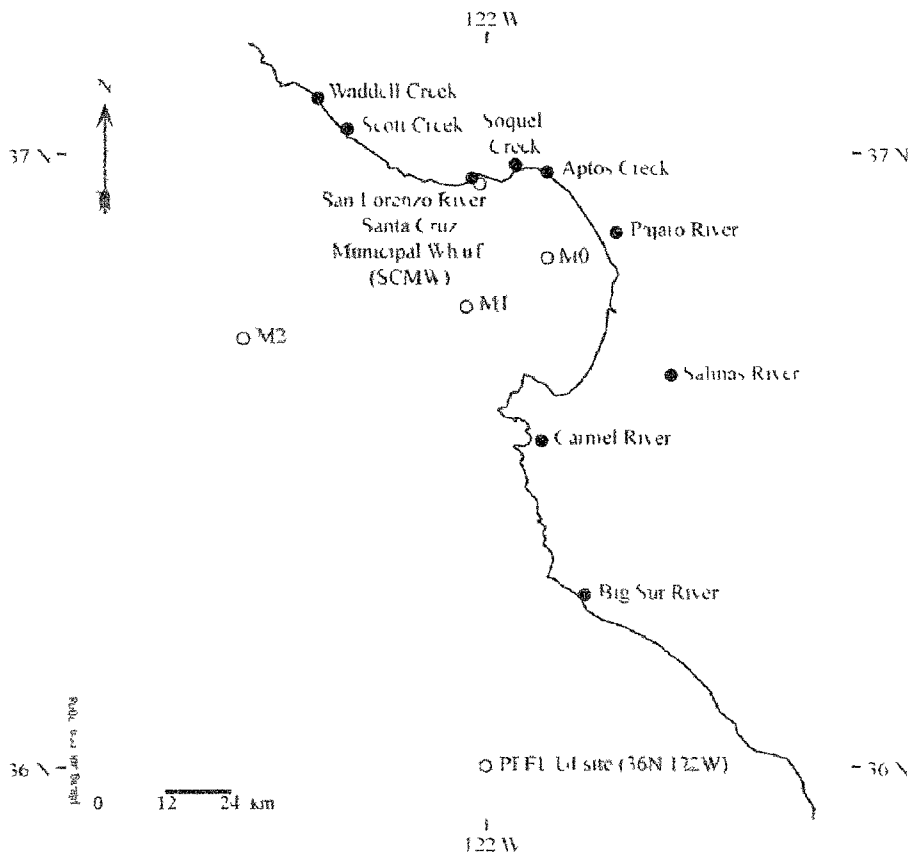


Figure 1. Map of the Monterey Bay region, annotated with Coastal Confluences Ambient Monitoring Project (CCAMP) river and creek coastal confluences (San Lorenzo River, Soquel Creek, Aptos Creek, Pajaro River, Salinas River, Carmel River, Big Sur River) which contributed to estimates of daily river nitrate-nitrogen (N_{NO_3}) loading to Monterey Bay, the coastal confluences sampled through the Pathogens Pollution Project for their characterization according to nutrient stoichiometry (same as CCAMP coastal confluence sites, omitting Aptos Creek and including Waddell Creek), the Monterey Bay Aquarium Research Institute (MBARI) offshore moorings (M0, M1, M2), the location of 36N 122W for which daily upwelling index (UI) is generated by the Pacific and Fisheries Environmental Laboratory (PFEL), and the location of the Santa Cruz Municipal Wharf (SCMW). Filled symbols denote river monitoring sites (versus sites used for coastal monitoring).

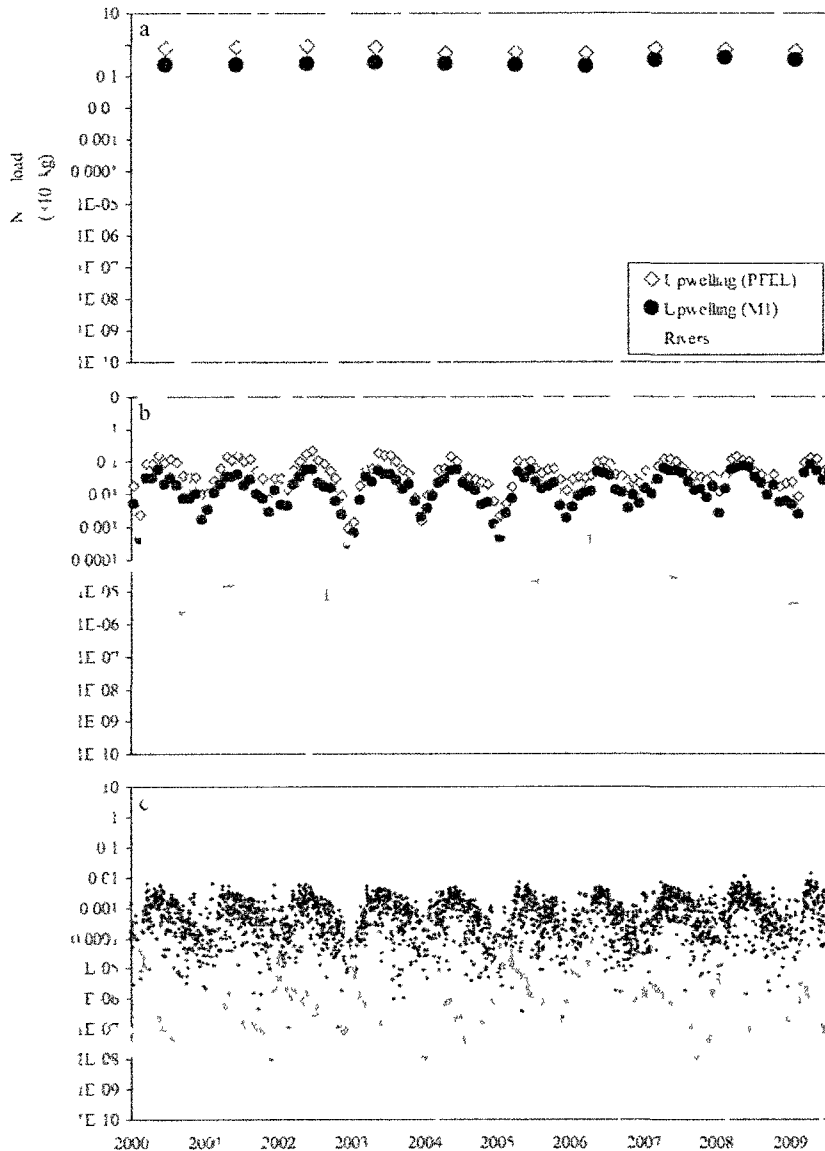


Figure 2. Nitrate-nitrogen (N_{NO_3}) loads introduced to Monterey Bay by rivers (grey bars) and by wind-driven upwelling estimated from observed winds at the Monterey Bay Aquarium Research Institute (MBARI) mooring M1 (filled circles) and from an upwelling index (UI) provided by the Pacific and Fisheries Environmental Laboratory (PFEL) for 36N 122W (open diamonds). The same N_{NO_3} load data are presented in each panel but at increasing temporal resolution, as follows: annual (A), monthly (B), and daily (C; daily N_{NO_3} loads are from M1 winds only). Note the unit difference between upwelling loads (plotted on the left vertical axis) and river loads (plotted on the right vertical axis).

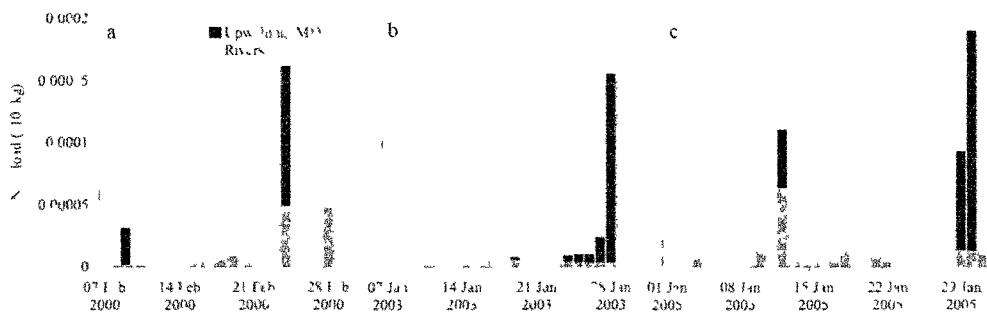


Figure 3. Daily nitrate-nitrogen (N_{NO_3}) loads introduced to Monterey Bay by rivers (grey bars) and by wind-driven upwelling estimated from observed winds at the Monterey Bay Aquarium Research Institute (MBARI) mooring M1 (black bars) across periods for which N_{NO_3} loads introduced by rivers were consistently higher than N_{NO_3} loads introduced by upwelling (i.e. upwelling winds were effectively turned ‘off’, while river loading remained switched ‘on’). This figure illustrates the relativity of river N_{NO_3} loading for only 3 select timeframes across which river loads are particularly competitive; across the entire study period (2000 – 2009), daily loads of N_{NO_3} from rivers exceed daily loads of N_{NO_3} from upwelling at a rate of 28%.

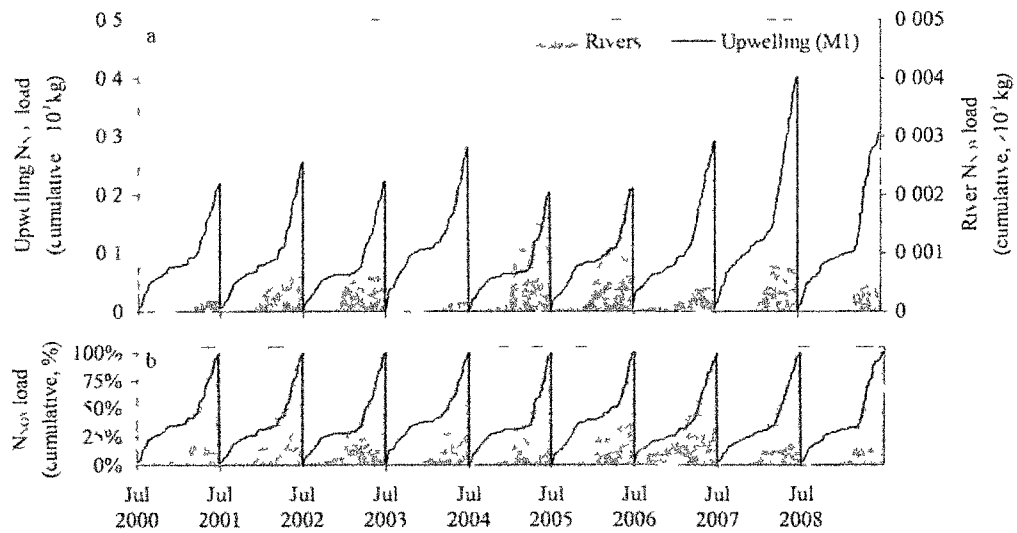


Figure 4. Nitrate-nitrogen (N_{NO_3}) loading by rivers (grey fill) and by wind-driven upwelling estimated from observed winds at the Monterey Bay Aquarium Research Institute (MBARI) mooring M1 (black line), as expressed in absolute cumulative sum (A), and percent cumulative sum (B). The cumulative sums are calculated and displayed according to hydrological year (July – June). Note in (A) the unit difference between upwelling loads (plotted on the left vertical axis) and river loads (plotted on the right vertical axis).

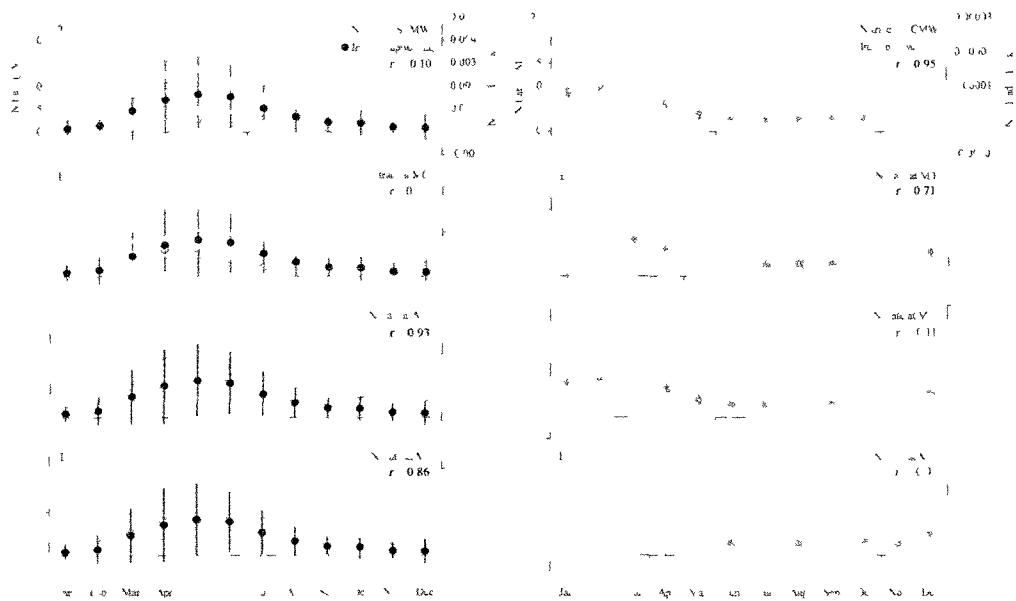


Figure 5. The surface nitrate climatology for Santa Cruz Municipal Wharf (SCMW; A and E), mooring M0 (B and F), mooring M1 (C and G), and mooring M2 (D and H) are shown; the climatologies are arranged top-to-bottom according to offshore distance (i.e. SCMW is a pier-based monitoring location; the M0, M1, and M2 moorings are located 8, 18, and 56 km offshore, respectively). The climatology of N_{NO_3} loading to Monterey Bay by upwelling is repeated through panels A-D for its comparison with the onshore (top panel) to offshore (bottom panel) series of surface nitrate climatology. The climatology for N_{NO_3} loading to Monterey Bay by rivers is repeated through panels E-H for its comparison with the onshore (top panel) to offshore (bottom panel) series of surface nitrate climatology. The correlation coefficient (r) for each pair of climatologies is shown. Light grey bars (surface nitrate climatology), black lines (upwelling load climatology) and dark grey lines (river load climatology) denote standard deviation for each month's climatological average.

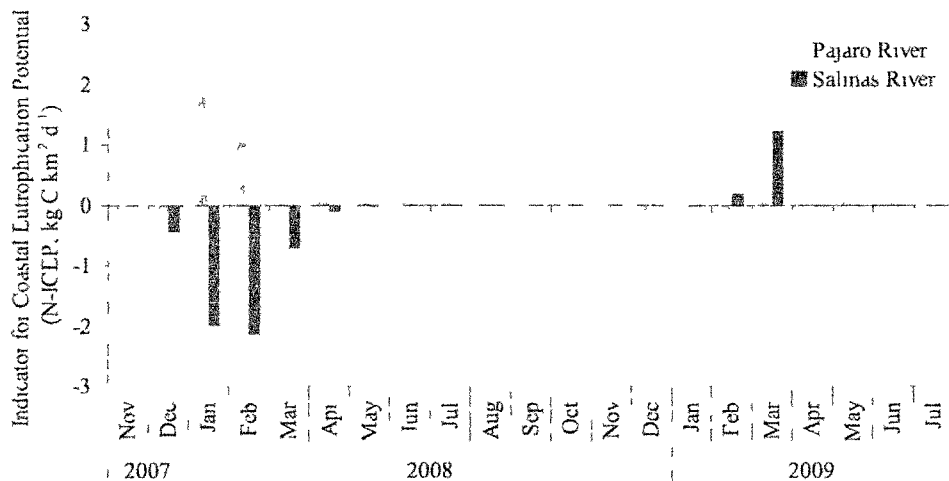


Figure 6. Monthly values of the Indicator for Coastal Eutrophication Potential with respect to nitrogen (N-ICEP) for the Pajaro and Salinas Rivers. The N-ICEP refers to the potential for new primary production (non-siliceous algae only) based upon the nutrient fluxes delivered by a river system. Designed as a summary characterization index, the N-ICEP encompasses and represents the relevant information contained in both absolute and relative values of nitrogen and silica fluxes delivered by large river systems (Billen and Garnier 2007). A negative value of the N-ICEP indicates silica delivery in excess over nitrogen delivery and the prevalence of relatively pristine conditions (i.e. the absence of eutrophication problems). A positive value of the N-ICEP indicates the reverse circumstance (nitrogen delivery in excess of silica delivery); positive values are generally indicative of eutrophication problems exerting their influence within the river basin.

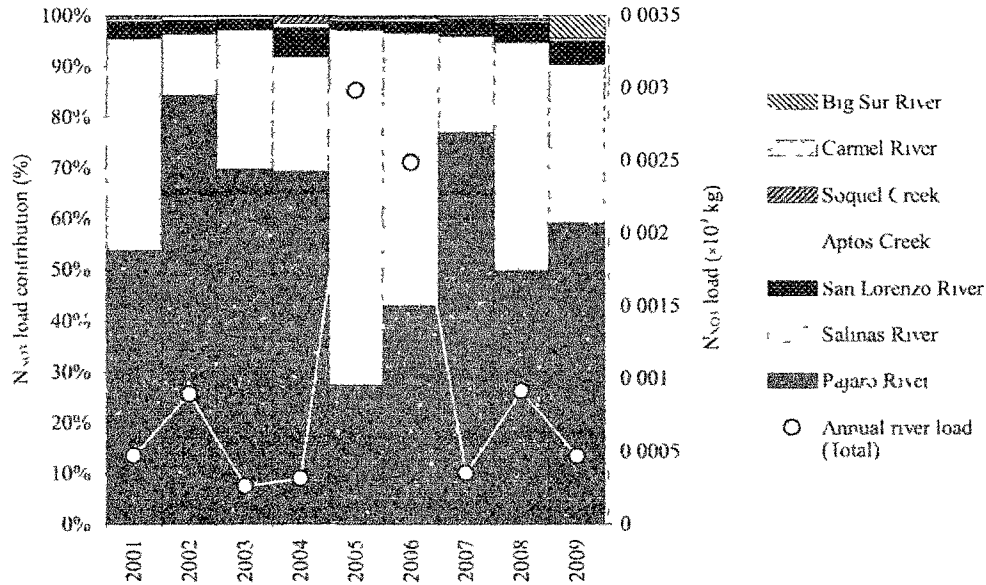


Figure 7. Relative percent nitrate-nitrogen (N_{NO_3}) load contribution (bars) from each of the rivers and creeks monitored by the Central Coast Ambient Monitoring Program (CCAMP). The total (absolute) N_{NO_3} load introduced to Monterey Bay in each year is shown (white circles) to illustrate the differential between the Pajaro and Salinas load contributions across years of moderate N_{NO_3} loading (corresponding to years of dry to normal hydrology) and years when N_{NO_3} loading was enhanced (i.e. the relatively wet years of 2005 and 2006).

CHAPTER THREE

Application of Solid Phase Adsorption Toxin Tracking (SPATT) for field detection of the hydrophilic phycotoxins domoic acid and saxitoxin in coastal California

Jenny Q. Lane¹*, C. Meiling Roddam¹, Gregg W. Langlois², and Raphael M. Kudela¹

¹Department of Ocean Sciences, University of California, 1156 High Street, Santa Cruz, CA 95064

²California Department of Public Health, Richmond Laboratory Campus, 850 Marina Bay Parkway, Richmond, CA 94804

Abstract

Recent publications have identified the analysis of phycotoxins in sentinel shellfish as a problematic tool for environmental monitoring purposes. Domoic acid (DA), a neurotoxin produced by some species of the diatom *Pseudo-nitzschia*, can remain undetected in sentinel shellfish stocks during toxic blooms and subsequent marine bird and mammal mass mortality events. Solid Phase Adsorption Toxin Tracking (SPATT) has previously been described for monitoring of lipophilic toxins, whereas resin based sampling methods are routinely employed for many other environmental contaminants. Here, we evaluate the applicability of SPATT for monitoring the hydrophilic phycotoxin DA and demonstrate that the same field sampling methods can be used for the detection of saxitoxins. We present laboratory based adsorption profiles characterizing the performance of SPATT with four resin types: (1) HP20, (2) SP700, (3) SP207, and (4) SP207SS. We present results from 17 mo of approximately weekly SPATT deployments in Monterey Bay, California (USA). This period included two significant toxicogenic *Pseudo-nitzschia* bloom events as well as low level saxitoxin events. SPATT signaled the presence of DA 3 and 7 weeks before the recognition of bloom conditions by traditional monitoring techniques (7 and 8 weeks before shellfish toxicity). Under ambient (non bloom) conditions, all resins detected DA when its presence was not apparent from traditional monitoring, highlighting the ubiquity of low level or transient toxin events in the environment. This study is the first to evaluate SPATT deployments in U.S. waters, and the first to demonstrate the applicability of SPATT toward detection of hydrophilic phycotoxins in the field.

The contamination of shellfish with phycotoxins is a public health risk encountered worldwide. In many countries, shellfish product safety is assured through biotoxin monitoring programs. In recent literature, the analysis of shellfish for

biotoxins has been described as difficult, expensive, problematic, time-consuming, technically demanding, and not ideal as a tool for monitoring the progress of toxicogenic blooms' (Fux et al. 2009, Mackenzie et al. 1993, Mackenzie et al. 2004, Mackenzie 2010, Rundberget et al. 2007). Although direct monitoring of shellfish for biotoxins has obvious benefits and unique significance, disadvantages include (1) an analytical process regarded as time-consuming, expensive, technically demanding, and labor-intensive; (2) analytical interferences resulting from biological matrix effects; (3) heterogeneity inherent to the employment of a biological matrix; (4) toxin bio-transformation and toxin degradation, both of which confound toxin detection and quantification; and (5) inability to control stock supply years of low shellfish recruitment can translate to a lack of shellfish stocks from or available for transfer to sentinel observation sites. Phytoplankton monitoring, often instated in conjunction with shellfish monitoring, offers valuable insight into the ecology and development of toxic blooms but is limited in its ability to signify biotoxicity in the target organisms because (1) phytoplankton samples can only describe a snapshot of the phytoplankton assem-

*Corresponding author. E-mail: jqlane@gmail.com

Acknowledgments

We thank Elizabeth Turrell (FRS Marine Laboratory), G. Jason Smith (Moss Landing Marine Laboratories), Bakthan Singaram (UCSC), and two anonymous reviewers for their guidance and suggestions. We appreciate the assistance of Kendra Hayashi (UCSC), Anna McCaraghan (UCSC), and the staff and volunteers of the CDPH Marine Biotoxin Monitoring Program. Partial funding was provided by NOAA Monitoring and Event Response for Harmful Algal Blooms (MER) AB Award NA04NO54/80239 (Cal PRE-MPT), NOAA California Sea Grant Award NA04GA00170036, and as a fellowship (GWL) from an anonymous donor through the Center for the Dynamics and Evolution of the Land-Sea Interface (CDELSI). This contribution is part of the Global Ecology and Oceanography of Harmful Algal Blooms (GEOHAB) Core Research Project on Harmful Algal Blooms in Upwelling Systems, and is MERHAB Publication #77.

DOI 10.4319/om.2010.8.45

blage at a single point in space and time, (2) observation of a phytoplankton assemblage can provide only circumstantial evidence for the possibility of toxin accumulation and (3) positive identification to the species level is difficult for some toxicogenic algae such as the genus *Pseudo-nitzschia*, a monitoring agency risks either increased incidence of false alarm or must further invest in, or develop, specialized tools required for species level identification of these groups (Mackenzie et al 2004; Mackenzie 2010; Müller and Scholin 1996, 1998, 2000; Rundberget et al 2009)

The use of a passive sampling method for determination of dissolved biotoxin levels in seawater Solid Phase Adsorption Toxin Tracking (SPATT) was first proposed in 2004 as a means by which the disadvantages associated with shellfish could be circumvented (Mackenzie et al 2004) SPATT extended the varied list of analytes and mediums toward which passive samplers had been applied (see reviews in Corecki and Namiesnik 2002; Kotwaniak et al 2007; Seethapathy et al 2008; Vrana et al 2005) As first described SPATT is the field deployment of adsorbent resin sealed within a polyester mesh bag SPATT bags of this design were tested by Mackenzie et al (2004) for a suite of lipophilic toxins, including the pectenotoxins (PTX 2, PTX 2 SA, PTX 11, PTX 11 SA), the okadaic acid complex toxins (OA, OA-ester), dinophysistoxin 1 (DTX 1), and yessotoxin (YTX) Studies subsequent to Mackenzie et al (2004) focused on the development of alternative sampler designs with DIONEX HP20, the resin identified as the most efficient for lipophilic toxin tracking, relatively fewer studies discussed the potential of alternative resins (Table 1) In all published studies to date SPATT has targeted lipophilic toxins exclusively for quantification This study is the first to evaluate semi-quantitative use of SPATT for field monitoring of the hydrophilic biotoxin domoic acid (DA, Fig. 1) as well as saxitoxin (STX) and related hydrophilic paralytic shellfish toxins (collectively referred to as PST), produced by species of the diatom genus *Pseudo-nitzschia* and the dinoflagellate genus *Alexandrium*, respectively

DA toxicosis manifests as Amnesic Shellfish Poisoning (ASP) in humans and is also referred to as Domoic Acid Poisoning (DAP, particularly for wildlife intoxication) to distinguish between shellfish and other vectors (Scholin et al 2000) The first reported outbreak of ASP occurred in 1987 when 3 people died and over 100 were hospitalized following the consumption of contaminated shellfish from Prince Edward Island, Canada (Bates and Trainer 2006) The California Department of Public Health (CDPH) Marine Biotoxin Monitoring Program included DA in their routine monitoring program in 1991, following identification of DA along the California coastline (Fritz et al 1992) Since 1987, no human deaths have been attributed to ASP in California, DA poisoning has, however, been identified as the causal factor in mass mortality events involving marine mammal and bird populations (Schretzer et al 2007; Scholin et al 2000) While the incidence of DA and its bio-accumulation in the food web is a public health concern first and foremost, the sudden or unan-

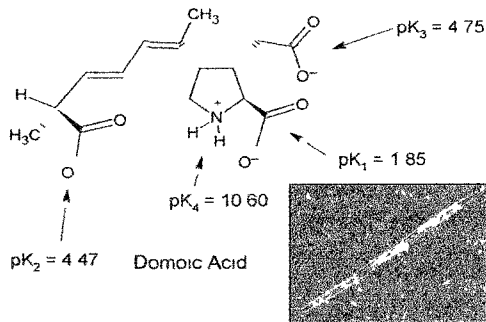


Fig. 1. The molecular structure of domoic acid, as protonated in seawater. Inset: a 3 cell chain of the diatom *Pseudo-nitzschia*

Table 1. Published studies on the employment of Solid Phase Adsorption Toxin Tracking (SPATT). Phycotoxin abbreviations are as follows: dinophysistoxin (DTX), okadaic acid (OA), pectenotoxin (PTX), yessotoxin (YTX), gymnodimine (GD), azaspiracid (AZA), spirrolide (SPX), domoic acid (DA), saxitoxin, and related paralytic shellfish toxins (PST). Bold text indicates the resin identified as optimal for the toxins addressed in the study

Study	Toxin group analyte	Resins	Region	Mode of deployment
Mackenzie et al (2004)	DTX, OA, PTX, YTX	HP20 , SP207, HP2MG	New Zealand	Sewn bags
Takahashi et al (2007)	CD, OA, PTX	HP20	Australia	Sewn bags
Rundberget et al (2007)	DTX, OA, PTX	HP20	Norway, Spain	Packed columns
Tunell et al (2007)	OA, PTX, YTX, AZA	HP20, SP700	Ireland	Zip-tied mesh bags
Tunell et al (pers. comm.)	DA	HP20, SP700	Ireland	Zip-tied mesh bags
Pizarro et al (2008a, 2008b)	DTX, OA, PTX	HP20	Spain	PVC frame
Fox et al (2008)	DTX, OA	HP20 , SP850, SP825L, XAD4, L-493	Ireland	Sewn bags, Embroidery disc
Fox et al (2009)	DTX, OA, PTX, YTX, AZA, SPX	HP20	Ireland	Embroidery disc
Rundberget et al (2009)	OA, PTX, YTX, AZA, SPX	HP20	Norway	Embroidery disc
This study	DA, PST	HP20, SP700 , SP207, SP20755	USA (California)	Heat sealed bags

implicated onset of a DA poisoning event within wildlife populations can prove detrimental through secondary impacts affecting area, unrelated to human health (i.e., ecologic, economic, aesthetic).


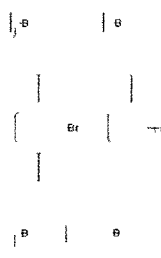
Here, as in preceding studies, SPATT is prescribed and evaluated as a monitoring technology for time-integrative detection of dissolved toxin (Mackenzie et al 2004; Mackenzie 2010; Pizarro et al 2008a, 2008b; Rundberget et al 2009; Takahashi et al 2007; Furrell et al 2007) and is assessed for its potential to provide "reliable, sensitive, time-integrated sampling to monitor the occurrence of toxic algal bloom events" (Mackenzie 2010). We evaluate the applicability of SPATT for the detection of DA in seawater in both controlled condition laboratory trials and coastal site field deployments. We compare SPATT to both particulate DA and sentinel shellfish data where as SPATT only detects toxins in the dissolved phase. Previous publications have discussed the prevalence of dissolved versus particulate or bio-accumulated toxins during harmful algal bloom events (e.g., Mackenzie et al 2004) and we do not further address this point herein. We specify four candidate SPATT resins and describe their DA adsorption efficiencies under controlled conditions. We present an adapted extraction protocol that provides rapid recovery of DA from SPATT bags deployed in the field and describe extraction efficiencies obtained under controlled conditions. We present a new method of SPATT passive sampler construction that minimizes labor and skill requirements while allowing for the manufac-

ture of a pliable sampling device. In the field trial component of our study, SPATT samplers of this new design were deployed approximately weekly over a 17 mo period in Monterey Bay, California (USA) in conjunction with weekly monitoring of DA in sentinel shellfish stocks, particulate DA (pDA), chlorophyll *a* phytoplankton abundance, and local oceanographic conditions. We present results from these field deployments which encompassed two significant bloom events of toxigenic *Pseudo-nitzschia* in spring and fall 2009. As a secondary effort, a subset of extracts from the HP20 resin SPATT deployments were selectively analyzed for identification of STX and closely related compounds, demonstrating the ability to successfully detect multiple analytes from a single field-deployed SPATT device. These data are presented in conjunction with measurements of Paralytic Shellfish Toxins (PSTs) in sentinel shellfish as reported by the California Department of Public Health (CDPH) and cell concentrations of *Alvandia catenella*, the presumed causative agent of PST in California coastal waters.

Materials and procedures

All macroporous resins (DIAION[®] HP20 and SEPABEADS[®] SP100, SP207, and SP2075S) were purchased from Sorbent Technologies, USA. The properties of these resins are summarized in Table 2. Water (Fisher W74), acetonitrile (Fisher A955), and methanol (MeOH, Fisher A456) used in liquid chromatography-mass spectrometry (LC-MS) analysis were purchased as Optima LC-MS grade from Fisher Scientific, USA.

Table 2. The physical characteristics of the resins evaluated for SPATT in the present study

Resin	HP20	SP700	SP207	SP2075S
Structure	Polystyrene-divinylbenzene (PS-DVB)		Modified PS-DVB	
				
Water content (%)	55-65	60-70		43-53
Particle size (µm)		>250	>250	75-150
Pore volume (mL/g)	1.3	2.3		1.3
Surface area (m ² /g)	600	1200		630
Pore diameter (Å)	520	180		210
Specific gravity (g/mL)	1.01	1.01		1.18

Ammonium acetate ($\geq 97\%$, MP Biomedicals 193848) formic acid ($\geq 99\%$, Acros Organics AC 27048 0010) isopropanol (Fisher A4644), ethylenediaminetetraacetic acid disodium salt dihydrate (EDTA Acros Organics AC32720-1000) and MeOH (HPLC grade, Fisher A452) used in SPATT extractions were purchased from Fisher Scientific USA.

DA analysis was conducted using an Agilent 6130 LC-MS system with an Agilent Zorbax Rapid Resolution column using an 8-point dilution series of CRM DA and domoic acid standards for calibration. The LC-MS was operated with a gradient elution of acidified water (0.1% formic acid) and acidified acetonitrile (0.1% formic acid). The same certified DA standard, obtained from the National Research Council (Canada) was used in LC-MS calibrations and incubation medium fortifications (NRC CRM DA I). Standards used the same extraction matrix as the samples (50% MeOH or 90% MeOH with 1 M ammonium acetate). DA was identified by the presence of a 312 nm peak in positive scanning ion mode (SIM) with concentration determined by signal integration of the peak area and back-calculations based on the standard curve. Our limit of detection was equal to or better than 34 pg DA on column. A modified solid phase extraction (SPE) clean up procedure (Wang et al. 2007) was applied to fortified seawater samples collected for adsorption profiling. In laboratory trials, the percent DA adsorbed and percent DA recovered were determined by mass balance, since no loss of DA was observed in the experimental control incubations, the loss of DA from the treatment incubations was attributed to the adsorption of DA by the experimental treatment (SPATT).

For a subset of samples, SPATT extracts were analyzed for the presence of STX and related compounds using Abraxis Saxitoxin ELISA kits (PN 52255B) using a modification of the manufacturer's directions. Briefly, SPATT extracts (in 50% MeOH) were either diluted in buffer solution or plated directly. Although the kits are not designed for analysis of MeOH extracts, verification using Abraxis STX standards with 50% MeOH exhibited no matrix issues (data not shown). Abraxis reports 100% cross reactivity for STX with varying sensitivity (0.2% to 2.9%) for neosaxitoxin, gonyautoxins (GTX) and derivatives.

To determine resin saturation values for DA, known quantities of resin (HP20 and unactivated SP700) were exposed to excess DA in Milli-Q for 45 d, and total adsorption was determined by mass balance to be 73001 ng g⁻¹ and 47090 ng g⁻¹, respectively. A second (non-saturating) trial was performed with known quantities of resin (non-activated SP700, activated SP257, and activated SP20755 $n = 3$ for each treatment) exposed for 8 d to DA in artificial seawater to better simulate field deployments, providing values of 8063 (CV = 20%), 8541 (CV = 13%), and 19644 (CV = 10%) ng g⁻¹ resin, respectively. PST saturation values were not determined as part of this study. Using a conservative value of 7300 ng g⁻¹ for HP20 and assigning 3 g SPATT deployments, we would expect saturation to occur at ~21,900 ng DA, the highest recorded value from

our time series was 182 ng g⁻¹ (546 ng DA). While 3 g deployments were determined sufficient for our field purposes, we note that during extreme bloom events, it is possible the various resins can saturate during a 7-d deployment and users may wish to adjust the amount of resin or the duration of deployment if this is a concern.

Sampler design and construction—A new method of SPATT bag construction was developed and applied. Unlike previously described construction methods (Table 1) the new method afforded quick manufacture of sealed, pliable SPATT bags without any requirement for specialized skills or equipment not generally found among oceanographic cruise supplies. As such, these bags could be quickly manufactured for deployment across a variety of configurations (e.g., narrow-neck flasks in laboratory trials clipped into an embroidery hoop for field deployment). SPATT bags were constructed from 100 μ m Nitex bolting cloth (Wildlife Supply Company, Product No. 24 C 31, \$45/yd). The bolting cloth was sealed on three sides using a plastic bag sealer (Clamco Impulse Sealer Model 210 121) to form an open bag of 55 mm width. The bag was filled with 3 g (dry weight) resin and the fourth side sealed with the bag sealer to form a finished SPATT bag of 55 \times 55 mm dimension. For activation, SPATT bags were soaked in 100% MeOH for 48 h, then rinsed thoroughly in deionized water (Milli-Q) and transferred into a fresh volume of Milli-Q for removal of MeOH residues by sonication using a probe sonicator (Fisher Scientific® Sonic Dismembrator, Model 100). The bags were stored in Milli-Q at 4-6°C prior to use.

Adapted extraction protocol (UCSC field protocol)—An unpublished extraction protocol for use with SP700 field-deployed SPATT resin was provided by the Fisheries Research Services [FRS] Marine Laboratory (Aberdeen, UK) and adapted for its application toward the extraction of field bags recovered by the University of California Santa Cruz (UCSC). Per the adapted protocol (hereafter referred to as the 'UCSC field protocol') the SPATT bag is rinsed with 3 \times 200 mL Milli-Q and inserted whole into a 1.5 \times 12 cm polypropylene chromatography column with a porous 30 μ m polyethylene bed (Bio Rad, Cat No. 732 1310), and 10 mL of 50% MeOH (v/v) is added. The column is vortexed for 1 min, placed on a vacuum manifold, and the extract is eluted into a glass scintillation vial. The extraction sequence is repeated with 10 mL ammonium acetate in 50% MeOH (1 M). The extraction sequence is repeated a final time with 10 mL ammonium acetate in 50% MeOH (1 M). The column and bag are rinsed with 10 mL ammonium acetate in 50% MeOH (1 M) and this rinse is collected as part of the final extraction. Each extraction is collected separately and analyzed, only the first extract (50% MeOH) was used for our determination of STX and related PSTs due to concerns about interference from the ammonium acetate in subsequent extracts. We did not concentrate the extracts before analysis by LC-MS due to concerns about DA stability (e.g., Wang et al. 2007) but inclusion of an evaporative step would increase the minimum detection limit proportionally to the concentration.

Evaluation of adsorption and extraction efficiency—The adsorption profile for SPATT bags of each resin type were determined by laboratory trial. SPATT resin bags were incubated, in triplicate, in aliquots of DA-fortified filtered seawater (or Milli-Q, where specified) in 125 mL glass flasks with rubber stoppers. The incubations were maintained at a controlled temperature (15°C) with constant agitation (70 rpm) with 12:12 illumination using “cool white” lamps at approximately 125 $\mu\text{mol photons m}^{-2} \text{s}^{-1}$. The sample water was regularly assayed for DA to monitor adsorption by the resin. The SPATT bags used for the determination of adsorption efficiencies were subsequently extracted according to the UCSC field protocol.

While DA could be extracted readily from HP20 (> 99% extraction efficiency when accounting for DA loss to Milli-Q rinses), extraction inefficiencies demonstrated for the other resins (2% to 11% extraction) prompted a secondary investigation into our extraction capacity with application of more extensive extraction techniques. A batch (9,200 g) of non-activated SP700 was soaked in DA-fortified Milli-Q (60 mg mL⁻¹ CRM DA-4) until DA in the incubation medium was below detection by LC-MS. The resin was then split into 4 batches (1,145, 1,192, 1,006, and 5,572 g, respectively). Resin batches 1, 2, and 3 were extracted with 50% MeOH, 50% MeOH with EDTA (10 mM), and ammonium acetate in 50% MeOH (1M), respectively, as follows: (1) 7 d soak, then elution/analysis, and (2) addition of fresh solvent, with elution/analysis on day 18. The solvents for resin batches 1 and 2 were reserved and used to extend the soak/extraction period; additional elution/analyses were performed at 29 d and 41 d. Resin batch 4 was packed into a Restek stainless steel column (250 × 4.6 mm), installed as an HPLC column, and run at 2 mL min⁻¹ with the following series of solvents: acidified water (0.1% formic acid; 40 mL), 50% MeOH (22 mL), 90% MeOH (18 mL), isopropanol (30 mL), 50% MeOH (10 mL), 50% MeOH with ammonium acetate (1M; 20 mL), and 50% MeOH (20 mL). The fortified Milli-Q was kept under the same storage conditions (room temperature, low light) and analyzed at each time point to check for degradation of the DA (none was observed).

The consistency of adsorption and extraction performance in field bags was investigated through the field-deployment of replicate SPATT bags and their extraction per the UCSC field protocol. SPATT bags of HP20, non-activated SP700 and SP207 were field-deployed [see “Field deployment at Santa Cruz Municipal Wharf (SCMW),” next section] in triplicate for 10 d (18–28 Nov 2009). The bags were processed as field bags (rinsed in Milli-Q, stored at -80°C) and extracted per the UCSC field protocol on 02 Dec 2009.

Field deployment at Santa Cruz Municipal Wharf (SCMW) — The resins HP20 and SP700 were evaluated in weekly field deployments at SCMW (36° 57.48'N, 122° 1.02'W) from 13 Jul 2008–01 Dec 2009; for 7 of these rotations, the deployment period exceeded 9 d. Deployment of SP700 as a nonactivated resin began on 29 Apr 2009, and the resin SP207 (non-activated) was added to the field rotations on 20 May 2009. For

deployment, SPATT bags were clamped into plastic embroidery hoops (Susan Bates® HOOP-La, 7.6 cm dia), and secured to a weighted rope with a plastic zip-tie at approximately 2.5 m depth. For SPATT bag retrieval and transport, the bag was unclamped from the embroidery hoop, immediately rinsed in ~200 mL Milli-Q, and transported to the lab in a glass container on ice. Upon arrival, the bag was rinsed twice more in Milli-Q (2 × 200 mL), then placed in a 20 mL glass scintillation vial and stored at -80°C. All archived bags were thawed entirely prior to extraction. Toxin values are reported normalized to 1 g resin and length of deployment (e.g., ng DA per gram resin per day) and were not corrected for estimated extraction efficiency.

SPATT bags were deployed at the same depth as bags of sentinel mussels (~2.5 m) maintained and sampled as part of the CDPH Marine Biotoxin Monitoring Program. Net-tow [5 × 10 ft vertical effort, 20 μm mesh with net dimensions 25 × 100 cm (leading diameter × length) and a 5 × 20 cm cod-end (internal diameter × length)] and whole-water samples were collected near the deployment site for qualitative evaluation of the phytoplankton assemblage (presence/absence and estimate of relative abundance to the genus level) and for the quantification of toxigenic *Pseudo-nitzschia* species (*P. australis* and *P. multiseres*) and *Alexandrium catenella*. Relative abundances of phytoplankton were determined with a Leica M7125 stereomicroscope within 1 h of sample collection. Whole water was collected by integration of water samples taken from 3 discrete depths (0, 1.5, and 3 m) with a FieldMaster 1.75 L basic water bottle. *Pseudo-nitzschia* and *Alexandrium* species identification and enumeration used species-specific large subunit rRNA-targeted probes following standard protocols (Miller and Scholin 1998). Samples were enumerated with a Zeiss Standard 18 compound microscope equipped with a fluorescence illuminator 100 (Zeiss). Duplicate filters were prepared for each species, and the entire surface area of each filter was considered in counting.

Assessment

Adsorption profiles—The DA adsorption profiles of the candidate resins in SPATT bags are characterized in Table 3 and are presented in Fig. 2. The profiles are two-phase exponential decay curves fit to time-point observations of DA concentration in the incubation medium (normalized to initial DA concentration) except for the adsorption profile of HP20 in seawater, which is best fit by linear regression (Fig. 2B). The estimated adsorption curves were poorest for HP20 in both Milli-Q and in seawater ($R^2 = 0.82$ and 0.55 , respectively). The adsorption curves of the SP700, SP207, and SP207SS resins fit the data well ($R^2 > 0.90$; Table 3). Adsorption profiles are presented for both activated and non-activated SP700 SPATT bags (Fig. 2B), since both were employed as part of our field deployment program. Through 192 h (8 d), there is no difference between the adsorption behavior of activated and non-activated SP700 (2-way ANOVA; $P = 0.11$); the difference becomes

Table 3 Adsorption characteristics for the SPATT resins evaluated in the present study. In all cases described here, domoic acid (DA) adsorption was from DA fortified 0.2 µm filtered seawater. Comparable results (not tabulated) were obtained for DA fortified Milli-Q water (e.g., Fig. 2A)

	HP20	SP700 (non-activated)	SP700 (activated)	SP207	SP20755
Adsorptive character	Slow/weak	Moderate/moderate	Moderate/strong	Fast/strong	Fast/strong
Adsorption in 7 d (%)	19	64	70	97	93
Time to full adsorption (d)	36	22	17	13	10
Profile fit (R^2)	0.55	0.93	0.99	0.94	0.91

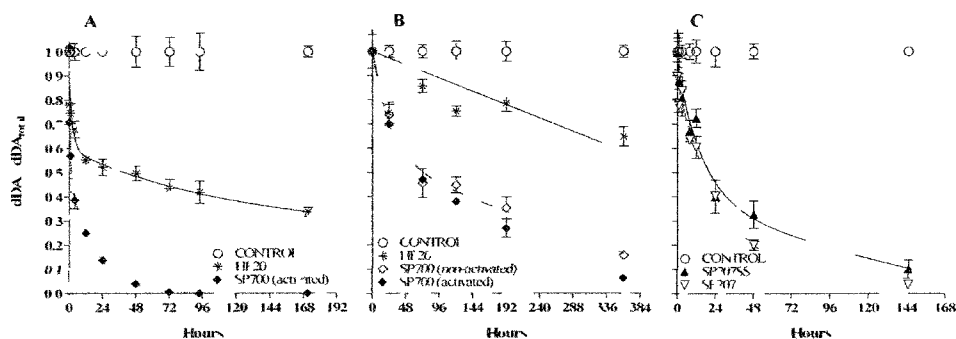


Fig. 2 Adsorption profiles for SPATT bags of the candidate resins assessed for application toward domoic acid (DA). (A) HP20 and SP700 in DA fortified Milli-Q. (B) HP20 and SP700 in DA-fortified seawater. (C) SP207 and SP20755 in DA fortified seawater. All adsorption profiles are presented as two-phase exponential decay curves except for the linear fit presented for HP20 in seawater (B). All exponential decay curves were significant ($R^2 > 0.9$, $P < 0.05$; see Table 3).

significant when the adsorption curve is extended to 360 hours (χ^2 days⁻¹ = 0.02).

Extraction efficiencies.—Instances of incomplete adsorption from the medium (e.g., HP20; Fig. 2) confounded the evaluation of extraction efficiencies across resin types. Regardless, HP20 could be distinguished as a relatively 'leaky' resin in preliminary trials. Our handling of HP20 bags per the original (FRS) extraction method indicated the unintended extraction (loss) of DA from the bags into pre-extraction Milli-Q rinses. While the leaky character of HP20 precludes a concise description of its extraction efficiency, losses of DA from HP20 field deployments into the pre-extraction Milli-Q rinses prescribed by the USYC field protocol could be (1) accounted for through the re-designation of the Milli-Q rinses as 'extractions' which are then received, cleaned on an SPE column and analyzed, or (2) encountered as a consistent loss term across HP20 field deployments which are handled and extracted according to the same field protocol. Compared with the HP20 resin, the three alternative resins (SP700, SP207, SP20755) were relatively aggressive in their retention of DA, and our DA recovery efficiencies from the experimental (non-HP20) SPATT bags were comparatively low (2% to 11%). The application of more exhaustive extraction techniques

toward a DA loaded batch of free non-activated SP700 resin demonstrated the capacity to recover DA from these resins exhibiting strong binding characteristics, but at higher analyte and material cost and with substantially longer time intervals between deployment and final analysis. Soak extraction of the SP700 resin in 50% MeOH and 50% MeOH with EDTA (10 mM) yielded 47% and 52% recovery (in day 7, cumulative recovery increased with prolonged soaking (61% to 62%, 68% to 69%, and 71% to 72% on day 18, 29, and +1, respectively). Soak-extraction in 50% MeOH with ammonium acetate (1M) demonstrated lower cumulative recovery (5% to 10% on day 7, 34% on day 18). Packing DA loaded (non-activated) SP700 into an HPLC column for pressurized extraction yielded 15.4%, 78.6%, and 82% cumulative recovery with the first 3 solvents used for column elution (acidified water, 50% MeOH, 90% MeOH) with no additional recovery of DA by solvent elutions thereafter, nor with removal of the resin from the column and 50% MeOH soak for an additional 10 d. Since we estimate recovery based on mass balance, we cannot determine whether the remaining DA (18% to 29%) was lost from the SP700 resin during processing, was still adsorbed, or was degraded. In consideration of loss to degradation, we note the >99% recovery from HP20, a similar resin (Table 2); this recov-

ery efficiency suggests that DA is not inherently unstable when exposed to resin. Although we did not extensively test storage effects as part of this study, our ad hoc results indicate that the resins and extracts (50% MeOH) are stable for at least several months with no loss or transformation of DA. Other extraction solvents and protocols were evaluated including longer chain alcohols (ethanol, isopropanol) of varying strength, pH adjusted methanolic solutions (both acidic and basic), sonication, heating, and warm (40°C) bath sonication (data not shown), with no improvement in extraction efficiency.

While adsorption profiles and extraction efficiencies can be estimated and described in the experimental setting, these data cannot be directly extrapolated to the field setting and presumed to hold constant in an uncontrolled environment. We therefore directly evaluated the variability inherent to our SPATT bag field deployment/extraction method through a deployment rotation of triplicate bags in the field: the coefficients of variation (CV) were 14.9% for HP20, 35.9% for SP700 and 15.8% for SP207. The relatively high CV for SP700 was caused by an outlier within the SP700 bag extractions. For comparison, an analogous assessment of variability among individual sentinel mussels ($n = 12$) determined CVs of 46.6% and 47.6% for analysis by LC-MS and Biosense ELISA, respectively, following standard extraction protocols and analysis in our laboratory.

Field deployment—The results of SPATT bag field deployment at SCMW are presented with *Pseudo-nitzschia* relative abundance (indexed by visual inspection of the sample and evaluation of the phytoplankton assemblage at the genus level, Fig. 3A), DA in shellfish (Fig. 3B), cell counts specific to toxicigenic species of *Pseudo-nitzschia* (Fig. 3C), and particulate DA (Fig. 3D). While the toxicigenic species *P. australis* and *P. multiseries* have been associated with toxic bloom events observed in Monterey Bay, their recognition as locally toxicigenic species does not eliminate the potential for DA production by species other than *P. australis* and *P. multiseries*, for this reason, we present the SPATT results with both discrete cell counts of these toxicigenic species and the index of relative abundance at the genus level. While we consider SPATT to be semi-quantitative because we can't directly relate resin toxin loads to quantitative toxin concentrations in the environment, field deployments used identical procedures, and are therefore internally comparable (i.e., low/high values for a given resin type are assumed to indicate low/high values in the environment). Of the three resins used in field testing, HP20 was the only resin deployed consistently (always activated) throughout the 17 month deployment period. The HP20 deployments successfully signaled the presence of DA periodically throughout the year. A significant episode of SPATT DA signaling by HP20 began in late February (deployment period 25 Feb – 03 Mar 2009) and had surpassed all previous signal magnitudes by mid-March: toxicigenic *Pseudo-nitzschia* and pDA were detected on 21 Apr 2009, 6 weeks after

the first week-rotation of SPATT-DA signaling. Toxicigenic *Pseudo-nitzschia* were identified at 'bloom level' concentrations ($>10,000$ cells l^{-1}) on 05 May 2009, and shellfish toxicity was detected on 11 May 2009. 7 and 8 weeks respectively, after the first rotation of elevated SPATT-DA signaling. Non-activated deployments of SP700 began on 29 Apr 2009 (near to the observed bloom-peak in pDA concentration), and SP207 deployments began on 20 May 2009 (near to the end of the bloom period). The DA signals from SP700 were initially high, and then SPATT DA signaling from all three resins declined in conjunction with, or in slight advance of, indicators afforded through traditional monitoring (i.e., cell counts and particulate toxin monitoring).

All three SPATT resins dropped to low and/or zero detection for three weekly rotations following the spring 2009 bloom event. Summer 2009 was a period of intermittent SPATT-DA signaling and disjointed signaling by traditional monitoring techniques (e.g., pDA detection without cell detection and vice versa single week detection incidents). The SP700 and SP207 SPATT resins signaled DA across two weekly rotations in late June/early July 2009 (HP20 signaled across only the latter of the two rotations). This signaling event may be recognized in the pDA record as a single detection incident (23 ng l^{-1} on 23 Jun 2009). Particulate DA (and toxicigenic *Pseudo-nitzschia* cell counts) remained below detection for the remainder of the summer, throughout a second summer period of sustained SPATT DA signaling (15 Jul–18 Aug 2009). SPATT DA signals then fell to zero over a two-week period of low *Pseudo-nitzschia* relative abundance and low (<1000 cells l^{-1}) toxicigenic *Pseudo-nitzschia* species abundance: both traditional measures of toxin incidence (pDA and DA in shellfish), indicated this as a period of non-toxicity (no detection of DA in the particulate fraction or in shellfish). SPATT DA began a consistent signal-response to the impending fall bloom on 02 Sept 2009, 3 weeks prior to the detection of 'bloom' conditions ($>10,000$ cells l^{-1}) and 7 weeks prior to the detection of shellfish toxicity. The consistency of the signal response by SPATT is unique among the monitoring data, toxicigenic *Pseudo-nitzschia* cell counts and *Pseudo-nitzschia* relative abundance both dropped to zero on 29 Sept and 12 Oct 2009, and pDA indicated declining toxin levels on those dates, the collection of a discrete sample which indicated an absence of *Pseudo-nitzschia* (toxicigenic species or otherwise) and declining toxin levels on 12 Oct is especially significant since the sentinel shellfish 'went toxic' the following week, jumping from zero to above the regulatory toxin limit within a matter of days (non-detect on 14 Oct 2009, 29 $\mu g g^{-1}$ on 21 Oct 2009).

While our record for PST is incomplete (e.g., no SPATT-PST data are available for the cell detection incident in Nov 2009), the detection of PST in HP20 field extracts exhibited patterns similar to those demonstrated for DA. Concentrations of PST in HP20 field extracts reflected both the presence of *Alexandrium catenella* and the toxin levels measured by CDPII in mussel samples (Fig. 4).

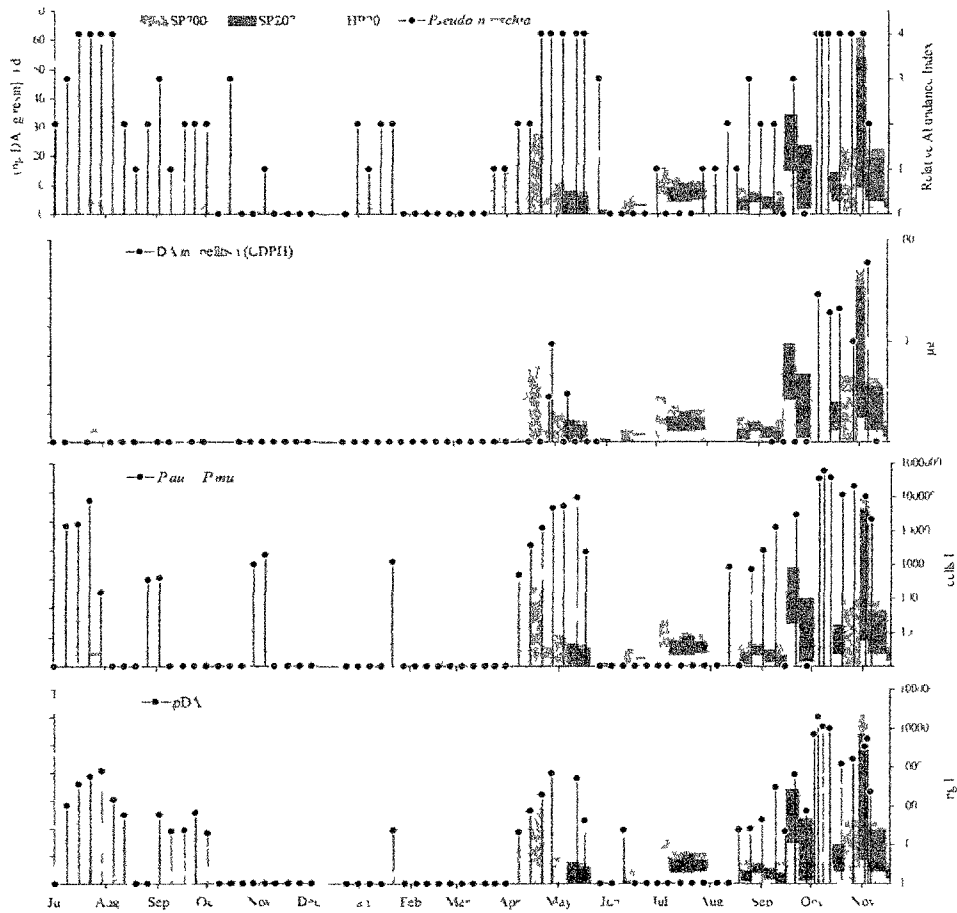


Fig. 3 Results from field deployment of SPATI bags at the Santa Cruz Municipal Wharf from 15 Jul 2008 – 01 Dec 2009. The SPATI field results are overlaid with total *Pseudo-nitzschia* relative abundance (0 = none, 1 = rare, 2 = present, 3 = common, 4 = abundant) (A) domoic acid in adjacent sentinel shellfish, as reported by the California Department of Public Health (CDPH) (B) cell abundance of toxicogenic *Pseudo-nitzschia* (*P. multiseries* + *P. australis*) (C) particulate domoic acid (pDA) concentration (D)

Discussion

Deployment strategy and cost – Biotoxin monitoring for the protection of human health requires a reliable resource that can be sampled consistently for monitoring purposes. In California, participants in the CDPH Marine Biotoxin Monitoring Program collect samples of sentinel or wild shellfish for delivery

to the state lab for analysis. In most years, the majority of biotoxin samples analyzed by CDPH are mussels (e.g. 69% in 2008). Special significance is given to monitoring activities along the outer coast, where toxin detection might afford advance warning to harvesters in more protected areas. The abundance of mussels along the outer coast of California is

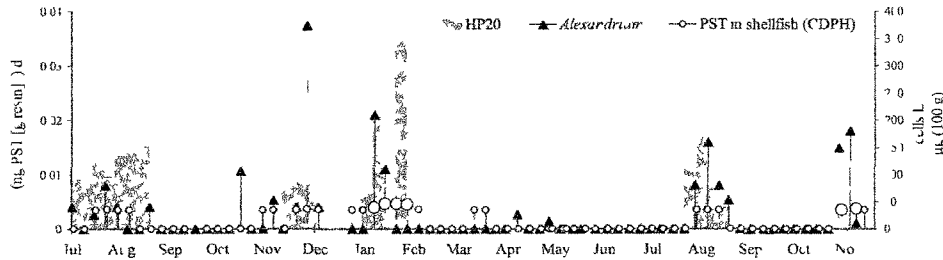


Fig 4 Results from the analysis of HP20 SPATT field bag extracts for saxitoxin and related paralytic shellfish toxin (PST). All extracts were obtained from HP20 field deployments at the Santa Cruz Municipal Wharf and assayed by Abraxis® ELISA. Also shown are PST in adjacent sentinel shellfish as reported by the California Department of Public Health (CDPH) and cell concentrations of *Alexandrium catenella*, a known source of PST in the marine environment. Enlarged open circles denote PST measurements by CDPH that were above the limit of detection; nonenlarged open circles denote PST detection through a rapid screening technique with non-detection by analytical means (value shown is the upper bounds or detection limit) or PST non-detection.

variable, however, both between regions (northern and southern California) and between sites within a region (Smith 2005). Mussel abundance is subject to change according to various factors including mesoscale oceanographic conditions, biotic and abiotic factors acting on local and broad scales (e.g. predation, tidal patterns), and larval supply and recruitment (cf. Smith et al. 2009). Within the Monterey Bay region, inconsistent mussel abundance has confounded monitoring activities; local monitoring agencies have recently reported low mussel recruitment to supply sites that had been generally reliable, and have expressed difficulty in sustaining and locating adult mussel stock (S. Peters, County of Santa Cruz Environmental Health and Safety, pers. comm.). While sentinel shellfish availability is inconsistent, the supply of SPATT is controlled only by the working capacity and preference of the monitoring agency. We have successfully deployed SPATT as a passive sampler in a freshwater lake, desalination system, feedwater tank, and in a flow through surface water sampling stream aboard a research vessel (data not shown). Given this flexibility, we anticipate that the primary impediments to widespread use of SPATT are primarily construction and analysis cost, and secondarily inter-calibration with mussels or other shellfish.

A comparative cost analysis for shellfish and SPATT is supplied in Table 4. Shellfish costs were estimated according to the extraction procedure and materials described in established protocols (Hess et al. 2005, Quilham et al. 1997, Quilham et al. 1998). While the overhead costs estimated for both monitoring programs are comparable (~\$200 USD), the programs differ in per-sampler cost. Relative to shellfish, a SPATT bag is lower in cost by >5 fold (HP20), 7.8-fold (SP700), and 2.5-fold (SP207). The SP207S test is the only case for which the cost of SPATT is higher than for shellfish (1.7 fold). One cost not represented in Table 4 (due to difficulty of quantification) is the cost of time and labor required to generate and

maintain a supply of SPATT bags or sentinel shellfish. The construction of 60 SPATT bags sufficient for over a year of weekly rotations could be completed within 6 h by a student volunteer. To maintain a sufficient supply of shellfish for deployment at SCMW, shellfish collection and bagging events occur 2-3 times per year by parties of 2-5 volunteers. While we present this comparison on a line-item basis for purposes of clarity, we do not suggest SPATT as a (less expensive) alternative to sentinel shellfish monitoring. With additional inter-calibration and validation studies, SPATT will most immediately be used to augment ongoing shellfish monitoring practices (Mackenzie 2010). If we reassess the potential of SPATT on a cost-savings basis (i.e. shellfish and SPATT are both sampled weekly, but the shellfish sample is extracted only when DA is detected in the SPATT extract), this screening approach within our field trial would have afforded 2% and 26% cost savings from HP20 and SP700, respectively. This is an internal cost savings estimate; the implementation of SPATT to screen for shellfish toxicity in a semi-quantitative capacity within the current CDPH monitoring design could afford significant cost savings by reducing both analytical and shipping costs, the latter of which is substantial component of the CDPH biotoxin monitoring budget.

It should be noted that the analytical and labor costs associated with shellfish biotoxin analysis proved prohibitive for all samples received by CDPH, especially when it became clear that multiple toxins were of concern (PST and DA versus PST alone). Phytoplankton monitoring was integrated into the CDPH Marine Biotoxin Monitoring Program in 1993 so that shellfish samples could be analyzed on the basis of risk probability, as such, only a fraction of the shellfish samples received by CDPH are actually analyzed (e.g. 26% in 2008). Extraction of a field SPATT sample is comparatively lower in time and labor requirements. The SPATT extraction described here includes a three-step series of column elutions that can be

Table 4. Comparative cost analysis of the supplies and equipment required for domoic acid monitoring by sentinel shellfish and by SPATT. Materials (supplies and equipment) required for sentinel shellfish are according to established protocols (Hess et al. 2005; Quilliam et al. 1995; Quilliam et al. 1998). All costs are in 2010 USD (\$). Costs included in "Construction & extraction" are for nonre-coverable supplies and expenses pro-rated for weekly sampling (e.g., weekly shellfish sampling includes \$41.20 for the collection permit distributed over 52 weeks, plus the weekly cost of an autoval filter and SPE column). In this study, SPATT and shellfish were both analyzed for DA by LC-MS; the analytical cost for the two monitoring methods was therefore equivalent. Reagents are listed but excluded from the cost estimate due to cost variability, whereas personnel costs are not included and assumed to be equivalent for the two methods

	Sentinel shellfish		SPATT	
Sampler construction	Field collections of shellfish, California Department of Fish & Game annual sport fishing license	41.20	HP20 (3 g) Sorbent, HP20-01	1.00
			SP700 (3 g) Sorbent, SP700-05L	0.60
			SP207 (3 g) Sorbent, SP207-01	2.50
			SP207SS (3 g) Sorbent, SP207SS-01	11.90
			Nitex (100 µm, per bag) Wildco, 24-C34	0.30
			Nitex (53 µm, per bag) Wildco, 24-C27	0.40
Extraction supplies (non-regenerative)	Autoval filter, Whatman Inc., AV125UNAO	2.90	—	—
	SPE column, Supelclean LC-SAX, 57-017	3.40	—	—
Construction & extraction (cost per sample)		7.10	HP20	1.30
			SP700	0.90
			SP207	2.80
			SP207SS	12.30
Specialized equipment	Commercial blender, Waring, 7011-G	211.50	Bag sealer (8"), Clamco, 210-21E	110.00
			Polypropylene columns (50), Bio-rad, 732-1010	104.50
Overhead (total cost)		211.50		214.50
Shipping (UCSC to CDPH)	FedEx Priority Overnight	33.54	FedEx 2Day	16.39
Processing time (per sample)	Shuck, homogenize, extract & SAX-prep	3 h	Rinse & extract	0.5 h
Reagents	Methanol, H ₂ O, Acetonitrile, Citric acid buffer, Formic acid		Methanol, H ₂ O, Ammonium acetate	

completed within 10-30 min, yielding extracts that are available for immediate analysis of a single toxin or of multiple toxins, as demonstrated (e.g., DA or DA plus PST). We note that others have already demonstrated the ability to use HP20 for a suite of marine toxins (Fux et al. 2008, 2009; Mackenzie et al. 2004; Pizarro et al. 2006a, 2006b; Rundberget et al. 2007, 2009; Takahashi et al. 2007). The toxin and extract are reasonably stable when stored at -80°C, providing the ability to archive samples for further analysis at a later time. An evaluation of variability among individual SPATT bags and individual sentinel mussels further demonstrates the advantage of

SPATT as an artificial sampling device: extractions of replicate field-deployed SPATT bags demonstrated significantly less variability than extractions of individual sentinel mussels that had been collected from the same deployment bag (14.9-36.9% versus 40.6%).

For some applications, such as ecological monitoring of toxin levels separate from shellfish, or for ecophysiological studies of harmful algae, direct comparison between shellfish and SPATT may not be necessary. For regulatory monitoring purposes, however, SPATT alone would not be acceptable since it does not conform to AOAC guidelines (AOAC International

2000; AOAC International 2006) SPATT may still be useful as an augmentation to regulatory monitoring of shellfish, similar to the phytoplankton observations, in that it can indicate the potential presence of biotoxins in the environment without or in addition to analysis of shellfish. Further inter-calibration, potentially on a site-by-site basis, would likely be required before SPATT could be fully integrated into existing monitoring programs (Mackenzie 2010). This present study supports the inclusion of hydrophilic toxins in future inter-calibration studies and provides evidence of their potential to augment regulatory practices worldwide, including within the United States.

Detection and early warning of a DA toxin event—Observations from a previous DA event along the California coastline established that the monitoring of shellfish alone is not always sufficient for adequate warning of food web contamination at levels that are threatening to marine mammal or human populations (Scholin et al. 2000). This previous DA event, triggered by a bloom of *Pseudo-nitzschia australis* in May and June 1998, resulted in the death of over 400 sea lions; although DA was detected in phytoplankton, northern anchovy (*Engraulis mordax*), and California sea lion (*Zalophus californianus*) samples, concurrent samples of blue mussels (*Mytilus edulis*) contained little to no DA (Scholin et al. 2000). The converse can also occur. DA-event observations of *M. edulis* populations in Cardigan Bay, Canada, reached toxin levels higher than could be explained by a single-compartment uptake-clearance model of DA flux (> 300 ppm), suggesting that biological factors (increased grazing or the suppression of metabolic efficiency, or both, under bloom conditions) complicate the relationship between the amount of DA available in particulate form in the water column and the amount that accumulates in mussels (Silver and Kao 1992). Both accretion and depuration vary according to seawater temperature and mussel size, with kinetics driven largely by the digestive gland (Blanco et al. 2006; Novacek et al. 1991). The efficiency at which DA is accumulated in *M. edulis* is 1% to 5% (Wohlgemuth 1991); the rate of depuration, originally estimated at 17% d^{-1} , has been recently corrected to 87% d^{-1} (Krogstad et al. 2009).

Synthetic passive sampling devices can be represented by a one-compartment sampling model (e.g., Fig. 1 in Stuer-Lauridsen 2005), with uptake according to chemical potential gradients. These chemical potential gradients can be affected by environmental conditions (flow, temperature, biofouling, etc.), and permeability reference compounds have been recommended as a means to quantify and correct for these factors (Booij et al. 1996; Huckins et al. 1996; Stuer-Lauridsen 2005). With the exception of semi-permeable membrane devices applied in conjunction with calibrated reference compounds, passive sampling devices are assessed semi-quantitatively, e.g., for the early-warning detection of toxin incidence or increase (Stuer-Lauridsen 2005).

Our field deployments of HP20 SPATT successfully signaled

two shellfish toxicity events 3 and 7 weeks prior to bloom onset (toxigenic *Pseudo-nitzschia* $> 10,000$ cells L^{-1}), and 7 and 8 weeks prior to the detection of shellfish toxicity; unlike traditional metrics, enhanced DA-signaling by SPATT consistently indicated the development of toxigenic blooms and impending incidents of shellfish intoxication (i.e., in the fall bloom, toxigenic *Pseudo-nitzschia* cell counts and *Pseudo-nitzschia* relative abundance both fell to zero the week prior to bloom onset and pDA declined the week prior to DA detection in shellfish). Sentinel shellfish samples collected and analyzed as part of the CDPH Marine Biotoxin Monitoring Program during the spring bloom period never exceeded $9.2 \mu g g^{-1}$ tissue (the regulatory closure limit is $20 \mu g g^{-1}$), and were not toxic above the CDPH detection limit until 8 weeks after DA detection with SPATT (Fig. 3). Unlike the spring bloom, mussel toxicity did exceed the regulatory closure limit during the toxigenic bloom event of fall 2009. This exceedance forced a regulatory reaction from CDPH: the annual mussel quarantine, lifted by CDPH according to schedule on 31 Oct 2009, had to be reinstated 2 weeks later through an emergency statewide press release (13 Nov 2009). Mussel toxicity was measured at its highest level on 20 Nov 2009 ($59 \mu g g^{-1}$), SPATT-DA signaling was unprecedented (high) from the deployment rotation immediately preceding that measurement (e.g., SP700, $60 ng DA g^{-1} d^{-1}$). Monitoring by SPATT successfully signaled the impending toxigenic blooms of spring and fall 2009, and tracked the unexpectedly sustained toxigenic bloom conditions of fall 2009. This demonstration of SPATT DA-signaling relative to shellfish toxicity and CDPH regulatory behavior indicates its potential to facilitate a more anticipatory, less reactionary, management perspective.

Detection of DA under 'non event' circumstances—Acute, fatal, or chronic sublethal exposure to DA is increasingly recognized as an emerging threat to both human and wildlife health (Goldstein et al. 2008; Grattan et al. 2007; Kreuder et al. 2005; Ramsdell and Zabka 2008). Data from long-term disease surveillance suggests that DA exposure may be one factor contributing to mortality and failure of population recovery of southern sea otters, a federally listed threatened species (M. A. Miller [CDFG], pers. comm.). Logistic regression models developed for toxigenic *Pseudo-nitzschia* blooms in Monterey Bay have been used to indicate the extent of potential exposure by signaling the incidence of toxigenic bloom events (Lane et al. 2009), but cannot directly address toxin incidence since toxigenic blooms can vary widely in toxicity (Anderson et al. 2006, 2009; Blum et al. 2006; Lane et al. 2009; Marchetti et al. 2004; Trainer et al. 2002). Irrespective of bloom prevalence or toxicity, SPATT affords the direct detection of DA, PST (including STX), and other phyco toxins in the water column and, as an integrative sampling tool, SPATT has the potential to signal the incidence of toxin between discrete sampling events. Observational data from SPATT deployments, applied in conjunction with toxigenic *Pseudo-nitzschia* bloom models or traditional sampling methods (phytoplankton identification,

sentinel shellfish monitoring, etc.) can help to interpret the extent to which the models describe the frequency of toxin exposure (not simply the potential for toxicogenic blooms). In this context, integrative toxin detection would be especially valuable across periods of low or transitory toxin incidence (e.g., across periods when modeled bloom predictions might otherwise be (erratically) categorized as false positive due to artifacts of discrete sampling).

As a time integrative sampling tool, SPATT is designed to detect toxin at levels that would otherwise elude detection. In our field study, SPATT deployments of HP20, SP700, and SP207 signal the presence of DA over periods in which resident toxicogenic *Pseudo-nitzschia* species were not detected by weekly phytoplankton observation. Concentration of pDA tracked closely with the toxicogenic *Pseudo-nitzschia* abundance, thus may in part be an artifact of their simultaneous measurement from the same discrete water sample. The patterns of DA signaling by SPATT specifically the detection of DA in advance of an impending bloom and the intermittent nature of DA signaling throughout the year suggest that SPATT deployment results the incidence of DA when toxicogenic species observation and pDA quantification otherwise fail as indicators. It is not to suggest that SPATT is designed to compete with these alternative monitoring measures; the semi-quantitative temporal integrated measure of DA in the dissolved component of the water is unique in subject purpose and as such in its potential to reveal otherwise unrecognized patterns of DA presence and absence. Rather, we envision SPATT as a supplementary technique which could help to reduce costs associated with traditional shellfish and plankton monitoring methods (Mackenzie 2010) while providing a time-integrated toxin monitoring record which is useful for regulatory purposes and in other contexts (e.g., toxin model development and validation).

Selection of SPATT resin—Other solid phase extraction techniques exist for the extraction of DA from natural media such as seawater and tissue (Chapman et al. 2007; Piletski et al. 2008); the currently described methods require specialized adsorption media, sample pretreatment (usually pH adjustment) or both such that their application toward in situ adsorption of DA is not feasible (and is not the purpose for which they were designed). The four SPATT resin evaluated exhibit different adsorption characteristics with DA (Table 3) and should be selectively applied according to the goals for which they are implemented.

The HP20 resin is characterized by relative weak adsorption behavior with DA. We have demonstrated the successful application of HP20 for detection of the hydrophilic toxins DA and PST in the field and previous studies have demonstrated its applicability for laboratory toxins (Busch et al. 2005; Hux et al. 2008; MacCenzie et al. 2004; Pizarro et al. 2008a, 2008b; Rundberg et al. 2006, 2009; Takahashi et al. 2007; Turner et al. 2007). HP20 chemical characteristics that perhaps most closely imitate those of a natural (i.e., a relatively

low rate of accumulation (19% over 7 d) and a relatively high rate of desorption. Of the resins evaluated here, the nonspecificity and weak adsorption behavior of the HP20 suggests that it would most accurately imitate the adsorption and desorption response of a sentinel mussel while affording the consistency of a non-biological passive sampler. The use of HP20 offers the added benefit that it can be applied toward simultaneous detection of both hydrophilic and lipophilic toxins (Table 1).

The SP700 resin is characterized by moderate adsorptive behavior with DA (Fig. 2). Deployment of SP700 by the Fisheries Research Services (FRS) Marine Laboratory are as non-activated resin. The activation of SP700 augmented its adsorptive behavior reducing extraction efficiency and hereby suppressing DA signaling. Field deployments of activated SP700 detected DA on five occasions (05/11/08 and 12/18/08 + 07 and 03/08/09, respectively). The first deployment of SP700 as a non-activated resin yielded a significant DA signal (29 Apr–05 May 2009, 2 ng DA g⁻¹ d⁻¹). Inactivated deployments of SP700 tracked declining DA signals throughout the period when HP20 DA signals fell to undetectable levels; these results are consistent with the characterization of HP20 as a weaker resin and SP700 as a more aggressive adsorptive medium.

The SP207 resin is a more responsive resin in terms of its adsorptive behavior with DA. SP207 field deployments did not begin until 20 May 2009 and its deployment record is therefore limited in coverage. Throughout the period of SP207 deployments, the pattern of DA signaling from SP207 agrees well with the pattern described by concurrent SP700 resin deployments. The highly responsive adsorption behavior of SP207 (Fig. 2) suggests that this resin may be most suitable for applications where fast adsorption kinetics would be a concern (e.g., in a flow through column or as an adsorptive on a filter or junctionous electrode).

The deployment of SP2075S for SPATT is the most expensive of the deployment options evaluated in this study and SP2075S was not evaluated as a field-deployed SPATT resin. In addition, SP2075S SPATT bags exhibited the same characteristics as those described for SP207; this is not unexpected since SP2075S and SP207 differ only in that SP2075S is of smaller particle size (75–150 µm versus > 250 µm). SP2075S was selected for evaluation to assess whether there is an advantage gained from use of the finer particulate version of SP207 resin type. Based on the adsorption and extraction profiles, adsorption speed and extraction efficiency were not improved in the relatively more expensive SP2075S resin.

In the creation of an improved extraction protocol, our priorities were (1) a low volume requirement for necessary solvents, (2) the use of safe and chemicals which would not interfere with analysis by LC-MS, (3) safe and easily disposed of reagents, and (4) the extraction of a whole (un-cut) SPATT bag. For our purposes, the preparation of the LC-MS field protocols both satisfied these priorities and provided sufficient

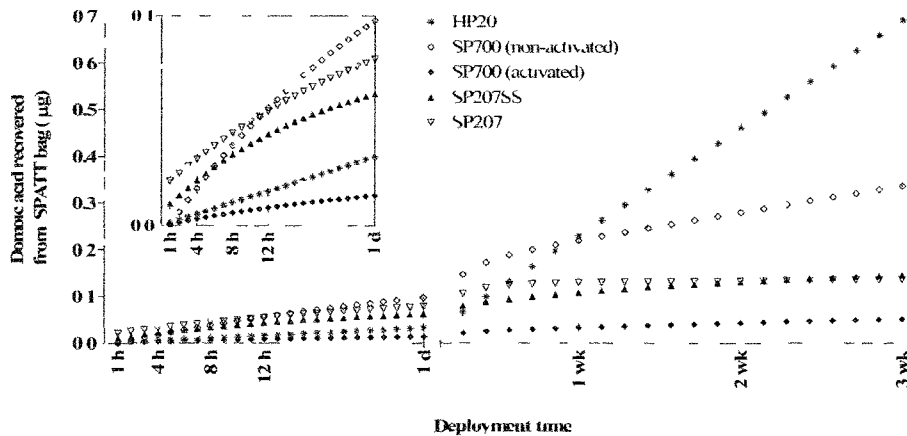


Fig. 5 A graph of hypothetical domoic acid (DA) recovery from SPATT bags of resin types evaluated in this study. The figure utilizes the experimentally determined adsorption and extraction efficiencies converted to the theoretical amount of DA recovered from SPATT bags of each resin type as a function of the duration of deployment. We assumed a closed system (1000 L) with an ambient dissolved DA concentration of 0.01 nM.

were able to observe DA signaling from our field deployed SPATT bags, and the DA signaling from the various resin types appeared to augment (rather than contradict) discrete observations of pDA toxicogen and *Pseudo-nitzschia* abundance, *Alexandrium catenella* abundance, and measurements of PST and DA in shellfish.

The adsorption behavior of each resin was representative of its relative extractability, i.e. faster adsorption translates to reduced (or more difficult) extraction. As such, the relative extraction efficiency of each resin must be considered in conjunction with its adsorption profile for proper identification of a resin that is optimal for any specific application. Figure 5 depicts the combination of adsorption and extraction efficiency for each resin to demonstrate the amount of DA that would be recovered from SPATT bags using our extraction protocols presented as a function of the hypothetical deployment period. While these results are theoretical, according to Fig. 5, deployment periods of 1 week would result in DA signaling from all three resin types at roughly the same magnitude, slight increases in the DA signal magnitudes from SP700 and SP207 may be owed to their greater capacity to adsorb DA during transient exposure to toxin. Fig. 5 also highlights the relative advantages of highly responsive resins such as SP207 for deployment via push through or tapping applications, and the benefits of using HP20 for prolonged deployments despite its leaky characteristics.

Much higher recoveries were obtained in non-activated SP700 laboratory trials when using either an HPLC column (82%) or successive room temperature soak/transfer with

MeOH (69% to 72%) while extraction of HP20 exceeded 99% when resin was removed from the SPATT bag and the Milli Q rinses were included in the analysis. Milli Q rinses did not extract DA from the other (non-HP20) resins. While it is important to demonstrate that maximal extraction efficiencies can be obtained, the time effort and cost required for achievement of those levels of efficiency detract from the utility of SPATT as a quick, efficient, and inexpensive new monitoring technology – without providing benefit beyond what larger resin bag deployments would provide (i.e. > 3 g dry weight resin). However, since the toxins appear to be stable when the resin is stored at -80°C, the end user always has the option of using our quick extraction protocol followed by more extensive (complete) extraction at a later time.

Comments and recommendations

A primary challenge in this method development was the identification of a reasonable and satisfactory extraction protocol. Just as we adapted an original extraction protocol for our purposes, we encourage further adaptation of our protocol (or the original protocol) for the improvement of extraction efficiency, the minimization of solvent volumes, and/or additional convenience. The resins performed adequately for the purpose of our SPATT DA field monitoring; this study therefore represents the successful expansion of SPATT technology (1) into US waters and (2) toward detection of DA, a hydrophobic phycotoxin (and in the case of HP20, simultaneous detection of STX and related PSTs). Whereas this is a demonstration of success, it is also a demonstration of broader

potential. The promise demonstrated here for SPATT technology warrants the future development and improvement of protocols allowing for expansion into a more diverse range of applications.

While not attempted as part of this study, we would particularly encourage investigation into the potential regeneration of SPATT resin for re-use. Synthetic adsorptive resins are relatively robust in structure and material, and are routinely regenerated as part of their application in an exceptionally wide variety of contexts. The development of a regenerative capacity would require: (1) the development of an extraction protocol that consistently provides 100% extraction efficiency, (2) a cleaning protocol to eliminate biofouling, and (3) a controlled assessment of resin resilience and performance through successive regeneration cycles. This would further reduce the expense and time associated with SPATT monitoring and would diminish the waste resin produced as a result of its application; these advantages would need to be balanced against the production of additional waste solvents generated as part of the recycling process as well as any loss of performance in the recycled resin.

We illustrate that passive sampling by SPATT is a powerful semi-quantitative tool that can afford new and unique insight into the distribution and prevalence of the hydrophilic biotoxins domoic acid and saxitoxin in the marine environment. Since the use of HP20 and SP700 with lipophilic toxins has been established, this work broadens their potential applicability toward the full range of phycotoxins currently monitored in sentinel shellfish. As such, SPATT is a technology that may support a more holistic regulatory approach, since its relevancy encompasses both lipophilic toxin exposure (e.g., neurotoxic shellfish poisoning, diarrhetic shellfish poisoning) and the hydrophilic toxins addressed in this study (amnesic shellfish poisoning, paralytic shellfish poisoning). Further, signaling by SPATT-DA in advance of shellfish toxicity may allow agencies to assume a more proactive (less reactive) regulatory stance. As an artificial sampling device, SPATT lacks the biological variability and analytical complications inherent to sentinel shellfish, and can be deployed in environments not conducive to sentinel organism monitoring. Since lipophilic and hydrophilic toxins are encountered and addressed by regulatory agencies and research institutes worldwide and within a range of environments, SPATT may afford more efficient and effective regulatory action, cost-savings, and enhanced toxin detection across an equally broad range of contexts. While its potential is apparent, SPATT should be considered complementary to quantitative observational methodologies until properly standardized to meet the reporting needs of regulatory agencies.

References

- Anderson, C. R., M. A. Brzezinski, L. Washburn, and R. M. Kudela. 2006. Circulation and environmental conditions during a toxicigenic *Pseudo-nitzschia* bloom. *Mar. Ecol. Progr. Ser.* 327:119-133 [doi:10.3354/meps327119].
- , D. A. Siegel, R. M. Kudela, and M. A. Brzezinski. 2009. Empirical models of toxigenic *Pseudo-nitzschia* blooms: potential use as a remote detection tool in the Santa Barbara Channel. *Harm. Algae* 8:478-492 [doi:10.1016/j.hal.2008.10.005].
- AOAC International. 2000. AOAC Official Method 991.26. AOAC International.
- . 2006. AOAC Official Method 2006.02. AOAC International.
- Bates, S. S., and V. L. Trainer. 2006. The ecology of harmful diatoms. In E. Granéli and J. Turner [eds.], *Ecology of harmful algae*. Springer-Verlag.
- Blanco, J., and others. 2006. Depuration of domoic acid from different body compartments of the king scallop *Pecten maximus* grown in raft culture and natural bed. *Aquat. Liv. Res.* 19:257-265 [doi:10.1051/alr/2006026].
- Blum, I., D. V. Subba Rao, Y. Pan, S. Swaminathan, and N. G. Adams. 2006. Development of statistical models for prediction of the neurotoxin domoic acid levels in the pennate diatom *Pseudonitzschia pungens* f. multiseriis utilizing data from cultures and natural blooms, p. 891-916. In D. V. Subba Rao [ed.], *Algal cultures, analogues of blooms and applications*. Science Publishers Inc.
- Booij, K., H. M. Sleiderink, and F. Smedes. 1998. Calibrating the uptake kinetics of semipermeable membrane devices using exposure standards. *Environ. Toxicol. Chem.* 17:1236-1245 [doi:10.1002/etc.5620170707].
- Chan, I. O. M., and others. 2007. Solid-phase extraction-fluorometric high performance liquid chromatographic determination of domoic acid in natural seawater mediated by an amorphous titania sorbent. *Anal. Chim. Acta* 283:111-117 [doi:10.1016/j.jaca.2006.09.063].
- Fritz, L., M. A. Quilliam, J. L. C. Wright, A. M. Beale, and T. M. Work. 1992. An outbreak of domoic acid poisoning attributed to the pennate diatom *Pseudonitzschia australis*. *J. Phycol.* 28:439-442 [doi:10.1111/j.0022-3646.1992.tb00439.x].
- Fux, E., C. Marcaillou, F. Mondeguer, R. Bire, and P. Hess. 2008. Field and mesocosm trials on passive sampling for the study of adsorption and desorption behavior of lipophilic toxins with a focus on OA and DTX1. *Harm. Algae* 7:574-583 [doi:10.1016/j.hal.2007.12.009].
- , R. Bire, and P. Hess. 2009. Comparative accumulation and composition of lipophilic marine biotoxins in passive samplers and in mussels (*M. edulis*) on the West Coast of Ireland. *Harm. Algae* 8:523-537 [doi:10.1016/j.hal.2008.10.002].
- Goldstein, T., and others. 2008. Novel symptomatology and changing epidemiology of domoic acid toxicosis in California sea lions (*Zalophus californianus*): an increasing risk to marine mammal health. *Proc. R. Soc. B* 275:267-276 [doi:10.1098/rspb.2007.1221].
- Górecki, T., and J. Namieśnik. 2002. Passive sampling. *Trends Anal. Chem.* 21:276-290 [doi:10.1016/S0165-2036(02)00407-7].

- Grattan, L. M., and others. 2007. Domoic acid neurotoxicity in Native Americans in the Pacific Northwest: human health project methods and update. *In* Fourth Symposium on Harmful Algae in the US. Woods Hole, Massachusetts (USA).
- Hess, P., and others. 2005. LC-UV and LC-MS methods for the determination of domoic acid. *Trends Anal. Chem.* 24:358-367 [doi:10.1016/j.trac.2004.11.019].
- Huckins, J., and others. 1996. Semipermeable membrane devices (SPMDs) for the concentration and assessment of bioavailable organic contaminants on aquatic environments. *In* G. Ostrander [ed.], *Techniques in aquatic toxicology*. Lewis Publisher.
- Kot-Wasik, A., B. Zabiega, M. Urbanowicz, E. Dominiak, A. Wasik, and J. Namie, nik. 2007. Advances in passive sampling in environmental studies. *Anal. Chim. Acta* 602:141-163 [doi:10.1016/j.aca.2007.09.013].
- Kreuder, C., and others. 2005. Evaluation of cardiac lesions and risk factors associated with myocarditis and dilated cardiomyopathy in southern sea otters (*Enhydra lutris nereis*). *Am. Vet. Res.* 66:289-299 [doi:10.2460/ajvr.2005.66.289].
- Krogstad, F. T. O., W. C. Griffith, E. M. Vigoren, and E. M. Faustman. 2009. Re-evaluating blue mussel depuration rates in 'Dynamics of the phycotoxin domoic acid: accumulation and excretion in two commercially important bivalves'. *J. Appl. Phycol.* 21:745-746.
- Lane, J. Q., P. T. Raimondi, and R. M. Kudela. 2009. Development of a logistic regression model for the prediction of toxicogenic *Pseudo-nitzschia* blooms in Monterey Bay, California. *Mar. Ecol. Progr. Ser.* 383:37-51 [doi:10.3354/meps07999].
- Mackenzie, A., D. A. White, P. G. Sim, and A. J. Holland. 1993. Domoic acid and the New Zealand Greenshell mussel (*Perna canaliculus*), p. 607-612. *In* T. J. S. a. Y. Shimizu [ed.], *Toxic phytoplankton blooms in the sea*. Elsevier Scientific Publ.
- Mackenzie, L., V. Beuzenberg, P. Holland, P. McNabb, and A. Selwood. 2004. Solid phase adsorption toxin tracking (SPATT): a new monitoring tool that simulates the biotoxin contamination of filter feeding bivalves. *Toxicol.* 44:901-918 [doi:10.1016/j.toxicol.2004.03.020].
- Mackenzie, L. A. 2010. In situ passive solid-phase adsorption of micro-algal biotoxins as a monitoring tool. *Curr. Opin. Biotechnol.* 21:326-331 [doi:10.1016/j.copbio.2010.07.013].
- Marchetti, A., V. L. Trainer, and P. J. Harrison. 2004. Environmental conditions and phytoplankton dynamics associated with *Pseudo-nitzschia* abundance and domoic acid in the Juan de Fuca eddy. *Mar. Ecol. Progr. Ser.* 281:1-12 [doi:10.3354/meps281001].
- Miller, P. E., and C. A. Scholin. 1996. Identification of cultured *Pseudo-nitzschia* (Bacillariophyceae) using species-specific LSU rRNA-targeted fluorescent probes. *J. Phycol.* 32:646-655 [doi:10.1111/j.0022-3646.1996.00646.x].
- and ———. 1998. Identification and enumeration of cultured and wild *Pseudo-nitzschia* (Bacillariophyceae) using species-specific LSU rRNA-targeted fluorescent probes and filter-based whole cell hybridization. *J. Phycol.* 32:371-382.
- and ———. 2000. On detection of *Pseudo-nitzschia* (Bacillariophyceae) species using whole cell hybridization: sample fixation and stability. *J. Phycol.* 36:238-250.
- Novaczek, I., M. S. Madhyastha, R. F. Albett, G. Johnson, M. S. Nijjar, and D. E. Sims. 1991. Uptake, dispersion and depuration of domoic acid by blue mussels (*Mytilus edulis*). *Aquat. Toxicol.* 21:103-118 [doi:10.1016/0166-445X(91)90009-X].
- Piletska, E. V., and others. 2008. Extraction of domoic acid from seawater and urine using a resin based on 2-(trifluoromethyl)acrylic acid. *Anal. Chim. Acta* 610:35-43 [doi:10.1016/j.aca.2008.01.032].
- Pizarro, G., L. Escalera, S. González-Gil, J. M. Franco, and B. Reguera. 2008a. Growth, behaviour and cell toxin quota of *Dinophysis acuta* during a daily cycle. *Mar. Ecol. Progr. Ser.* 353:89-105 [doi:10.3354/meps07179].
- , B. Paz, J. M. Franco, T. Suzuki, and B. Reguera. 2008b. First detection of Pectenotoxin-11 and confirmation of OA-D8 diol-ester in *Dinophysis acuta* from European waters by LC-MS/MS. *Toxicol.* 52:889-896 [doi:10.1016/j.toxicol.2008.09.001].
- Quilliam, M. A., M. Xie, and W. R. Hardstaff. 1995. A rapid extraction and cleanup for liquid chromatographic determination of domoic acid in unsalted seafood. *J. AOAC Int.* 78:543-554.
- , K. Thomas, and J. L. C. Wright. 1998. Analysis of domoic acid in shellfish by thin-layer chromatography. *Nat. Toxins* 6:147-152 [doi:10.1002/(SICI)1522-7185(199805/06)6:3/4<147::AID-NTX63(1-0)>3.0.CO;2-#1].
- Ramsdell, J. S., and T. S. Zabka. 2008. In utero domoic acid toxicity: a fetal basis to adult disease in the California sea lion (*Zalophus californianus*). *Mar. Drugs* 6:262-290.
- Rundberget, T., and others. 2007. Extraction of microalgal toxins by large-scale pumping of seawater in Spain and Norway, and isolation of okadaic acid and dinophysistoxin-2. *Toxicol.* 50:960-970 [doi:10.1016/j.toxicol.2007.07.003].
- , E. Gustad, I. A. Samdal, M. Sandvik, and C. O. Miles. 2009. A convenient and cost-effective method for monitoring marine algal toxins with passive samplers. *Toxicol.* 53:542-550 [doi:10.1016/j.toxicol.2009.01.010].
- Schnetzler, A., and others. 2007. Blooms of *Pseudo-nitzschia* and domoic acid in the San Pedro Channel and Los Angeles harbor areas of the Southern California Bight, 2003-2004. *Harm. Algae* 6:372-387 [doi:10.1016/j.hal.2006.11.004].
- Scholin, C. A., and others. 2000. Mortality of sea lions along the central California coast linked to a toxic diatom bloom. *Nature* 403:80-84 [doi:10.1028/47461].
- Seethapathy, S., T. Görecki, and X. Li. 2008. Passive sampling in environmental analysis. *J. Chromatogr. A* 1184:234-253

- [doi:10.1016/j.chroma.2007.07.070].
- Silvert, W., and D. V. S. Rao. 1992. Dynamic model for the flux of domoic acid, a neurotoxin, through a *Mytilus edulis* population. *Can. J. Fish. Aquat. Sci.* 49:400-405 [doi:10.1139/f92-045].
- Smith, J. R. 2005. Factors affecting geographic patterns and long-term change of mussel abundances (*Mytilus californianus* Conrad) and bed-associated community composition along the California coast. Ph.D. thesis, Univ. California Los Angeles.
- , P. Fong, and R. E. Ambrose. 2009. Spatial patterns in recruitment and growth of the mussel *Mytilus californianus* (Conrad) in southern and northern California, USA, two regions with differing oceanographic conditions. *J. Sea Res.* 61:165-173 [doi:10.1016/j.seares.2008.10.002].
- Stuer-Lauridsen, F. 2005. Review of passive accumulation devices for monitoring organic micropollutants in the aquatic environment. *Environ. Poll.* 136:503-524 [doi:10.1016/j.envpol.2005.12.004].
- Takahashi, E., and others. 2007. Occurrence and seasonal variations of algal toxins in water, phytoplankton and shellfish from North Stradbroke Island, Queensland, Australia. *Mar. Environ. Res.* 64:429-442 [doi:10.1016/j.marenvres.2007.03.005].
- Trainer, V. L., B. M. Hickey, and R. A. Horner. 2002. Biological and physical dynamics of domoic acid production off the Washington coast. *Limnol. Oceanogr.* 47:1438-1446 [doi:10.4319/lo.2002.47.5.1438].
- Turrell, E., L. Stobo, J.-P. Lacaze, E. Bresnan, and D. Gowland. 2007. Development of an 'early warning system' for harmful algal blooms using solid-phase adsorption toxin tracking (SPATT). *Oceans '07. Marine Challenges: Coastline to Deep Sea.*
- Vrana, B., and others. 2005. Passive sampling techniques for monitoring pollutants in water. *Trends Anal. Chem.* 24:845-868 [doi:10.1016/j.trac.2005.06.006].
- Wang, Z., K. L. King, J. S. Ramsdell, and G. J. Doucette. 2007. Determination of domoic acid in seawater and phytoplankton by liquid chromatography-tandem mass spectrometry. *J. Chromatogr. A* 1163:169-176 [doi:10.1016/j.chroma.2007.06.054].
- Wohlgeschaffen, G. D. 1991. Uptake and loss of the neurotoxin domoic acid by mussels (*Mytilus edulis*) and scallops (*Placopecten magellanicus* Gmelin). M.S. thesis, Dalhousie Univ.

Submitted 30 March 2010

Revised 19 August 2010

Accepted 6 October 2010

CHAPTER THREE (ADDENDUM)

Update on the Application of Solid Phase Adsorption Toxin Tracking (SPATT) for Field Detection of Domoic Acid

Lane, J.Q.¹, Langlois, G.W.² & Kudela, R.M.¹

¹University of California Santa Cruz, 1156 High Street, 95064, Santa Cruz, California U.S.A.

JQuay@ucsc.edu

²California Department of Public Health, 850 Marina Bay Parkway, 94804, Richmond, California U.S.A.

Abstract

Recent publications have identified the analysis of phycotoxins in sentinel shellfish as a problematic tool for environmental monitoring purposes. Domoic acid (DA), a neurotoxin produced by some species of the diatom *Pseudo-nitzschia*, can remain undetected in sentinel shellfish stocks during toxic blooms and subsequent marine bird and mammal mass mortality events. Solid Phase Adsorption Toxin Tracking (SPATT) has previously been described as a new tool useful for monitoring of lipophilic toxins; a methodology extending its applicability towards the hydrophilic phycotoxins [DA and paralytic shellfish toxin (PST)] has been recently described. The original method development included 18 months of weekly SPATT deployments in Monterey Bay, California (U.S.A.). Here, we update the original results with new field data from 2010 (January – November), presenting DA-signaling from SPATT deployments in conjunction with data from concurrent, traditional monitoring practices. The sensitivity of SPATT to the onset of a toxic *Pseudo-nitzschia* bloom (spring 2010) is presented for comparison to the sensitivity described in the original method development publication. Unlike in years for which SPATT-DA signaling has been described, toxigenic *Pseudo-nitzschia* abundance remained elevated throughout 2010, allowing for a unique and new evaluation of SPATT-DA performance during an exceptionally sustained toxic event.

Introduction

Solid Phase Adsorption Toxin Tracking (SPATT) is a passive sampling technology designed to monitor and detect lipophilic phycotoxins as a ‘man-made’ sentinel mussel, enabling the detection and monitoring of lipophilic toxins in coastal waters without the cost and complications of sentinel shellfish analysis (MacKenzie *et al.* 2004, Fux *et al.* 2009, Rundberget *et al.* 2009, MacKenzie 2010). The SPATT technology has most recently been extended for the detection of the hydrophilic phycotoxin domoic acid (DA), a neurotoxin produced by toxigenic species of the diatom genus *Pseudo-nitzschia* (Lane *et al.* 2010). The method development of SPATT for its application with DA included 18 months (July 2007 – December 2009) of weekly-rotation field deployments at Santa Cruz Municipal Wharf (SCMW) in northern Monterey Bay, California. As described, 3 adsorptive synthetic resins identified as SPATT-DA candidate resins (HP20, SP700, SP207) were sealed separately into Nitex mesh using a plastic bag sealer. The SPATT ‘bags’ were secured to a weighted rope and

suspended in the water column alongside sentinel mussels sampled weekly as part of the California Department of Public Health (CDPH) Marine Biotoxin Monitoring Program. After one week the bags were recovered (and replaced with new bags), transported to University of California Santa Cruz (UCSC) on blue ice, and extracted; the extract was then analyzed for DA (and additional phycotoxins; see Lane *et al.* 2010). Concurrent traditional sampling techniques included (a) the collection of integrated-depth whole water (0, 1 and 3 m) for cell counts of toxigenic *Pseudo-nitzschia* species (*P. australis* and *P. multiseriata*) and the analysis of DA (particulate and dissolved), and (b) the collection of a net tow [5 x 10 ft (50 ft) vertical tow effort] for the assessment of *Pseudo-nitzschia* (genus) relative abundance within the phytoplankton community by light microscopy. Two significant toxic events occurred during the 18-month period; in both, DA detection by SPATT preceded shellfish toxicity by 7-8 weeks and afforded unique advance warning of the toxic bloom events.

Here we update the initial performance report described as part of the development of SPATT

for application with DA. The timeseries described in Lane *et al.* 2010 is updated for Jan – Nov 2010 with data from continued field deployments of SPATT at SCMW and concurrent sampling of *Pseudo-nitzschia* (genus) relative abundance, toxigenic *Pseudo-nitzschia* cell counts, particulate DA, and sentinel mussels. We describe two refinements instituted since description of the original extraction protocol: (1) the extraction of SPATT as free resin, and (2) same-day preparation of an ammonium acetate reagent for use in SPATT extractions.

Methods

Continued weekly field deployments of SPATT and concurrent sampling of *Pseudo-nitzschia* relative abundance, toxigenic *Pseudo-nitzschia* cell counts, particulate DA and sentinel mussels were conducted as described in Lane *et al.* 2010. High resolution (daily) sampling of particulate DA was carried out 06-21 Oct across 2 week-long SPATT rotations, allowing for a comparison between the two sampling approaches (discrete daily grab sampling of particulate toxin versus week-integrative SPATT deployment). The treatment of SPATT resins recovered from the field was consistent with Lane *et al.* 2010 until 08 Feb 2010; from that rotation forward all SPATT resins were extracted in-column as free resins. The extraction of SPATT as free resin is made possible with adjustment of the original extraction protocol, as follows: the SPATT bags are recovered from the seawater, immediately rinsed with Milli-Q (2 x ~200 mL) and transported from the field to the analytical lab on blue ice. One side of the bag is cut open and the resin is Milli-Q-rinsed out of the bag and into an extraction column. During this process the extraction column spigot is in the ‘closed’ position, so that the volume of Milli-Q used in resin transfer can be held constant from week to week (~10 mL). The resin is then extracted as described in Lane *et al.* 2010, with the specification that the 1M ammonium acetate in 50% MeOH reagent is prepared the same day it is used for extraction.

Results and Discussion

DA detection data from week-integrative SPATT deployments at SCMW are shown in Figure 1, with concurrent (weekly) data for *Pseudo-nitzschia* (genus) relative abundance, toxigenic

Pseudo-nitzschia cell abundance, particulate DA, and DA in mussels. *Pseudo-nitzschia* (genus) and toxigenic species of *Pseudo-nitzschia* were observed every week from 31 Mar onward, with few exceptions. Particulate DA tracked closely with toxigenic cell counts, although the detection of particulate DA was sporadic in the weeks prior to (and zero the week of) the initial observation of toxigenic *Pseudo-nitzschia* on 14 Apr. Shellfish data from UCSC indicate low-level DA in sentinel mussels for all samples collected in 2010, and elevated DA (>1 ppm) in sentinel mussels collected during the height of the bloom event (05 May – 08 Sept) with only a single exception (28 Jul; 0.679 ppm).

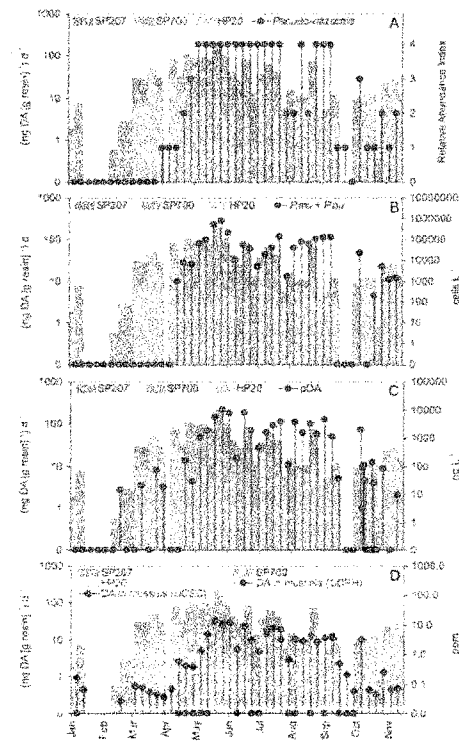


Figure 1. Domoic acid (DA) detection by week-integrative deployments of SPATT (HP20, SP700, SP207) at the Santa Cruz Municipal Wharf, with the following weekly data from discrete sample collections: *Pseudo-nitzschia* (genus) relative abundance within the phytoplankton community [0, 1=1% or less, 2=1-9%, 3=10-49%, 4=50% or more] (A), toxigenic *Pseudo-nitzschia* species cell abundance (*P. australis* + *P. multiseriata*) (B), particulate DA (C), and DA in mussels (D).

DA was detected in the first SPATT deployments of the year, from 29 Dec 2009 – 12 Jan 2010 (Figure 1). SPATT and sentinel mussel monitoring was disrupted from 13 Jan – 09 Feb due to loss of the wharf deployment platform in a winter storm. DA was detected by SPATT upon the resumption of weekly deployments on 10 Feb, and was detected in every deployment rotation thereafter until 08 Sept, with a single exception (rotation 31 Mar – 06 Apr) which coincided with two weekly samples in which particulate DA was not detected (0.00 ng L^{-1} ; 07 and 14 Apr). The continual detection of DA by SPATT began on 07 Apr; this signal preceded the observation of toxigenic *Pseudo-nitzschia* by 1 week, the detection of particulate DA and *Pseudo-nitzschia* (genus) at relative abundance >1% by 2 weeks, the recognition of bloom onset (toxigenic *Pseudo-nitzschia* abundance $>10,000 \text{ cells L}^{-1}$) and impending shellfish toxicity ($>1 \text{ ppm}$) by 4 weeks, and the detection of shellfish toxicity by the regulatory agency (CDPH) by 6 weeks. SPATT DA with daily-sampled particulate DA and weekly-sampled DA in sentinel mussels are presented for 06-21 Oct (Figure 2). Particulate DA was variable from day-to-day, ranging from zero to 1935 ng L^{-1} . In the most exceptional example of this variability, particulate DA fell to 3.22 ng L^{-1} on 07 Oct after its highest measurement the day before (1935 ng L^{-1}). DA detection by SPATT was moderate for the first two week-long deployment rotations (06-13 Oct and 13-20 Oct), then became relatively weak [$(0.78 \text{ ng g}^{-1} \text{ d}^{-1})$ by SP700]. Weekly samples of DA in sentinel mussels indicated low and decreasing shellfish toxicity during this period (3 ppm on 06 Oct; $<1 \text{ ppm}$ on 13 & 20 Oct). These data illustrate the utility of SPATT, which, as an integrative passive sampling technology, can provide a monitoring perspective that is less susceptible to the variability introduced through discrete sample collections (i.e. SPATT data inform the collector of toxin encounters across the



Figure 2. Domoic acid (DA) detection by week-integrative deployments of SPATT (HP20, SP700, SP207) at the Santa Cruz Municipal Wharf, with DA in mussels (sampled weekly).

deployment period, while discrete-sample data inform the collector of conditions in the water parcel that was collected). However, since SPATT is not approved for regulatory decisions, it remains complementary to traditional sampling.

Acknowledgements

We thank K. Hayashi (UCSC) and the staff and volunteers of the CDPH Marine Biotxin Monitoring Program. Partial funding was provided by NOAA Monitoring and Event Response for Harmful Algal Blooms (MERHAB) Award NA04NOS4780239 (Cal-PReEMPT), NOAA California Sea Grant Award NA04OAR4170038, as a fellowship (JQL) from an anonymous donor through the Center for the Dynamics and Evolution of the Land-Sea Interface (CDELSI), and as a scholarship (JQL) from the Achievement Rewards for College Scientists (ARCS) Foundation. This contribution is part of the Global Ecology and Oceanography of Harmful Algal Blooms (GEOHAB) Core Research Project on Harmful Algal Blooms in Upwelling Systems, and is MERHAB Publication #144.

References

- MacKenzie, L., Beuzenberg, V., Holland, P., McNabb, P. & Selwood, A. (2004). *Toxicon* 44: 901-918.
- Fux, E., Bire, R. & Hess, P. (2009). *Harmful Algae* 8: 523-537.
- Rundberget, T., Gustad, E., Samdal, I.A., Sandvik, M. & Miles, C.O. (2009). *Toxicon* 53: 543-550.
- MacKenzie, L.A. (2010). *Current Opinion in Biotechnology* 21: 326-331.
- Lane, J.Q., Roddam, C.M., Langlois, G.W. & Kudela, R.M. (2010). *Limnology and Oceanography: Methods* 8: 645-660.

DISSERTATION CONCLUSION

In the first chapter of this dissertation, I developed statistical models to identify the *chemical* and *physical* oceanographic conditions associated with the incidence of toxigenic *Pseudo-nitzschia*, blooms in Monterey Bay, California. The statistical models are logistic regressions that identify and use predictor variables (chlorophyll, silicic acid, nitrate, water temperature, an upwelling index, and river discharge) to generate bloom probabilities (a 0–100% ‘chance-of-bloom’ estimate, analogous to a weather model ‘chance-of-rain’ prediction). The models that I developed demonstrate excellent ($\geq 75\%$) predictive ability with unknown (future) blooms events of toxigenic *Pseudo-nitzschia*. Prior to this contribution, the development of robust *Pseudo-nitzschia* bloom models had been hindered by a general lack of long-term and consistent monitoring efforts. Thus, in both scope and functionality, my modeling effort was unprecedented: it was the first to (1) produce *Pseudo-nitzschia* models from long-term (>1.5 y) monitoring efforts, and (2) address blooms of toxigenic *Pseudo-nitzschia*. Although the seasonality of blooms is widely recognized, my study was the first to incorporate seasonality in model development. As such, the study revealed important seasonal patterns in the factors contributing to bloom proliferation; nitrate and river discharge emerged as significant bloom predictors during the summer/fall/winter period, while temperature and upwelling emerged as significant factors for springtime bloom events.

The identification of seasonal (and year-round) predictor variables represented an important step towards understanding *Pseudo-nitzschia* bloom dynamics and establishing guidelines for comprehensive monitoring and preventative regulatory measures. This advancement is of widespread and immediate public and scientific interest: the recent implication of cultural eutrophication as a factor in HAB proliferation is an alarming and unresolved subject requiring analysis of specific and, most helpfully, seasonal contributing factors. My development of toxigenic *Pseudo-nitzschia* bloom models, in lieu of direct toxin models, ensured their applicability to an emerging ecosystem threat, namely the exposure of humans and marine mammals to ‘background’ levels of DA introduced by low to mildly toxigenic *Pseudo-nitzschia* blooms. The power of the models to predict toxigenic *Pseudo-nitzschia* blooms offers pathologists, public health regulators, shellfisheries, and others a new tool for hindcast and future prediction of bloom dynamics.

The first chapter of this dissertation represents the first rigorous consideration and synthesis of the environmental factors significant to proliferation of toxigenic *Pseudo-nitzschia* and provides the research and regulatory communities with a powerful new tool for toxigenic *Pseudo-nitzschia* bloom prediction. The modeling study also contributes to a collection of literature in which two eutrophication processes had been alternately suggested as promotional of *Pseudo-nitzschia* blooms in Monterey Bay: (1) ocean upwelling, the vertical flux of deep, nutrient-rich water into surface waters, and (2) river flow, which has been otherwise regarded as a non-competitive influence along upwelling-dominated coastlines (Breaker and Broenkow

1994; Rosenfeld et al. 1994; Olivieri and Chavez 2000; Ramp et al. 2005; Shulman et al. 2010). Ultimately, the modeling exercise identified both of these processes as significant according to their seasonality, reconciling their previous regard as alternative hypotheses, rather than co-conspirators. To understand this duality further, the second chapter of this dissertation was developed as an explicit examination of those environmental processes (river discharge and upwelling) within the context of a third seasonally predictive ‘fertilizer’ component (nitrate).

In the second chapter of this dissertation, I evaluate the timing and magnitude of nitrate loading by rivers to Monterey Bay, i.e. freshwater nitrate loading within the context of a coastal upwelling regime. As an open embayment on the ‘upwelling-dominated’ central coast of California, it is typically assumed that fluvial nitrate inputs to Monterey Bay are insignificant compared to coastal upwelling. Recent publications describing eutrophic river discharge as a significant contributor of nutrients promotional of HAB development along the California, Oregon and Washington coastlines (Warrick et al. 2005; Hickey and Banas 2008; Lane et al. 2009; Hickey et al. 2010), and increasing nitrate concentrations in rivers draining to Monterey Bay (Ruehl et al. 2007), indicate that this assumption may be inaccurate. The test of that assumption and long standing paradigm required the identification and use of a water quality dataset that was unprecedented as a high-resolution, long-term record (daily, across 10 years: 2000–2009), matched with an equally rigorous and high-resolution record of upwelling nitrate load estimates. The comparison between river and upwelling nitrate loading across the 10 years shows that while

upwelling loads 'dominate' at low temporal resolution (monthly, annual), rivers exceed upwelling as a source of nitrate on short timescales (daily, weekly) at a significant rate (28% of days in a given year). The study also provided evidence of a clear onshore-offshore gradient in fluvial load influence: the correlation between annual climatologies of nitrate concentration measured in Monterey Bay waters and fluvial nitrate input to Monterey Bay is highest at a pier-based monitoring site and weakens with distance offshore (the reverse general spatial pattern is identified for upwelling load influence). The 10-year record of river nitrate loads enabled identification of a significant upward trend across the decade (i.e. river nitrate loads increasing in size), while no similar trend was identified in upwelling loads. The load record also allowed for novel characterization of the eutrophic conditioning of the largest rivers in Monterey Bay (the Salinas and Pajaro rivers) according to the Indicator for Coastal Eutrophication Potential for nitrogen (N-ICEP), which permitted their comparison to rivers worldwide. Within this global context, the patterns identified for the Pajaro and Salinas rivers align with patterns described for rivers of non-industrialized countries, where rapidly increasing agricultural production and urbanization have led to worsening eutrophic conditions. The characterization of the Pajaro and Salinas rivers according to the N-ICEP suggests that the eutrophic conditioning of these central coast rivers will persist (or worsen) and may be expected to contribute to the incidence of HABs at present and into the future.

The second chapter of this dissertation represents the first comparative synthesis of river and upwelling nitrate inputs at temporal scales which are (1)

ecologically relevant, and (2) appropriate for resolution of fluvial loading, which is highly episodic. Further, and perhaps most significantly, it provides the research and regulatory communities with insight into when, and why, historical assumptions about water quality require re-evaluation. The value of executing a comparison between riverine and upwelling nitrate loading to Monterey Bay, an embayment centrally located along an ‘upwelling-dominated’ coastline, was initially an open question. While nitrate loading by large rivers to *non*-upwelling regimes is widely regarded as an environmental threat (e.g. regional anoxia in the Gulf of Mexico resulting from nitrogen loading by the Mississippi River), classical oceanography dictates that eutrophication by upwelling processes along the California coastline occurs on spatial and temporal scales so large as to render riverine inputs negligible. The eutrophic state of our rivers has changed dramatically, however, even over the career spans of present day water quality specialists, and warrants new consideration by coastal ocean researchers. Even to the more arid south, the Santa Clara River has been identified as a significant source of nutrients to the coastal waters of the Santa Barbara Channel according to both its timing (loading primarily occurs during episodic, high-flow/‘flush’ events) and its nutrient load stoichiometry [upwelling injects silicic acid (Si), nitrate (N) and *ortho*-phosphate (P) into the surface waters at ratios of 13:10:1 (Si:N:P) while the Santa Clara River does the same but at ratios of 16:5:1 (Warrick et al. 2005)].

The third and final chapter of this dissertation is my development of a new monitoring technology, Solid Phase Adsorption Toxin Tracking (SPATT), for

use with hydrophilic algal toxins (DA and saxitoxin) in the coastal environment. SPATT is the deployment of synthetic resin for time-integrated, semi-quantitative tracking purposes: the toxin of interest is passively adsorbed from seawater onto the resin, the resin is recovered and extracted, and the extract is analyzed. First described by MacKenzie et al. (2004), the development and application of SPATT has remained limited to lipophilic toxin tracking within its region of origin (New Zealand) and across Europe (MacKenzie et al. 2004; Rundberget et al. 2007; Takahashi et al. 2007; Turrell et al. 2007; Fux et al. 2008; Pizarro et al. 2008a; Pizarro et al. 2008b; Fux et al. 2009; Rundberget et al. 2009; MacKenzie 2010; Rodriguez et al. in press). My method development work with SPATT is unprecedented in two central aspects: (1) it is the novel development of SPATT for use with hydrophilic toxins, and (2) it is the first to describe and evaluate the application of SPATT in the United States.

The method development of SPATT for DA included the identification of four potential SPATT resins for hydrophilic biotoxin monitoring and their evaluation in laboratory-based trials (adsorption efficiencies, saturation thresholds, extraction efficiencies) and as part of a field biotoxin monitoring effort. I describe a new deployment strategy that allows for quick manufacture of pliable, resin-filled SPATT bags without specialized skills or equipment, and an extraction protocol appropriate for use with these bags upon their retrieval from the field. I identify three (of the four) resins as cost-effective SPATT candidates for toxin monitoring, and evaluate their performance based on 17 months of field deployment at the Santa Cruz Municipal Wharf (SCMW) alongside weekly California Department of Public Health (CDPH)

sentinel shellfish monitoring. Observations of the phytoplankton assemblage, oceanographic conditions, and particulate DA concentrations were also performed concurrently. Two significant toxigenic *Pseudo-nitzschia* blooms were observed during the deployment period: SPATT successfully signaled these blooms events 3 and 7 weeks prior to the recognition of bloom conditions by traditional monitoring techniques (7 and 8 weeks prior to the detection of shellfish toxicity). Following their analysis for DA, a selection of extracts recovered from field-deployed HP20 (one of the four resins) was analyzed for saxitoxin; HP20 was targeted since it was originally identified for simultaneous monitoring of multiple lipophilic toxins. Our detection of both DA and saxitoxin in HP20 field-extracts signifies its potential with an array of biotoxins that is broader than previously recognized.

SPATT was developed as a synthetic alternative to biotoxin monitoring with sentinel shellfish; while we recognize the employment of sentinel shellfish as a uniquely valuable practice, the use of a biological matrix introduces analytical costs and challenges. Gregg Langlois, Senior Research Scientist at CDPH and co-author on the publication that comprises the third chapter of this thesis, oversees the statewide Marine Biotxin Monitoring Program and is charged with balancing these costs and challenges with the provision of public health protection. His participation as part of this study allowed us to develop this new hydrophilic-SPATT method while maintaining (and providing) a unique and valuable ‘real-world’ perspective on method efficiency, relevance, utility, and potential. Our discussion and assessment of SPATT application for DA includes the consideration of cost (material, time, effort,

shipping, etc.), character (e.g. which resin might best mimic a sentinel shellfish) and contribution (what new information SPATT provides, and the significance and value of that information). In the case of the latter, the development of this method has allowed us to reconsider the prevalence of biotoxins in local waters; the SPATT deployments at SCMW indicate that DA is present at times when it is otherwise not detected by traditional monitoring techniques. I therefore provide a method that delivers useful, efficient, and cost-effective information, and can provide unique insight into coastal biotoxin prevalence and dynamics.

Included as an addendum to the third chapter of this dissertation is a manuscript prepared for submission to the 14th International Conference on Harmful Algae (ICHA 14) Conference Proceedings. The manuscript provides two refinements to the SPATT methodology and provides an overview of SPATT monitoring performance during the 2010 SCMW field season.

References

- Breaker, L. C., and W. W. Broenkow. 1994. The circulation of Monterey Bay and related processes. *Oceanography and Marine Biology* **32**: 1-64.
- Fux, E., R. Bire, and P. Hess. 2009. Comparative accumulation and composition of lipophilic marine biotoxins in passive samplers and in mussels (*M. edulis*) on the West Coast of Ireland. *Harmful Algae* **8**: 523-537.
- Fux, E., C. Marcaillou, F. Mondeguer, R. Bire, and P. Hess. 2008. Field and mesocosm trials on passive sampling for the study of adsorption and desorption behavior of lipophilic toxins with a focus on OA and DTX1. *Harmful Algae* **7**: 574-583.
- Hickey, B. M., and N. S. Banas. 2008. Why is the Northern End of the California Current System So Productive? *Oceanography* **21**: 90-107.
- Hickey, B. M. and others 2010. River Influences on Shelf Ecosystems: Introduction and synthesis. *J Geophys Res-Oceans* **115**: -.
- Lane, J. Q., P. T. Raimondi, and R. M. Kudela. 2009. Development of a logistic regression model for the prediction of toxicogenic *Pseudo-nitzschia* blooms in Monterey Bay, California. *Marine Ecology Progress Series* **383**: 37-51.
- MacKenzie, L., V. Beuzenberg, P. Holland, P. McNabb, and A. Selwood. 2004. Solid phase adsorption toxin tracking (SPATT): a new monitoring tool that simulates the biotoxin contamination of filter feeding bivalves. *Toxicon* **44**: 901-918.
- MacKenzie, L. A. 2010. *In situ* passive solid-phase adsorption of micro-algal biotoxins as a monitoring tool. *Current Opinion in Biotechnology* **21**: 326-331.
- Olivieri, R. A., and F. P. Chavez. 2000. A model of plankton dynamics for the coastal upwelling system of Monterey Bay. *Deep-Sea Research II* **47**: 1077-1106.
- Pizarro, G., L. Escalera, S. González-Gil, J. M. Franco, and B. Reguera. 2008a. Growth, behaviour and cell toxin quota of *Dinophysis acuta* during a daily cycle. *Marine Ecology Progress Series* **353**: 89-105.
- Pizarro, G., B. Paz, J. M. Franco, T. Suzuki, and B. Reguera. 2008b. First detection of Pectenotoxin-11 and confirmation of OA-D8 diol-ester in *Dinophysis acuta* from European waters by LC-MS/MS. *Toxicon* **52**: 889-896.
- Ramp, S. R., J. D. Paduan, I. Shulman, J. Kindle, F. L. Bahr, and F. Chavez. 2005. Observations of upwelling and relaxation events in the northern Monterey Bay during August 2000. *J Geophys Res-Oceans* **110**: -.
- Rodriguez, P., A. Alfonso, E. Turrell, J. Lacaze, and L. M. Botana. in press. Study of solid phase adsorption of paralytic shellfish poisoning toxins (PSP) onto different resins. *Harmful Algae*.
- Rosenfeld, L. K., F. B. Schwing, N. Garfield, and D. E. Tracy. 1994. Bifurcated flow from an upwelling center: a cold water source for Monterey Bay. *Continental Shelf Research* **14**: 931-964.
- Ruehl, C. R. and others 2007. Nitrate dynamics within the Pajaro River, a nutrient-rich, losing stream. *Journal of the North American Benthological Society* **26**: 191-206.
- Rundberget, T., E. Gustad, I. A. Samdal, M. Sandvik, and C. O. Miles. 2009. A convenient and cost-effective method for monitoring marine algal toxins with passive samplers. *Toxicon* **53**: 542-550.
- Rundberget, T. and others 2007. Extraction of microalgal toxins by large-scale pumping of seawater in Spain and Norway, and isolation of okadaic acid and dinophysistoxin-2. *Toxicon* **50**: 960-970.

- Shulman, I., S. Anderson, C. Rowley, S. DeRada, J. Doyle, and S. Ramp. 2010. Comparisons of upwelling and relaxation events in the Monterey Bay area. *J Geophys Res-Oceans* **115**: -.
- Takahashi, E. and others 2007. Occurrence and seasonal variations of algal toxins in water, phytoplankton and shellfish from North Stradbroke Island, Queensland, Australia. *Marine Environmental Research* **64**: 429-442.
- Turrell, E., L. Stobo, J.-P. Lacaze, E. Bresnan, and D. Gowland. 2007. Development of an 'early warning system' for harmful algal blooms using solid-phase adsorption toxin tracking (SPATT). *Oceans '07. Marine Challenges: Coastline to Deep Sea*.
- Warrick, J. A., L. Washburn, M. A. Brzezinski, and D. A. Siegel. 2005. Nutrient contributions to the Santa Barbara Channel, California, from the ephemeral Santa Clara River. *Estuarine, Coastal and Shelf Science* **62**: 559-574.